1977

Studies into the electronic structure of transition metal complexes

John A. Land
University of Wollongong

STUDIES INTO THE ELECTRONIC STRUCTURE OF TRANSITION METAL COMPLEXES

A thesis presented for the degree

of

Master of Science

at

The University of Wollongong

John A. Land B.Sc.
A.R.A.C.I.

1977

TO BIMP, CHRISTINE

AND

LAUREN, BARRY AND ERIC

ACKNOWLEDGEMENTS

I would like to express my thanks to the many people who have contributed in the development of the work presented in this thesis.

In particular I thank my supervisor, Dr. P.G. Burton.

Special thanks are due to the staff of the University of Wollongong Computer Centre, particularly Mr. Q. Addison, for his assistance.

I also thank Mrs. G. Gregor for the excellent work done in typing this thesis.

SUMMARY

The aim of this work is to determine the computationally optimal route to the reliable first principles evaluation of the electronic structure parameters for transition metal complexes by molecular orbital theory. Three hexafluoride complexes have been studied as test systems.

This thesis has examined experimental techniques which probe electronic structure, and hence may provide data for comparison with theory. We have also discussed theoretical investigations of electronic structure including, of course, our results in relation to previous studies.

We have investigated three different matrix element methods of various levels of sophistication with the aim of establishing the minimum acceptable computational effort required to describe them within a given basis set.

We have shown that the development of better methods of calculating integrals has led to improved accuracy and as a result, agreement with experiment has also improved.

Our model has behaved in an orderly and predictable way when variations of a chemically interpretable nature were introduced. Within the limitations of this work we believe our method will be capable of producing reliable wavefunctions for molecular systems which are chemically more interesting than the simple complexes studied here.

We have illustrated that the octahedral cluster approximation even in very ionic crystals such as $KNiF_3$ is entirely inadequate (in contrast to the case of crystals such as K_2NaCrF_6 and K_2NaFeF_6) because of the pronounced electrostatic differentiation of metal and ligand species in the fluoroperovskites. The results of our elaborate modelling of the influence of the lattice contradict a long standing assumption of the literature in regard to the fluoroperovskites.

CONTENTS

1.0 INTRODUCTION

Molecular Orbital studies at the present state of development are a compromise between the accuracy of the calculated wavefunction and the cost, or computational effort, involved in obtaining it. The present study is concerned with the development of a MO technique which reduces the number of molecular integrals to a minimum to allow more accurate basis sets to be used in the expansion of the MO's. Thus it is hoped to effect a considerable saving in effort with minimal loss of precision.

We have studied the systems CrF_6^{3-}, FeF_6^{3-} and NiF_6^{4-} representing 3d orbital configurations of 3, 5 and 8 electrons respectively. Three distinct matrix element methods of varying complexity have been evaluated using localized orbitals, the Mulliken and Roby population analysis schemes together with the calculated spin distribution on the above systems.

The stimulus for this study came from the success of these matrix element methods in the study of HF, H_2O, NH_3, FCN, O_3, OF_2 and the n-alkanes[1] when the integrals were evaluated rigorously.

Chapter 2 outlines the experimental investigations of the electronic structure of transition metal systems together with a summary of MO theory applied to transition metal complexes. The transition metal hexafluoride literature has been monitored hopefully exhaustively while other areas such as the tetroxyanions the coverage has not been as great. Both ground and excited state experimental methods are examined but in this thesis considerable emphasis is placed on the study of spin distributions by magnetic resonance and magnetic neutron diffraction techniques.

The theoretical framework of molecular calculations, in particular, Hartree-Fock theory is presented in Chapter 3 while an analysis of MO methods currently being applied to transition metal systems is given in Chapter 4. The literature results, both for the 3 ions in this study and other systems are given in Chapter 5.

An outline of the ESEMO method and discussion of its use in this study are given in Chapter 6 and the discussion of results obtained are given in Chapter 7.

References : Chapter 1.

1. P.G. Burton, N.R. Carlsen, To be published.

2.0 EXPERIMENTAL INVESTIGATIONS OF THE ELECTRONIC STRUCTURE OF TRANSITION METAL SYSTEMS.

2.1.0 Molecular Orbital Theory of Transition Metal Complexes

Initially we are studying simple octahedral complexes of a 3d transition metal ion using Molecular Orbital (MO) theory. The relation of the MO formalism to the more complete Configuration-Interaction (C-I) description has been discussed by Owen and Thornley[1].

The ionic wave functions of the components of each complex of particular interest are the metal 3d orbitals and the ligand 2s and 2p orbitals. Sigma (σ) bonds may be formed between the $3d_{x^2-y^2}$ and the $3d_{z^2}$ (e_g) metal orbitals, the six ligand 2s orbitals and the six ligand p_σ orbitals. Pi (π) bonds may be formed between the $3d_{xy}$, $3d_{xz}$ and $3d_{yz}$ (t_{2g}) orbitals. The nature of the overlap of the 3d orbitals with $2p_\sigma$ and $2p_\pi$ orbitals is shown schematically in Figs. 1 and 2.

The filled bonding orbitals of mainly ligand character are:

$$\psi_S^B = N_S^B \left[\chi_{2s} + \gamma_S \, d\sigma + \gamma_{S\sigma} \, \chi_{2p\sigma}\right] \qquad 2.1$$

$$\psi_\sigma^B = N_\sigma^B \left[\chi_{2p\sigma} + \gamma_\sigma \, d\sigma + \gamma_{\sigma S} \, \chi_{2s}\right] \qquad 2.2$$

$$\psi_\pi^B = N_\pi^B \left[\chi_{2p\pi} + \gamma_\pi \, d_\pi\right] \qquad 2.3$$

N_S^B, N_σ^B and N_π^B and normalization constants and χ_{2s}, $\chi_{2p\sigma}$ and $\chi_{2p\pi}$ are the appropriate symmetry adapted linear combination (SALC) of ligand 2s, 2pσ and 2pπ orbitals, respectively. γS and $\gamma\sigma$ are the admixture parameters describing the σ covalency between dσ and the ligand 2s and 2pσ orbitals respectively, and $\gamma\pi$ measures the π covalency between dπ and 2pπ orbitals.

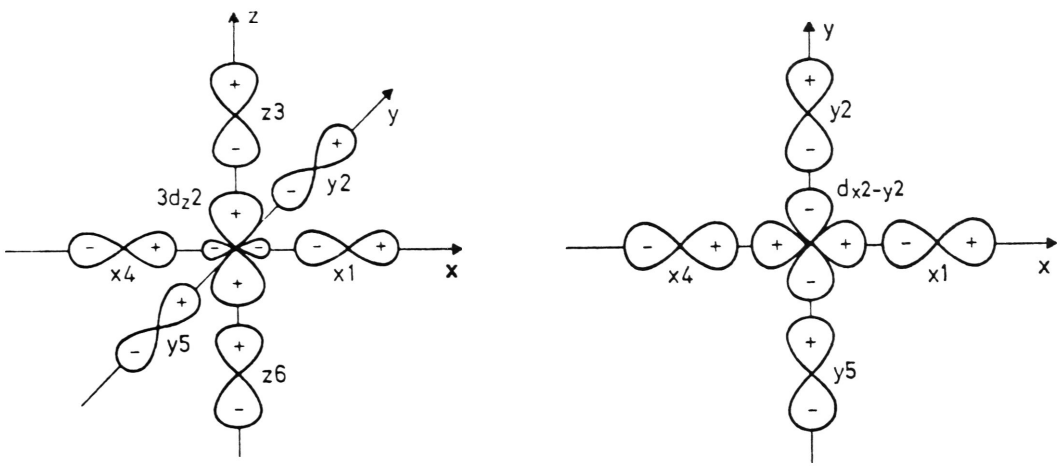

FIG. 1. Schematic overlap of $3dz^2$ and $3dx^2-y^2$ metal orbitals with $2p\sigma$ ligand orbitals.

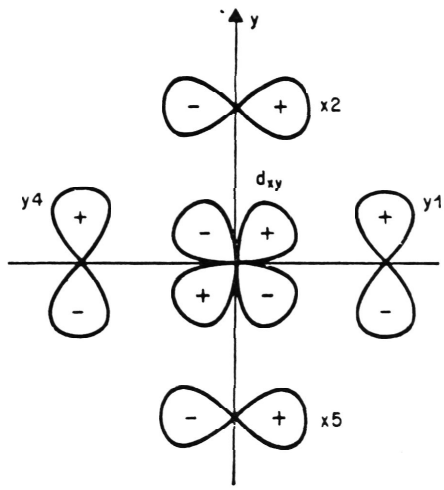

FIG. 2. Schematic overlap of <u>one</u> of the metal t_{2g} orbitals ($3d_{xy}$) with ligand $2_{p\pi}$ orbitals.

Because the bonding orbitals are filled in the complexes of interest they do not directly contribute to the magnetic properties of a complex; the magnetic interactions associated with transition metal ions mainly reflect the distribution of the unpaired electrons in the antibonding orbitals, which have mainly metal d character. Orthogonalized to the bonding orbitals, these may be written:

$$\psi_\sigma = N_\sigma\left(d_\sigma - \lambda_\sigma\chi_{2p\sigma} - \lambda_S\chi_{2s}\right) \qquad 2.4$$

$$\psi_\pi = N_\pi\left(d_\pi - \lambda_\pi\chi_{2p\pi}\right) \qquad 2.5$$

In full, (4) and (5) are:

$$\psi_{z^2} = N_\sigma\left[d_{z^2} - \frac{1}{\sqrt{12}}\lambda_\sigma\left(-2p_{z_3} + 2p_{z_6} + p_{x_1} - p_{x_4} + p_{y_2} - p_{y_5}\right) - \frac{1}{\sqrt{12}}\lambda_S\left(2s_3 + 2s_6 - s_1 - s_2 - s_4 - s_5\right)\right] \qquad 2.6$$

$$\psi_{x^2-y^2} = N_\sigma\left[d_{x^2-y^2} - \frac{1}{2}\lambda_\sigma\left(p_{x_4} - p_{x_1} + p_{y_2} - p_{y_5}\right) - \frac{1}{2}\lambda_S\left(s_1 + s_4 - s_2 - s_5\right)\right] \qquad 2.7$$

$$\psi_{xy} = N_\pi\left[d_{xy} - \frac{1}{2}\lambda_\pi\left(p_{y_1} - p_{y_4} + p_{x_2} - p_{x_5}\right)\right] \qquad 2.8$$

$$\psi_{xz} = N_\pi\left[d_{xz} - \frac{1}{2}\lambda_\pi\left(p_{z_2} - p_{z_5} + p_{y_3} - p_{y_6}\right)\right] \qquad 2.9$$

$$\psi_{yz} = N_\pi\left[d_{yz} - \frac{1}{2}\lambda_\pi\left(p_{x_3} - p_{x_6} - p_{z_1} - p_{z_4}\right)\right] \qquad 2.10$$

The normalization constants in equations 2.6 to 2.10 are defined by $\langle\psi|\psi\rangle = 1$ and

$$N_\sigma = \left(1 - 2\lambda_\sigma S_\sigma - 2\lambda_S S_S + \lambda_\sigma^2 + \lambda_S^2\right)^{-\frac{1}{2}} \qquad 2.11$$

$$N_\pi = \left(1 - 2\lambda_\pi S_\pi + \lambda_\pi^2\right)^{-\frac{1}{2}} \qquad 2.12$$

where the overlap integrals S are defined by $\langle d|\chi\rangle$ and

$$S_\sigma = 2\ \langle d_\sigma|p_{2p\sigma}\rangle\ , \quad S_S = 2\ \langle d_\sigma|s_{2s}\rangle$$

and $S_\pi = 2 \langle d_\pi | p_{2p\pi} \rangle$

Because of the orthogonality relations

$$\langle \psi_\sigma | \psi_\sigma^B \rangle = \langle \psi_\sigma | \psi_S^B \rangle = \langle \psi_\pi | \psi_\pi^B \rangle = 0$$

it follows that, to first order in λ, γ and S

$$\lambda_\sigma = \gamma_\sigma + S_\sigma$$
$$\lambda_S = \gamma_S + S_S$$
$$\lambda_\pi = \gamma_\pi + S_\pi \quad .$$

Thus, we see that experiments which measure λ are sensitive to a combination of the covalency admixture parameters γ and the overlap integrals.

Bonding also takes place between the ligand valence orbitals and the outer, initially unoccupied, 4s and 4p orbitals of the transition metal ion. Although it is generally thought that the metal 3d - ligand 2p bonding is the most significant covalent interaction in relatively ionic complexes, the 4s orbitals, being of larger radial extent, have a greater overlap with the ligand orbitals. For d^3 ions such as Cr^{3+} and Mn^{4+}, effects attributed to spin polarization of charge transferred to the empty e_g orbitals have been observed by spin resonance and neutron diffraction.

A schematic molecular orbital diagram is shown in Fig. 3 for bonding involving ligand 2s and 2p orbitals and metal 3d, 4s and 4p orbitals. The ligand field splitting Δ is shown and from the simple MO model this is given by

$$\Delta = (\lambda_\sigma^2 - \lambda_\pi^2)(E_d - E_{2_p}) + \lambda_S^2(E_d - E_{2_S}) \qquad 2.13$$

where Ed, E_{2_p} and E_{2_s} are the initial energies of the 3d, 2p and 2s orbitals.

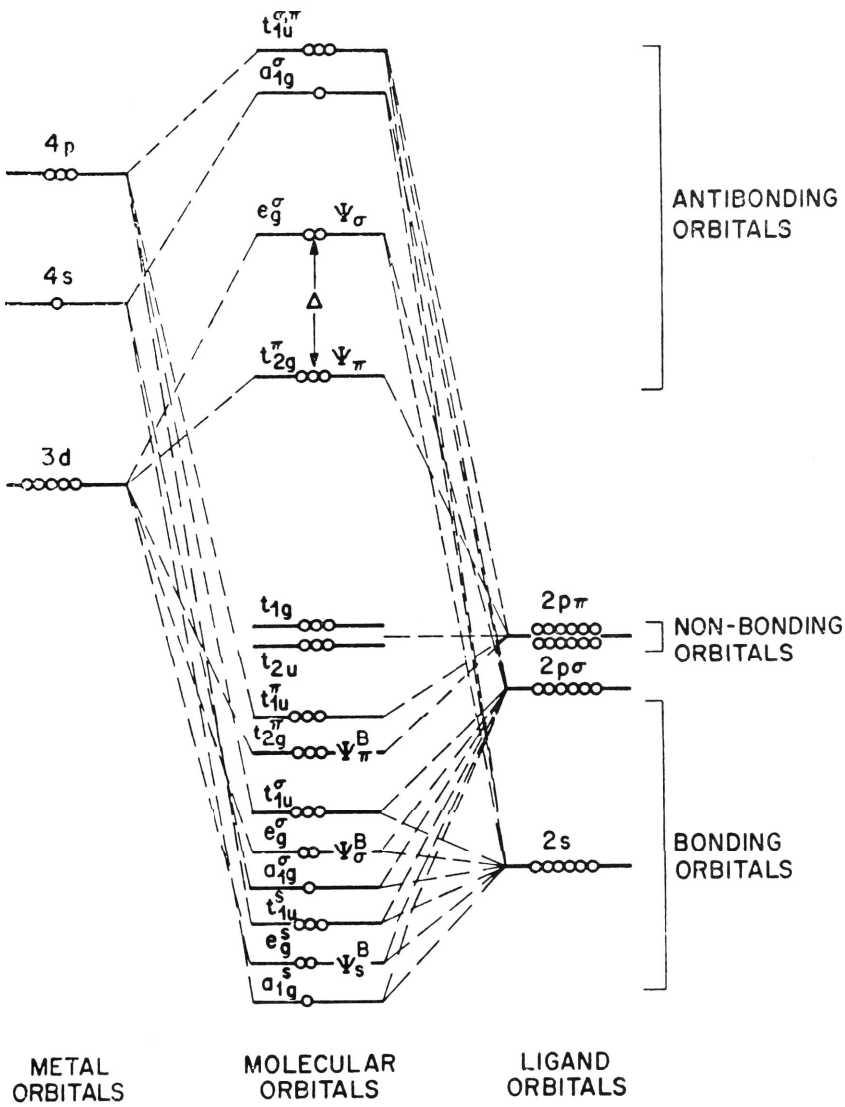

FIG. 3. Schematic molecular orbital diagram for bonding involving ligand 2s and 2p orbitals and metal 3d, 4s and 4p orbitals.

Types of Available Experimental Information

When classifying physical methods applied to inorganic chemistry, and, in particular transition metal chemistry, it is convenient to divide them into two groups. Firstly, techniques which give information about a single electronic state, normally the ground-state includes Nuclear Magnetic Resonance (NMR), Electron Spin Resonance (ESR), vibrational and Mössbauer spectroscopy. Secondly, energy differences between states are probed by electronic and photoelectron spectroscopy and magnetic optical activity.

2.2.0 Ground State Methods

2.2.1 The Measurement of Spin and Spin Distributions

2.2.1.1 Magnetic Resonance Techniques

Eaton[2], in his review has discussed magnetic resonance methods and their utility in the study of electronic structures of transition metal complexes. In paramagnetic complexes electron spin - nuclear spin interactions provide a detailed probe of electronic structure. Transitions involving a change in electron spin quantum number and those involving a change in nuclear spin quantum number are studied by ESR and NMR, respectively.

Electron Spin Resonance (ESR)

ESR spectroscopy permits the determination of the number and distribution of unpaired electrons and may also reveal the hyperfine structure of the metal atom energy levels. It allows precise determination of the lowest energy levels in paramagnetic transition metal ions and it may yield information on the symmetry properties of the ligands and on the character of the bonds between the transition metal and the ligands.

With good resolution it is possible to observe hyperfine splittings caused by interaction between electron spin and nuclear spin or even **superhyperfine** ("ligand" or "transferred" hyperfine) splittings due to interactions of the electron spin with nuclear spins on neighbouring atoms.

The phenomenon of electron spin resonance may be observed when molecules or ions containing one or more unpaired electrons are placed in a magnetic field. In a molecule containing a single unpaired electron in an S state the effect of the magnetic field is to lift the spin degeneracy, i.e. to make the energy of the electron different for its two M_s values $\pm\frac{1}{2}$.

Since the lower state is slightly more populated thermally, with radiation of frequency ν such that $h\nu = g\beta H$ there is a net absorption because stimulated absorptive transitions upward are more numerous than stimulated radiative transitions downward. By sweeping the frequency of an oscillator (in the microwave region) through the appropriate frequency range, ν is observed as the frequency of maximum absorption.

Nuclear Magnetic Resonance (NMR)

NMR spectroscopy reveals the electronic environment around those atomic nuclei which possess a magnetic moment and may furnish information on structure and symmetry. It is a well established method for identifying and studying the structure of molecules in the liquid state though unfortunately solids are in general characterized by broad resonance lines with little fine structure.

Multiple Nuclear Resonance (MNR)

In the usual NMR experiment the sample is irradiated with a single monochromatic radiofrequency and experiments involving simultaneous irradiation at two frequencies are know as double resonance techniques. Double resonance depends on the experimental observation that if two sets of different nuclei A and B are coupled by a spin - spin coupling constant J_{AB}, under the correct conditions, irradiation at the A frequency results in loss of spin - spin structure at the B resonance and similarly irradiation of B collapses the multiplet of A. In this way the values of the chemical shift can be read directly from the spectrum and the spectra of complicated molecules are simplified.

Electron Nuclear Double Resonance (ENDOR)

ENDOR is a combination of ESR and NMR that permits excellent resolution of the HFS or SHFS while retaining good sensitivity. The technique is to pump at a microwave frequency with sufficient power to saturate the population of the upper state. If this is done, there is no resonant absorption, since nearly as much energy is being emitted as absorbed. The populations within the two main energy levels responsible for the ESR transition can be altered by the additional application of r.f excitation. The r.f field produces NMR between the fine-structure levels, removing the saturation condition, and causing the ESR absorption to reappear.

In the ENDOR technique the NMR's of nuclei adjacent to a paramagnetic centre are scanned, giving a spectrum which depends on the local fields created by the paramagnetic ion.

In this way it is possible to identify the position of each of the surrounding nuclei with nonzero nuclear magnetic moments, providing a detailed map of the environment of the paramagnetic centre.

Magnetic Resonance Studies of Crystals

Magnetic resonance studies of transition metal ions have been a productive technique in the study of electron distributions and covalency in solids. g values and metal hyperfine interactions are both affected by covalency, but almost all quantitative information has been obtained by study of ligand hyperfine interactions (LHFI). These may be observed both by NMR of ligand nuclei in undiluted paramagnets and by ESR of magnetic ions at dilute concentration in diamagnetic host crystals.

In an isolated paramagnetic complex, such as is studied in the measurement of LHFI by paramagnetic resonance the LHFI measures the spin density transferred to the ligands. For such experiments, it is customary to refer to the fraction of unpaired spin (f) transferred to a single ligand orbital when the metal d orbitals of the appropriate symmetry are singly occupied. For two e_g α electrons (e.g. d^5 high spin) spin density $2\lambda_\sigma^2$ and $2\lambda_s^2$ is transferred to six p_σ and six 2s orbitals respectively. For three t_{2g} electrons (e.g. d^3, d^5 high spin) spin density $3\lambda_\pi^2$ is transferred to 12 p_π orbitals. Therefore[3]

$$f_\sigma = \frac{1}{3}\lambda_\sigma^2 , \quad f_s = \frac{1}{3}\lambda_\sigma^2 , \quad f_\pi = \frac{1}{4}\lambda_\pi^2$$

In general, imprecise knowledge of the relaxed metal-ligand distance of a complex provides considerable uncertainty in the reduction of ESR data for magnetic ions doped into host crystals. So the ESR f values have significant errors. However, the ENDOR results for Cr^{3+} and Fe^{3+} doped into MgO closely parallel the covalency parameters determined from NMR and ESR studies in fluoride hosts[3].

Tofield[3] has also suggested that the ENDOR technique may provide LHFI parameters for second and third nearest neighbour ions.

Further ESR studies of first row transition metal ions in halide crystals have been reported. Sootha[4] has studied ESR absorption of a series of first row transition metal ions in sodium and potassium fluoride crystals. Shields[5] in a similar study has determined covalency parameters from his measurements. The ENDOR technique has been applied[6] to the study of V^{3+} and Ti^{2+} doped into Cd F_2, Sr F_2 and Ca F_2 but no other ions were studied.

2.2.1.2 Magnetic Neutron Diffraction

Neutrons (unlike X-rays) are magnetically scattered, and in systems with unpaired electrons, the magnetic scattering intensity is superimposed on the nuclear scattering. The latter, being effectively scattering by point charges, has a form factor which is constant with scattering angle, in contrast to neutron scattering by the electric charge distribution[3].

The magnetic electrons in systems containing transition metal ions are associated with outer electron orbitals, and consequently magnetic neutron scattering shows a strong angular dependence, defined by the magnetic form factor $f(Q) = \int e^{iQr} D(r)\, dr$, where Q is the scattering vector (magnitude $4\pi \sin \theta/\lambda$) and D(r) is the magnetic moment density normalized so that $f(Q) = 1$ at $Q = 0$.

The most complete information on magnetic systems may be obtained by polarized neutron experiments on single crystals whereby the complete spin distribution may be mapped out in 3-dimensions. The recent study[7] of the Cr^{3+} form factor in K_2NaCrF_6 is an impressive demonstration of the technique.

Fourier transformation of the form factor data directly reveals the shape of the t_{2g} orbitals and shows spin density covalently transferred to the fluorines.

This experiment was carried out at 4.2°K together with an accurate structure analysis to provide the set of nuclear structure factors. The spin density covalently transferred to the fluorines is not exactly centred on the F^- sites because the antibonding nature of the wavefunctions with unpaired spin gives rise to the negative overlap region between the metal and ligand ions which pushes out the maximum of the ligand spin density. Because of the finite resolution of the map the nodes along the x and y axes of the chromium were washed out and the shape of the spin density distribution on the fluorines could not be precisely seen. The majority spin density appears to be associated with the p_π orbital, however. This experiment demonstrates the shape of the $d^3\ t_{2g}$ magnetic electron distribution.

2.2.2 Mössbauer Spectroscopy

This technique has been used to great advantage in the determination of chemical structure but, unfortunately, the effect is only observed with very few nuclei. It complements the other hyperfine interaction spectroscopies in several ways. The technique observes the changes in two nuclear energy levels within the nucleus as a function of chemical environment, while techniques such as ESR and NMR refer to the nuclear ground state.

The Mössbauer technique, in contrast to NMR is primarily used in the solid state. The broadening of NMR spectra caused by solid state interaction is absent in Mössbauer spectroscopy because recoilless emission demands no solid state (phonon) interaction.

The Mössbauer effect permits direct measurement of electron density and changes in electron density at the nucleus of the central atom.

Several recent applications of the Mössbauer effect to the study of electronic structures have been reported. The interaction of the nuclear quadrupole moment and the electric field gradient at the nucleus in various Fe^{3+} components at very high pressure[8] provides an effective means of studying perturbations in electronic distributions. It was found that quadrupole splitting increased with increasing pressure. In a second application, in combination with X-ray emission K_α shifts, the effective electronic configuration of Fe in K_3FeF_6 and $K_3Fe(CN)_6$ were determined[9].

The Mössbauer study[10] of the spin-flop transition in $Fe^{2+}:MnF_2$ at 4.2°K and subsequent measurements of the hyperfine interaction were in good agreement with theory. The compounds NH_4MnCl_3, NH_4FeCl_3 and NH_4CoCl_3 have also been studied[11].

2.2.3 Vibrational Spectroscopy

Vibrational spectra reveal the vibrations of a molecule, the character of the bonds between its atoms, the force constants and bonding strengths. It may also give information regarding the structure and symmetry in a complex.

Vibration spectroscopy finds its most common application in the analysis of vibronic transitions which will be discussed later under electronic absorption spectra. However, two recent articles studying the low frequency vibrations of inorganic complex salts are notable exceptions. Nakagawa[12] has examined the metal-ligand and complex ion-outer ion interactions of some $FeCl_6^{3-}$ complexes utilizing Infra-Red and Raman spectroscopy.

In the second report Flint et al[13] have further investigated compounds of the form A_2MF_6 in an effort to explain various resonances in the Raman spectrum of these complexes.

2.3.0 Excited State Methods

2.3.1 Electronic Absorption Spectra

The electronic spectra of octahedral hexahalide complexes of transition metal ions have been of interest for many years. The interpretation of these spectra has provided much of the impetus for the development of ligand field theory and for the application of MO theory to extremely complex systems. These theories provide the framework for understanding bonding and assigning transitions in these complexes.

It is necessary to have a general feeling for the nature of the experimental data that are available. A great number of studies have been made at room temperature but these do not provide the sort of information that is most useful to interpretation of the spectra. Under such conditions only broad band absorptions are observed; details of the individual vibronic transitions which comprise the band are completely obscured. Only at low temperature is vibronic structure resolved. The importance of this vibronic data cannot be overemphasised.

Two excellent discussions of the vibronic spectra of coordination compounds, particularly cubic complexes have been given by Flint[14] and Kettle and Kahn[15].

In the electronic absorption spectra of, for instance, transition metal hexafluoro complexes bands corresponding basically to two kinds of electronic transitions may be detected: (1) d-d bands (2) charge-transfer bands.

In the case of a d-d transition the electron is transferred by excitation from one largely "metal d orbital" to another, whilst charge-transfer bands may arise from the transition of an electron from a ligand π orbital to an unfilled orbital of high metal character.

In general, in the electronic spectra of transition metal complexes, the charge-transfer bands are found in the UV spectral region, while the much less intense bands due to d-d transitions appear in the visible region. If the energy of the C.T. transition is small, the charge-transfer band may move into the visible spectrum, as in MnO_4^- and, owing to its higher extinction coefficient, it may obscure the d-d band.

The four types of transition that would be expected are indicated in Fig. 4. Actually each of the transitions shown is a group of transitions, since the excited orbital configuration gives rise to several different states of similar but not identical energies.

Most solid state electronic spectra of transition metal complexes reported is relectance data which only provides quantitative information on band position. Several excellent reviews have reported the diffuse reflectance spectra of the octahedral transition metal complexes[16-19]. The data reported for the charge-transfer bands in MF_6^{n-} species of the 3d series is presented in Table (1).

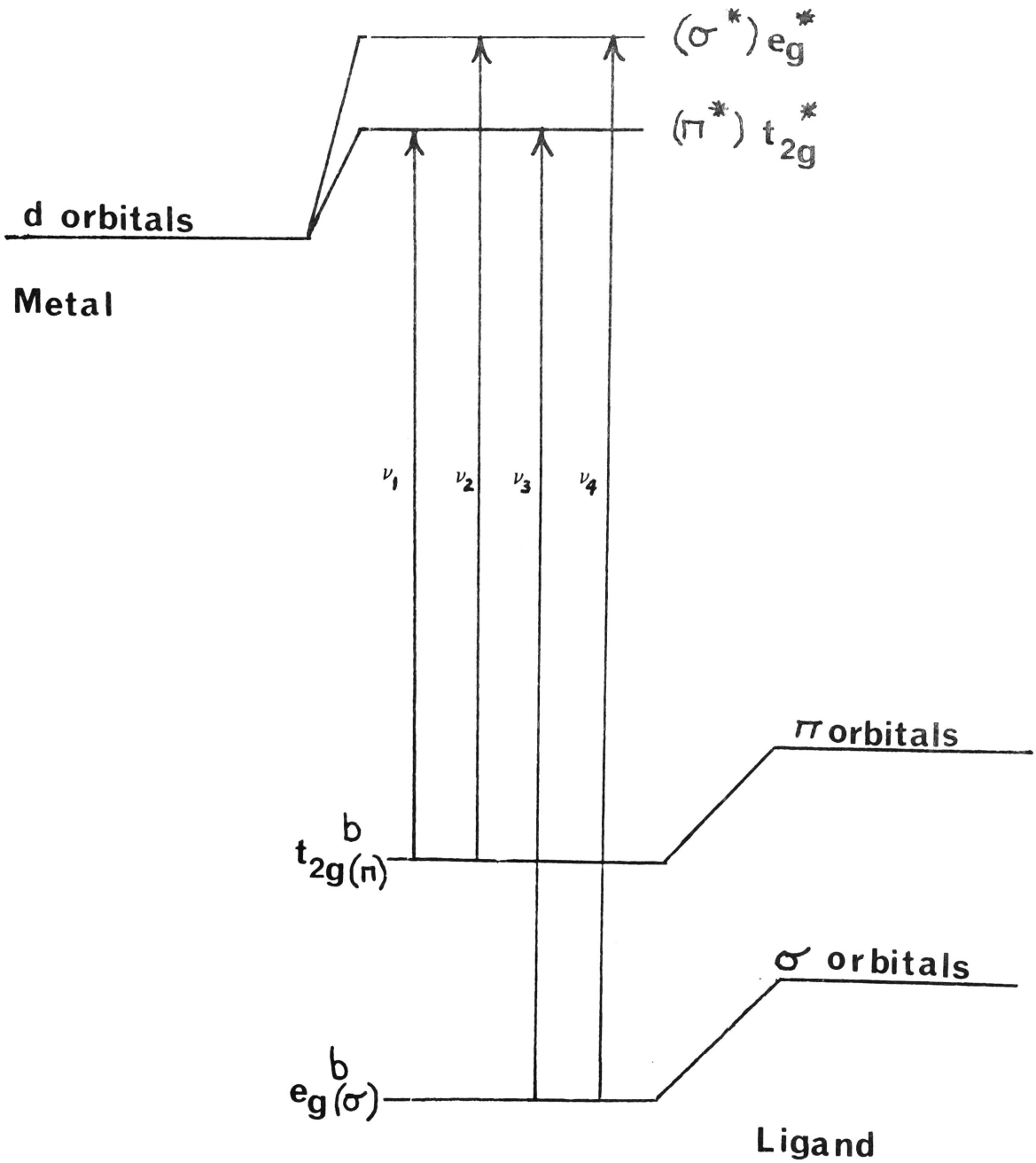

FIG. 4. Partial MO diagram for an octahedral MX_6 complex showing the four main classes of Ligand to Metal Charge-Transfer Transition.

Table 1 : Charge Transfer Bands of MF_6^{n-} Complexes

	Transition	Position (kK)
MF_6^{3-} Anions		
Ti	$\pi \longrightarrow t_{2g}$	48
V	$\pi \longrightarrow t_{2g}$	43
Cr	$\pi \longrightarrow t_{2g}$	55 - 60
Mn	$\pi \longrightarrow t_{2g}$	50 - 55
Fe	$\pi \longrightarrow t_{2g}$	49
Co	$\pi \longrightarrow t_{2g}$	41
Ni	$\pi \longrightarrow e_g$	32
Cu	$\pi \longrightarrow e_g$	30
MF_6^{2-} Anions		
V	$\pi \longrightarrow t_{2g}$	34
Cr	$\pi \longrightarrow t_{2g}$	30
Mn	$\pi \longrightarrow t_{2g}$	39
Co	$\pi \longrightarrow t_{2g}$	28
Ni	$\pi \longrightarrow e_g$	31

2.3.1.1 Low Temperature Crystal Spectra

Spectral assignment is greatly simplified by low temperature studies of both isomorphous single crystals of transition metal complexes and the complementary technique of "doping" the complex into a host crystal. This area of chemistry research is most active; the assignments of the electronic bands of transition metal complexes being complementary to the development of MO schemes for inorganic systems.

The 3d series tetroxyanions and hexafluoroanions have been most widely studied using these techniques but for a more exhaustive coverage the reader is directed to Reference 20.

Tetroxyanions

Tetroxo-ions, particularly the permanganate ion, have played a central part, as model compounds, in the development of approximate molecular orbital schemes for inorganic molecules and thus their electronic spectra have frequently been examined.

By analyzing the site group splittings when d° ions CrO_4^{2-} and MnO_4^- are doped into orthorhombic hosts K_2SO_4 and $KClO_4$ Ballhausen[21,22] and his co-workers and Butowiez[23] have identified the lowest energy absorption. Butowiez[24] has also given positive identifications of weak bands first reported by Teltow[25] in pure crystals of $K_2Cr_2O_7$ and K_2CrO_4.

The d' tetroxo-ions MnO_4^{2-} and CrO_4^{3-} have been investigated by Kosky and Holt[26] and Day and his co-workers[27] but there is still much controversy concerning the assignments. Systems studied were MnO_4^{2-} doped into $BaSO_4$ and K_2SO_4. Another paper by Holt and co-workers[28] has studied CrO_4^{3-} in Ca_2PO_4Cl where the site symmetry is lowered to D_{2d}.

The intensity of the $^1A_1 \longrightarrow {}^1T_2$ ($t_1 \longrightarrow e$) transition in CrO_4^{2-} has been calculated in both dipole length and velocity transition moment approximations as functions of the metal-ligand mixing coefficients. The velocity moment gives better results.

Further efforts to assign the charge transfer spectrum of the MnO_4^- ion have been made by McGlynn and his co-workers[29-31]. Their studies have included the electronic spectroscopy of MnO_4^- doped $Li(ClO_4)\ 3H_2O$ and $Ba(ClO_4)\ .3H_2O$ hosts using polarized light at liquid He temperature and the study of a weak near ir also in the same lattices. Butowiez[32] has also studied these weak bands at low temperature.

Further work on the assignment of the MnO_4^- spectrum is reported by Ballhausen and co-workers[33], while the low temperature spectrum of MnO_4^- has been measured[34] in a new host lattice, KBr where the ion substitutes for a Br^-.

The spectrum of MnO_4^{2-} has been re-investigated by Day et al[35] who used K_2SO_4 as host lattice and Holt et al[36] who used $BaSO_4$. Both agree that the weak band with extensive vibrational structure in the near infra red is the $^2E \longrightarrow {}^2T_2$ ligand field transition, thus defining Δ for the ion. For example, in K_2SO_4 the average frequency of the three components split by the C_s site perturbation is 11177 cm^{-1} with a total site splitting of 667 cm^{-1}. In $BaSO_4$ the site group is C_{2v}. The two studies also agree that the tetrahedral parentage of the first charge transfer band, near 18000 cm^{-1}, is $^2T_2$. If by analogy with MnO_4^-, this state arises from transferring an electron from the non-bonding t_1 to the partly occupied 2e orbital, the fact that it lies below $^2T_1$ which also comes from the same configuration, can be rationalized by examining the effect of electron repulsion using a simplified model which only takes into account one centre metal (d-d) contributions. In this way the sequence of the first four charge-transfer transitions ($^2T_2 < {}^2T_2 < {}^2T_1 < {}^2T_2$ from site group splittings) are accounted for.

In alkali halide hosts the first charge-transfer transition of CrO_4^{2-} exhibits a progression in the totally symmetric stretching node of the ion[37]. In the same hosts, $Cr_2O_7^{2-}$ has two bands with well resolved fine structure at 77°K. The first at 360 nm, was assigned[38] as $t_1 \longrightarrow 2e$ and the second, at 250 nm, as $t_1 \longrightarrow 3t_2$.

As already mentioned CrO_4^{2-} in K_2SO_4 has two broad bands covering the regions 330 - 375 nm and 230 - 265 nm, both of which exhibit vibrational fine structure at low temperatures.

In a re-examination of this spectrum[39,40] it has been suggested that one of the two sets of vibrational intervals attached to the lowest energy transition should be assigned to transitions from an excited vibrational level of the ground state, instead of a single quantum of the upper state $e(v_2)$ bending mode, attached to each member of the main $a_1(v_1)$ progression.

$CsCrO_3Br$ has been prepared and characterized and its charge transfer spectrum resembles those of CrO_3Cl^- and CrO_3F^-.[41]

The trinegative chromium manganese tetraoxo ions are difficult to stabilize in host lattices but Holt and co-workers[42] have investigated phosphate and vanadate lattices and have assigned the 4°K polarized spectrum.

Extensive study has been made of MnX_4^{2-} and NiX_4^{2-} salts where X = Cl or Br by Ballhausen's group[43] and Smith and his colleagues[44,45] respectively.

A further contribution from Day and co-workers[46] has examined the crystal lattice effects on the electronic spectrum of MnO_4^{2-}. Another technique which aids assignment of bands is to replace one of the ligands of a complex ion with another and observe the consequent changes in the spectrum. Day et al[47] report the use of this method in the study of mono-substituted oxo ions using low temperature polarized absorption spectra and magnetic circular dichroism (MCD).

Hexafluoroanions

The crystal K_2NaGaF_6 is of interest because in it the Cr^{3+} ion occupies a site with full cubic symmetry. The crystal field and electron repulsion parameters are such that in this lattice the ^2E_g and $^2T_{2g}$ states are quite close to the $^4T_{2g}$ and are heavily mixed with it

by spin orbit coupling. At 4°K the absorption and fluorescence profiles for $^4A_{2g} \longrightarrow {}^4T_{2g}$ yield well resolved vibrational progressions, the major frequency being one of 556 cm^{-1}. In the spectrum of this region[48] the origin of ^2E_g is at 15045 cm^{-1}, whilst both $^2T_{1g}$ and $^4T_{2g}$ are above 16000 cm^{-1}.

It has been known for some time that the $3d^3$ ion $[MnF_6^{2-}]$ has an elaborate sharpline spectrum, parts of which have now been definitely assigned[49] using Cs_2GeF_6 and K_2GeF_6, in which the site symmetries are respectively O_h and D_{3d}, as host lattices. Transitions gain electric dipole intensity by vibronic coupling with all three of the odd parity intramolecular modes of the octahedral complex, and many also appear in combination with the totally symmetric modes. The $^4A_{2g} \longrightarrow {}^2E_g$ and $^2T_{1g}$ transitions can be assigned quite unambiguously, but for $^4T_{2g}$ it is necessary to assume that the spin-orbit coupling factor is reduced about tenfold. In contrast to the MnF_6^{2-} ion, the spectrum of $MnCl_6^{2-}$ contains only broad transitions, and unfortunately the complex disproportionates[50].

The vibronic structure of the $^1A_{1g} \longrightarrow {}^1T_{1g}$ transitions of NiF_6^{2-} seems to consist of an a_{1g} progression built on a t_{1u} vibration[51] rather than arising from an upper state J-T distortion as previously suggested by Reisfield et al[52].

Diffuse reflectance spectra of the Mn^{IV} salts of M_2MnF_6 (M = K,Rb,Co) and $BaMnF_6$ show vibrational fine structure on the lowest d-d band[53].

The spectrum of MnF_6^{2-} studied on a sample of high purity Cs_2MnF_6 contains both vibrational and spin-orbit fine structure[54].

The vibronic structure of the $^2E_g \longrightarrow {}^4A_{2g}$ emission in d^3 ions indicates[55] that a 2nd order JTE is operative in the ^2E_g states. The spectra of Cs_2MnF_6 and $K_2NaGaF_6:Cr^{3+}$ have different vibronic structures, though in both cases the d^3 ion is in a perfectly octahedral environment.

2.3.2 Luminescence Spectra of Transition Metal Complexes

One of the most important reasons for studying luminescence is to obtain information about processes which de-activate excited states, other than the radiative one. Hence it is the main method of measuring rates of radiationless transitions, energy transfer processes and photochemical reactions.

Schlafer et al[56] point out that Cr^{3+} in octahedral microsymmetry could give rise to two types of emission depending upon the field strength of the ligands coordinated to it. In most cases a narrow band phosphorescence, due to the transition $^2E_g \longrightarrow {}^4A_{2g}$ is seen. Little Stokes loss is apparent between the maxima in emission and absorption as the strong field configurations of the ground and excited states are identical, being t^3_{2g}. However if the field strength of the ligands is low, a broad banded fluorescence may be detected which is due to the transition $^4T_{2g} \longrightarrow {}^4A_{2g}$. The Stokes shift of this band from the equivalent absorption band is always large.

Below 20°K, K_3CrF_6 shows both the sharp phosphorescence spectrum and the broad fluorescence band[57]. However, above 20°K only the fluorescence band is detectable. It is concluded that the local site symmetry of the Cr^{3+} ion is octahedral since the $^2E \longrightarrow {}^4A_2$ transition is not split. The vibronic side bands of both this transition and the $^4T_2 \longrightarrow {}^4A_2$ fluorescence are compared with IR and Raman data.

The positions of the zero phonon lines of both transitions could be derived and the temperature dependence of the quantum yield of fluorescence to phosphorescence was studied.

Manganese (IV) is a well known activator of phosphors. Early work[58] on this ion doped into magnesium germanate assigned the luminescence to the $^4T_{2g} \longrightarrow {}^4A_{2g}$ fluorescence, even though the large crystal field splitting expected from a quadrivalent ion is likely to push the quartet excited states well above the doublets. More recently a number of studies of the MnF_6^{2-} ion have identified unambiguously the $^2E \longrightarrow {}^4A_2$ phosphorescence.

Flint[59] has studied the pure solid Cs_2MnF_6 in which the Mn^{4+} site is perfectly O_h. An extremely intense $^2E_g \longrightarrow {}^4A_{2g}$ phosphorescence is observed even at room temperature, which becomes remarkably sharp at 80°K. By comparison with the reflectance spectrum the zero phonon line is identified at 16031 cm^{-1}. This is very weak compared with the three intense false origins due to the 3 modes $v_3(t_{1u}$ stretch), v_4 (t_{1u} bend) and $v_6(t_{2u})$. These odd fundamental vibrations carry more than 95% of the intensity of the transition. A progression in v_2, an e_g mode, is also seen. This progression carries more intensity than in a_{1g}. This indicates that there is more difference between the PE surfaces of the ^2E and $^4A_{2g}$ states along this coordinate than along the totally symmetric coordinate. At 80°K a broad featureless emission at ~ 13000 cm^{-1} was detected, which was absent at room temperature. This was assigned to the fluorescent transition $^4T_{2g} \longrightarrow {}^4A_{2g}$. Since the maximum in absorption of this transition lies at 21600 cm^{-1} a huge Stokes shift must occur.

Reisfield et al as well as investigating the low temperature absorption spectrum[54] reported their luminescence study, although their spectrum is not as detailed as Flint's[59]. The $^4A_{2g} \longrightarrow {}^4T_{2g}$ was well resolved and three progressions in the a_{1g} mode, equal to 500 ± 15 cm^{-1}, based upon the spin-orbit components of τ_6, τ_8 and $\tau_{7.8}$ were identified. However Pfeil's emission spectrum[60] allowed him to identify the $v_2(e_g)$ mode in this band, which he took as evidence for a Jahn-Teller distortion in the $^4T_{2g}$ state. This led to an explanation, proposed by Flint[55] for the presence of an e_g mode both in the phosphorescence, $^2E \longrightarrow {}^4A_2$, of Cs_2MnF_6 and in Cr^{3+} - K_2NaGaF_6. It was pointed out that second order spin-orbit coupling mixes the τ_8 component of $^4T_{2g}$ with $\tau_8(^2E_g)$, the mixing being inversely proportional to the energy separation of the two components. In Cs_2MnF_6 the separation is 6000 cm^{-1} whereas in Cr^{3+}/K_2NaGaF_6 it is only ~ 800 cm^{-1}. Hence the mixing is strong in the latter case and leads to a similar distortion of the potential surface of the $\tau_8(E_g)$ state, so that a progression in the e_g mode is seen. The e_g modes are much less intense in the case of Cs_2MnF_6.

The emission of MnF_6^{2-} doped into lattices Cs_2GeF_6 and K_2GeF_6 has also been reported[49]. The $^2E \longrightarrow {}^4A_{2g}$ phosphorescence was measured at 4.2°K. In Cs_2GeF_6 the 0-0 line is identified at 16040.7 cm^{-1} and again intensity is built upon three false origins due to $v_6(t_{2u})$ at 222 cm^{-1}, $v_4(t_{1u})$ at 334 cm^{-1} and $v_3(t_{1u})$ at 602 cm^{-1}. In K_2GeF_6 the lower site symmetry splits the ^2E_g state into a pair of Kramers doublets. Both emission and absorption spectra at 77°K show two magnetic dipole 0-0 lines at 16070 and 16081 cm^{-1}. At 4.2°K only the lower energy line is seen in emission, but is doubled with a separation of 0.7 cm^{-1}. This separation agrees with the ESR data which show a zero field splitting of 0.75 cm^{-1} in MnF_6^{2-} doped into this host.

The g values of the ground state and the Zeeman splitting of the ^2E_g state all depend upon second order spin-orbit interaction with the $^4T_{2g}$ state. These authors conclude that there is little if any effect of Jahn-Teller distortion in the $^4T_{2g}$ state upon the magnitude of the spin-orbit coupling constant which might be expected.

The emission of MnF_6^{2-} in two other hosts K_2SiF_6 and K_2TiF_6 has been measured by Paulusz[61]. The quenching temperature of the $^2E_g \longrightarrow {}^4A_{2g}$ emission is ~490°K. However no fluorescence from $^4T_{2g}$ is found even at 890°K.

Flint and co-workers have provided two further studies of the MnF_6^{2-} ion. Their study[62] of excitation and luminescence spectra of K_2MnF_6 prepared by different methods shows that the intense emission observed at low temperatures between 14700 and 13500 cm^{-1} is caused by an impurity. Further work[13] on Cs_2MnF_6 and Mn^{4+} in various cubic crystals has attempted to assign the weak bands of the luminescence spectra which are due to low frequency vibrations and are not assignable using the unit cell model. Their comparison of these spectra with infra red and Raman spectra and with a model for the lattice dynamics has suggested *probable* assignments for the vibrational and luminescence spectra.

2.3.3 Magnetic Circular Dichroism

Another useful spectrophotometric technique for assigning the symmetries and orbital configurations of excited states of transition metal complexes is based on the phenomenon of magnetic circular dichroism (MCD), where, in a magnetic field all molecules become optically active.

The magnitude of this induced optical activity depends on three factors; the magnetic moment of the ground state, the magnetic moment of the excited state, and the amount of magnetically induced mixing of ground and excited states with non-zero magnetic moments. It is this last contribution which ensures that all molecules are optically active in a magnetic field.

Two phenomena occur when light interacts with matter in a magnetic field, the first being the rotation of plane polarized light and the second being a difference in absorptivity between left and right circularly polarized light. These two effects are respectively, Magnetic Optical Rotatory Dispersion (MORD) and Magnetic Circular Dichroism (MCD).

The MCD effect is the one of primary interest here and arises from the fact, that, in an external magnetic field the absorption of left circularly polarized light is not equal to the absorption of right circularly polarized light[63]. An excellent review, outlining details of the theory and experimental methods used in MCD experiments, has been made by Stephens[64] and some relevant aspects will be presented.

The wavelength where a given maximum or minimum in an MORD or MCD curve depends only on the material in the sample cell but the absolute magnitude of the Faraday Effect is proportional to the total amount of material in the light path and the magnetic field strength. The magnitude of the Faraday Effect is small compared to natural optical activity as very few compounds will yield more than 0.5° rotation in a 10 kG field where the absorbance of the sample is one or less. The difference in absorbance of left and right circularly polarized light is seldom as great as 0.1 whilst most instruments are accurate to 10^{-6} absorbance and use magnetic fields of about 40 to 100 kG.

The MCD band has a shape similar to the absorption band, with MCD going to zero at wavelengths not far from the centre of the band. One useful feature of the Faraday Effect is that rotation and dichroism are proportional to the total length of sample traversed by the light, even when a reflection has occurred during traversal. Since reflection back through the sample cell cancels rotation and dichroism arising from natural optical activity and doubles rotation and dichroism that are magnetically induced an instrumental method is thus provided for separating the natural from the magnetically induced effects.

The emission analogue of MCD referred to, as magnetic circularly polarized emission (MCPE) results from the differential longitudinal emission of left and right circularly polarized ratiation arising from an excited sample in a magnetic field. In MCD, transitions originate in thermally equilibrated ground states and terminate in Franck-Condon excited states which are not in thermal equilibrum. In MCPE, transitions generally originate from relaxed or partially relaxed electronic excited states and terminate in an unrelaxed electronic ground state. MCD and MCPE therefore generally probe different sets of spectroscopic states even though the electronic parentage of these states may be the same. Additional differences in MCD and MCPE spectra can arise due to non zero Boltzmann populations (lack of thermal equilibration) within the manifold of emitting states.

A preliminary report[65] of both MCD and MCPE of crystalline $Cs_2GeF_6:Mn^{4+}$ has studied the $^4A_{2g} \longrightarrow {}^2E_g$ emission and absorption with analysis of the 0-0 (including MCD) and the 0-1 (t_{2u}) vibronic components.

The MCD spectrum of MnO_4^- in $Ba(ClO_4)_2.2H_2O$ has been measured in the region of the first allowed band and in the weak near-infra red band[66]. The hypothesis that the weak band corresponds to the ^1E component of the $^1T_1$ (t_1^5e) tetrahedral-field transitions is tested by assuming that the trigonal field perturbation is responsible for the mixing with ^1E from the allowed $^1T_2$ state. In such a case B terms of opposite sign are calculated for the $^1T_2$ and $^1T_1$ regions. The magnitude can be related to the known trigonal field parameter and is in excellent agreement with observation.

Further studies, not directly related to the present work are given in Stephen's review[64].

2.3.4 Photoelectron Spectroscopy (PES)

This technique involves the measurement of the kinetic energy of electrons which have been ejected from a molecule by monochromatic UV or X-Ray Radiation. The former source provides good resolution, after allowing vibrational structure to be resolved. However, to avoid significant charging effects on electronic levels in solids gaseous samples are required and hence its application in transition metal chemistry is restricted. Solid state PES are obtained with soft X-rays of $\lambda \sim 10°A$ and ionization energies up to about 1400 eV can be measured with a resolution of leV.

X-Ray Photoelectron Spectroscopy (XPS) has proved to be a very powerful tool for the study of molecular bonding. In this method the binding energies of core electrons E_B are determined by means of the well-known photoelectric effect.

$$E_B = h_\nu - E_e$$

h_ν is energy of incident radiation ($Al_{k\alpha}Mg_{k\alpha}$) and

E_e is the measured KE of the photoelectron.

The inner shell or core orbitals are basically in atomic type orbitals and their binding energies are characteristic of the atoms. However, slight changes occur for the inner shell binding energies that are dependent on the nature of the chemical environment. These changes in the core level binding energies, or chemical shifts, are due to alterations in the electron density of the valence shell: A more highly oxidized species gives rise to a higher binding energy, while a more reduced species shows the opposite effect[64].

When core electrons are ejected from compounds they come from orbitals which are primarily atomic in nature. However, these electrons do reflect their chemical environment. For an atom in a more oxidized state, the ejected electron exhibits a lower binding energy. These changes in binding energy for a given orbital or a given atom in different environments are the observed photoelectron chemical shifts.

Chemical shift measurements have been made on numerous occasions and the following equation has been used to describe them[67]

$$\Delta E_B = k\,\Delta q_N + \Delta V$$

where ΔE_B is the change in binding energy based upon a comparison to some reference compound, k is a constant approximately equal to e^2/r (r = atomic radius), Δq_N is the change in calculated atomic charge, and ΔV is the change in crystal potential.

Fadley et al[68] and more recently Clark and Adams[69] have shown that the photoelectron spectra of transition metal compounds can yield additional information on bonding from the examination of multiplet splitting. The appearance of these splittings in the photoelectron spectra is due to the interaction of electrons in the partially filled

inner orbital, produced by photon bombardment, with electrons in a partially filled valence shell.

The binding energy of an electron (E_b) within a molecule is defined as the negative of the work required to move the electron from its orbital to a position of rest an infinite distance from the molecule. Since the electron in this final state has no kinetic or potential energy E_b is equal to the difference in the energies of the initial and final states of the species:

$$E_b = E_i - E_f$$

where E_i and E_f are the total electronic energies of the initial and final states, respectively.

Koopman's Theorem[70] assumes that the same orbitals can be used to describe both states of the species. Within the applicability of this theorem a direct comparison can be made between the binding energies measured by XPS and the one electron eigenvalues calculated by theory.

The chemical shifts, relative to the free atoms, of the iron 3p orbital in K_3FeF_6 is reported as 57.7 eV[71] while shifts in the chromium 3p orbital in $K_2Cr_2O_7$ and $Na_2CrO_4.4H_2O$ are given as 48.7 and 47.9 eV, respectively[72].

The fluorine 1s orbital[73] and the chromium 2p orbital[74] have been studied in $(NH_4)_3CrF_6$ and K_3CrF_6, respectively.

Ejection of a core electron from a given orbital in a molecule or atom having a closed shell configuration normally will result in only one final state. However, if there are unpaired valence electrons, more than one final state can occur upon creation of an inner shell vacancy, because the exchange interaction will affect the α and β core electrons differently.

If the ejected electron is from a core s level of a paramagnetic ion, two final states will occur. The lower energy state will be the one having the spin of the remaining electron parallel to the unpaired valence electrons. However, the number of final states is much larger if the vacancy is created in an orbital of higher angular momentum. In addition, the exchange interaction causes the greatest energy separation to occur when both unfilled shells have the same principal quantum number.

Several studies of the valence region PES of the 3d tetroxyanions have been made[75-78] in an effort to unambiguously interpret the electronic transitions of these complexes in terms of a one electron orbital scheme. Fortunately the results are in good agreement with each other. The highest energy line at 22 eV seems to be due to ionization from the a_1 and t_2 orbitals of predominantly O character and the line at 6.6 eV is due to ionization from the a_1, e, t_1, t_2 and t_2 orbitals with O 2p and partly 3d character. The total spread of energy of the fine low energy orbitals is 4 eV.

Discussion of these results with the theoretical calculations will be made later.

References : Chapter 2

1. J. Owen, J.H.M. Thornley. Rept. Progr. Phys., 29, 675 (1966).

2. D.R. Eaton, Coord. Chem. Revs., 7, 2, (1971).

3. B.C. Tofield, Progress in Inorganic Chemistry, Vol. 20 (1976) John Wiley Ed. S.J. Lippard.

4. G.D. Sootha, Phys. Stat. Sol. A 5, 293, (1971).

5. L. Shields, Journal Chem. Soc. A 8, 1048, (1971).

6. Yu. F. Mitrofanov, Yu. E. Pol'skii, M.L. Falin, Spektrosk. Krist. Mater. Simp. Spektrosk. Krist., Aktiv. Ionamic Redkozemel Perckodnykh Metal 3rd 1970. Publ. 1973 Ed P.P. Feocilov, 313.

7. F.A. Wedgwood, Proc. R. Soc. Lond. A. 349, 447 (1976).

8. H.G. Drickamer, C.W. Christie, Phys. Rev B [3], 1, 1813 (1970).

9. J. Blomquist, M. Sundbom, B. Roos, Chem. Phys. Lett., 9, 160 (1971).

10. C.R. Abeledo, R.B. Frankel, A. Misetich, N.A. Blum, J. Appl. Phys., 42, 1723 (1971).

11. L. Asch, J. Friedt, Chem. Phys. Lett., 21, 595 (1973).

12. I. Nakagawa, Can. J. Spectr., 18, 1, (1973).

13. S.L. Chodos, A.M. Black, C.D. Flint, Chem. Phys. Letts., 33, 344 (1975).

14. C.D. Flint, Coord. Chem. Revs., 14, 47, (1974).

15. O. Kahn, S.F.A. Kettle, Mol. Phys., 29, 61 (1975).

16. G.C. Allen and K.D. Warren, Structure and Bonding, 9, 49 (1971).

17. G.C. Allen, R. Al-Moborak, G.A.M. El-Sharkawy and K.D. Warren, Inorg. Chem., 11, 787 (1972).

18. G.C. Allen and K.D. Warren, Structure and Bonding, 19, 101 (1974).

19. G.C. Allen and K.D. Warren, Coord. Chem. Revs., 16, 227 (1975).

20 Specialist Periodical Reports - Electronic Structure and Magnetism of Inorganic Compounds, Vols. 1-4, Chemical Society London.

21. S.L. Holt, C.J. Ballhausen, Theor. Chem. Acta, 7, 313 (1967).

22. J. Duinker, C.J. Ballhausen, Theor. Chem. Acta, 12, 325 (1969).

23. B. Butowiez, Compt. Rend., B. 271, 1141 (1970).

24. B. Butowiez, J. Phys. (Paris), 31, 477, (1970).

25. J.Teltow, Z. Phys. Chem. B 40, 397 (1938); B 43, 198 (1939).

26. C.A. Kosky, S.L. Holt, Chem. Commun., 668 (1970).

27. P. Day, L. O'Leari, L. Disipio, Chem. Phys. Letts, 5, 533 (1970).

28. S.L. Holt, C. Simo, E. Banks, Inorg. Chem., 9, 183 (1970).

29. L.W. Johnson, S.P. McGlynn, J. Chem. Phys., 55, 2985 (1971).

30. L.W. Johnson, S.P. McGlynn, Chem. Phys. Letts., 10, 595 (1971).

31. L.W. Johnson, S.P. McGlynn, E. Hughes, J. Chem. Phys., 55, 4476 (1971).

32. B. Butowiez, Compt. Rend., B 272, 534 (1971).

33. C.J. Ballhausen, J.P. Dahl, I. Tralijerg, Colloq. Internat. C.N.R.S., 191, 69 (1970).

34. S.C. Jain, D. Pooley, R. Singh, J. Phys., 5, 1307 (1972).

35. L. Disipio, L. O'Leari, P. Day, J. Chem. Soc. Faraday II, 68, 776 (1972).

36. C.A. Kosky, B.R. McGarvey, S.L. Holt, J. Chem. Phys., 56, 5904 (1972).

37. S.C. Jain, A.V.R. Warrier, S.K. Agrawal, Chem. Phys. Letts., 14, 211 (1972).

38. S. Radhakrishna, B.D. Sharma, Chem. Phys. Letts., 17, 578 (1972).

39. S. Radhakrishna, K.P. Pande, Chem Phys. Letts., 13, 62 (1972).

40 S. Radhakrishna, K.P. Pande, Phys. Stat. Solidii, B 55, 155 (1973).

41. E. Ahlborn, E. Diemann, A. Muller, Z. Naturforsch 27B, 1108 (1972).

42. J.B. Milstein, J. Ackerman, S.L. Holt, B.R. McGarvey, Inorg. Chem., 11, 1178 (1972).

43. M.T. Vala, C.J. Ballhausen, R. Dingle, S.L. Holt, Mol. Phys., 23, 217 (1972).

44. A. Mooney, R.H. Nuttall, W.E. Smith, J.C.S. Dalton, 1096 (1972).

45. A. Mooney, R.H. Nuttall, W.E. Smith, J.C.S. Chemical Commun. 1290 (1972).

46. P. Day, L. Disipio, G. Ingletto, L. O'Leari, J.C.S. Dalton, 2595 (1973).

47. D.B. Jeans, J.D. Penfield, P. Day, J.C.S. Dalton, 1777 (1974).

48. J. Ferguson, H.I. Guggenheim, D.L. Wood, J. Chem. Phys., 54 504 (1971).

49. L. Helholz, M.E. Russo, J. Chem. Phys., 59, 5455 (1973).

50. R.J. McCarthy, R.D. Bereman, Inorg. Chem., 12, 1909 (1973).

51. G.C. Allen, K.D. Warren, J. Mol. Spectr., 33, 180 (1970).

52. M.J. Reisfield, L.B. Asprey, R.A. Penneman, J. Mol. Spectr., 29, 109 (1969).

53. D.S. Novotry, G.D. Sturgeon, Inorg. Nucl. Chem. Letts., 6, 455, (1970).

54. M.J. Reisfield, N.A. Matwiyoff, L.B. Asprey, J. Mol. Spectr., 39, 8 (1971).

55. C.D. Flint, Chem. Phys. Letts., 11, 27 (1971).

56. H.L. Schlafer, H. Gausman, H. Witzke, J. Chem. Phys., 46, 1423, (1967).

57. E. Koglin, W. Krasser, Z. Naturforsch, 28A, 1131 (1973).

58. G. Kenemy, C.H. Haake, J. Chem. Phys., 33, 783 (1960).

59. C.D. Flint, J. Mol. Spectr., 37, 414 (1972).

60. A. Pfeil, Spectr. Acta, 26A, 1341 (1970).

61. A.G. Paulusz, J. Electr. Soc., 120, 942 (1973).

62. A.M. Black, C.D. Flint, J.C.S. Dalton, 977 (1974).

63. K. Burger, "Coordination Chemistry: Experimental Methods", Butterworth, (1973).

64. P.J. Stephens, page 201, Annual Reviews of Physical Chemistry, 25, (1974), H. Eyring, Ed.

65. C.K. Luk, W.C. Yeakel, F.S. Richardson, P.N. Schatz, Chem. Phys. Letts., 34, 147, (1975).

66. J.C. Collingwood, P. Day, R.G. Denning, D.J. Robbins, L. Disipio, L. Oleari, Chem. Phys. Letts., 13, 567, (1972).

67. V. Gelius, P.F. Heden, J. Hedman, B.J. Lundberg, R. Manne, R. Nordberg, C. Nordling, K. Sieghbahn, Physica Scripta, 2, 70, (1970).

68. C.S. Fadley, D.A. Shirley, Phys. Rev., A 2, 1109, (1970).

69. D.T. Clark, D.B. Adams, Chem. Phys. Letts., 10, 121, (1971).

70. T. Koopmans, Physica, 1, 104, (1933).

71. L.N. Kramer, M.D. Klein, J. Chem. Phys., 51, 3618, (1969).

72. D.N. Hendricksen, J.M. Hollander, W.H. Jolly, Inorg. Chem., 9, 612, (1970).

73. C.K. Jorgensen, H. Berthou, L. Balsenc, J. Fluorine Chem., 1, 327 (1971-72).

74. M.V. Zeller, R.G. Hayes, Chem. Phys. Lett., 10, 610 (1971).

75. R. Prins, T. Novakov, Chem. Phys. Lett., 9, 593 (1971).

76. R. Prins, T. Novakov, Chem. Phys. Lett., 16, 86, (1972).

77. A. Calabrese, R.G. Hayes, J. Amer. Chem. Soc., 95, 2819 (1973).

78. R. Prins, J. Chem. Phys., 61, 2580 (1974).

3.0 THEORETICAL STUDIES OF ELECTRONIC STRUCTURE

3.1.0 The Molecular Problem

The electronic structure and properties of any molecule in a stationary state may be determined by solution of the time-independent Schrodinger equation:

$$\hat{H}\psi = E\psi$$

where $\hat{H}$ is the Hamiltonian of the molecule, ψ is the total molecular wave function which describes the motion of nuclei and electrons and E is the total energy. In practice this equation is difficult to solve unless approximations are made.

3.1.1 Born - Oppenheimer (B-O) Approximation

The B-O approximation[1] assumes electronic motion to be independent of nuclear motion and allows the total wavefunction to be represented as a product of nuclear (ψ_n) and electronic (ψ_e) parts. In most theoretical studies the electronic wavefunction ψ_e is calculated at some fixed nuclear geometry, normally the experimental geometry.

The appropriate electronic Hamiltonian operator in atomic units when spin-spin and spin-orbit interactions are neglected is

$$\hat{H}_e = \hat{T} + \hat{V}_{ne} + \hat{V}_{ee}$$

$$= \sum_i -\frac{1}{2}\nabla_i^2 + \sum_i \sum_n \frac{Z_n}{r_{in}} + \sum_{i>j} \frac{1}{r_{ij}}$$

and represents the kinetic energy, nuclear-electron attraction and electron-electron repulsion operators, respectively.

3.1.2 The Electronic Wavefunction

The total electronic wavefunction ψ_e may be approximated as a product of one electron wave functions ψ_i, anti-symmetrized to meet the requirements of the Pauli principle. It is normally written in determinant form

$$\psi_e = \frac{1}{\sqrt{N!}} \begin{vmatrix} \psi_1(1) & \cdots & \psi_N(1) \\ \vdots & & \\ \psi_1(N) & \cdots & \psi_N(N) \end{vmatrix} = \det \left\{ \psi_1 \psi_2 \cdots \psi_N \right\}$$

The one electron wavefunctions, ψ_i are called molecular spin orbitals and can be factored into a spatial part and a spin part

$$\psi_i(N) = \phi_i(N) \begin{cases} \alpha(N) \\ \beta(N) \end{cases}$$

3.1.3 The Hartree-Fock Method

In addition to the above approximation, where each electron is described by a one-electron spin orbital, it is usually necessary for molecular systems to assume that each electron is independent of the instantaneous motion of the other electrons. Hence the dynamic correlation between electrons is neglected and each electron is assumed to be influenced by the <u>average</u> potential produced by the other electrons.

This corresponds to solving the Hartree-Fock equations

$$F(1)\ \phi_i(1) = E_i\ \phi_i(1)$$

where F is the effective Hartree-Fock Hamiltonian incorporating the average electronic field, and E_i is the energy of an electron in MO ϕ_i. Because of the average electronic field the above equation must be solved iteratively until self consistency is achieved: this is known as the <u>Self-Consistent Field</u> (SCF) method.

The state of a closed shell molecule may be represented by a Slater determinant built from doubly occupied MO's.

$$\psi_e = \det \{\phi_1 \bar{\phi}_1 \phi_2 \bar{\phi}_2 \cdots \phi_N \bar{\phi}_N\}$$

where $\phi_1 = \phi_1 \alpha$

and $\bar{\phi}_1 = \phi_1 \beta$

The state of an open shell molecule can also be represented by a single Slater determinant utilizing the unrestricted Hartree-Fock (UHF) method[2]. In this situation there are now no a priori constraints on the form of the occupied MO's. Hence, different spatial orbitals are associated with electrons of different spin.

The UHF wave function has the form

$$\psi_{UHF} = [(p+q)!]^{-\frac{1}{2}} \det\{\phi_1(1)\ \alpha(1) \ \cdots \ \phi_p(p)\ \alpha(p) \ \cdots \ \cdots \ \phi_1(p+1)\ \beta(p+1) \ \cdots \ \phi_q(p+q)\ \beta(p+q)\}$$

where p = number of electrons with α spin

q = number of electrons with β spin

$\{\phi_i\}$ and $\{\phi_j\}$ form two different orthonormal sets.

Generally, the MO's (of both closed and open shell systems) are explicitly represented as a linear combination of basis orbitals χ_μ:

$$\phi_i = \sum_\mu \chi_\mu C_{\mu i}$$

or in matrix notation

$$\underline{\phi} = \underline{\chi}\,\underline{C}$$

where $\underline{\phi}$ and $\underline{\chi}$ are row matrices of MO's and basis orbitals respectively, and $\underline{C}$ is the coefficient matrix. When $\{\chi_\mu\}$ are atomic orbitals, the above approximation is known as the linear combination of atomic orbitals (LCAO) approximation. If the complete basis set $\{\chi_\mu\}$ is used the $\{\phi_i\}$ are given exactly.

In practive, however, an incomplete set is used because of the complexity of the problem.

3.2.0 Solution of the Molecular Problem

Roothaan[3] systematized and developed the procedure for solving the integro-differential equations in the LCAO-MO approximation. In matrix form the fundamental equation may be written over basis orbitals:

$$\underline{FC} = \underline{SCE} \qquad 3.1$$

where $\underline{F}$ and $\underline{S}$ are known matrices and $\underline{C}$, the coefficient matrix and $\underline{E}$, the orbital energy matrix, are unknown. $\underline{S}$ is the overlap matrix with elements:

$$S_{\mu\nu} = \langle \chi_\mu | \chi_\nu \rangle$$

and $\underline{F}$ is the effective Hartree-Fock Hamiltonian matrix, which may be expressed as:

$$\underline{F} = \underline{H} + G$$

where $\underline{H}$ is the one-electron matrix, representing electron-kinetic energy and electron-nuclear attraction effects, and has elements of the form:

$$H_{\mu\nu} = \langle \chi_\mu | -\tfrac{1}{2}\nabla^2 | \chi_\nu \rangle + \langle \chi_\mu | -\sum_n \frac{Z_n}{r_n} | \chi_\nu \rangle$$

The $\underline{G}$-matrix is the two-electron Hamiltonian matrix, representing electron-electron repulsion effects, and has elements:

$$G_{\mu\nu} = \sum_{\lambda\sigma} R_{\lambda\sigma} \left[2\langle \mu\lambda | \nu\sigma \rangle - \langle \mu\lambda | \sigma\nu \rangle \right]$$

where $$\langle \mu\lambda | \nu\sigma \rangle = \iint \chi_\mu^*(1)\ \chi_\lambda^*(2)\ \frac{1}{r_{12}}\ \chi_\nu(1)\ \chi_\sigma(2)\ d_{\tau 1}\ d_{\tau 2}$$

The elements of $\underline{R}$ are given by:

$$R_{\mu\nu} = \sum_i^{occ} C_{\mu i}\ C_{\nu i}^*$$

From the density matrix representation, $\underline{R}$, the total electronic energy (in a.u.) may now be calculated as:

$$E_e = 2\mathrm{Tr}\,[\underline{R}\,\underline{F}] - \mathrm{Tr}\,[\underline{R}\,\underline{G}]$$

$$= \mathrm{Tr}\,[\underline{R}\,\underline{H}] + \mathrm{Tr}\,[\underline{R}\,\underline{F}]$$

The total energy (in a.u.) is:

$$E_{total} = E_e + V_{nn}$$

$$= \mathrm{Tr}[\underline{R}\,\underline{H}] + \mathrm{Tr}[\underline{R}\,\underline{F}] + \sum_{n<m} \frac{Z_n Z_m}{r_{nm}}$$

The problem of solving Roothaan's equations is essentially a matrix-eigenvalue problem and involves finding the roots of the secular equation:

$$|F - SE| = 0$$

Because $\underline{F}$ depends on $\underline{C}$ via the density matrix $\underline{R}$, the SCF technique is needed; the initial values of $\underline{C}$ are estimated, $\underline{F}$ is calculated, FC = SCE is solved and new values of $\underline{C}$ are obtained. This cyclic procedure is continued until self-consistency is achieved.

In practice the Roothaan equation in the non-orthogonal $\{\chi_\mu\}$ atomic basis

$$\underline{FC} = \underline{SCE} \qquad 3.1$$

is best solved by transforming to an orthogonal $\{\lambda\}$ basis

$$\underline{F}^{\lambda}\underline{C}^{\lambda} = \underline{C}^{\lambda}\underline{E} \qquad 3.2$$

Equation 3.2 is readily solved by diagonalization. The above transformation is achieved by using the Lowdin[4] transformation:

$$\underline{C} = \underline{S}^{-\frac{1}{2}}\,\underline{C}^{\lambda}$$

and premultiplying 3.1 by $S^{-\frac{1}{2}}$ to give

$$\underline{S}^{-\frac{1}{2}}\,\underline{F}\,\underline{S}^{-\frac{1}{2}}\,\underline{C}^{\lambda} = \underline{S}^{-\frac{1}{2}}\,\underline{S}\,\underline{S}^{-\frac{1}{2}}\,\underline{C}^{\lambda}\underline{E}$$

which reduces to 3.2 on defining:

$$\lambda\underline{F} = \underline{S}^{-\frac{1}{2}}\,\underline{F}\,\underline{S}^{-\frac{1}{2}} \qquad \text{and noting}$$

$$\underline{S}^{-\frac{1}{2}}\,\underline{S}\,\underline{S}^{-\frac{1}{2}} = \underline{1}$$

The solution so far described applies to closed shell systems only. As mentioned earlier the open shell cases are described by the UHF approach and analagous equations are derived for both α and β MO's

$$\begin{aligned} \underline{F}^{\alpha}\,\underline{C}^{\alpha} &= \underline{S}\,\underline{C}^{\alpha}\,\underline{E}^{\alpha} \qquad \text{(for α-MO's)} \\ \underline{F}^{\beta}\,\underline{C}^{\beta} &= \underline{S}\,\underline{C}^{\beta}\,\underline{E}^{\beta} \qquad \text{(for β-MO's)} \end{aligned} \qquad 3.3$$

where $\underline{F}^{\alpha} = \underline{H}^{\alpha} + \underline{G}^{\alpha}$

$\underline{F}^{\beta} = \underline{H}^{\beta} + \underline{G}^{\beta}$

In terms of the non-orthogonal χ-basis, the MO's are:

$$\theta_i = \sum_{\mu} \chi_{\mu}\, C^{\alpha}_{\mu i} \qquad \phi_i = \sum_{\mu} \chi_{\mu}\, C^{\beta}_{\mu i}$$

The $\underline{H}$ and $\underline{G}$ matrices are defined as:

$$H_{\mu\nu} = \langle \chi_{\mu} \left| \frac{\nabla^2}{2} - \sum_{n} \frac{Z_n}{r_n} \right| \chi_{\nu} \rangle$$

$$G^{\alpha}_{\mu\nu} = \sum_{\lambda,\sigma} \left[R_{\lambda\sigma} \langle \mu\lambda | \nu\sigma \rangle - R^{\alpha}_{\lambda\sigma} \langle \mu\lambda | \sigma\nu \rangle \right]$$

$$G^{\beta}_{\mu\nu} = \sum_{\lambda,\sigma} \left[R_{\lambda\sigma} \langle \mu\lambda | \nu\sigma \rangle - R^{\beta}_{\lambda\sigma} \langle \mu\lambda | \sigma\nu \rangle \right]$$

$$R^{\alpha}_{\mu\nu} = \sum_{i}^{p} C^{\alpha}_{\mu i}\, C^{\alpha *}_{\nu i} \quad ; \quad R^{\beta}_{\mu\nu} = \sum_{i}^{q} C^{\beta}_{\mu i}\, C^{\alpha *}_{\nu i}$$

and $R_{\mu\nu} = R^{\alpha}_{\mu\nu} + R^{\beta}_{\mu\nu}$

Solution of equations 3.3 is effected in a similar manner to that employed for the closed shell case. Thus $\underline{F}^{\alpha}$ and $\underline{F}^{\beta}$ are transformed into the orthogonal λ-basis by the transformations:

$$\lambda\underline{F}^{\alpha} = \underline{S}^{-\frac{1}{2}}\,\underline{F}^{\alpha}\,\underline{S}^{-\frac{1}{2}}$$

$$\lambda\underline{F}^{\beta} = \underline{S}^{-\frac{1}{2}}\,\underline{F}^{\beta}\,\underline{S}^{-\frac{1}{2}}$$

The new eigenvalue equations

$$\lambda_{\underline{F}}^{\alpha}\ \lambda_{\underline{C}}^{\alpha} = \lambda_{\underline{C}}^{\alpha}\ \underline{E}^{\alpha}$$

$$\lambda_{\underline{F}}^{\beta}\ \lambda_{\underline{C}}^{\beta} = \lambda_{\underline{C}}^{\beta}\ \underline{E}^{\beta}$$

are then solved by diagonalization of $\lambda_{\underline{F}}^{\alpha}$ and $\lambda_{\underline{F}}^{\beta}$. Subsequent Löwdin transformations on $\lambda_{\underline{C}}^{\alpha}$ and $\lambda_{\underline{C}}^{\beta}$ allow $\underline{C}^{\alpha}$ and $\underline{C}^{\beta}$, and hence $\underline{R}^{\alpha}$ and $\underline{R}^{\beta}$ to be obtained.

The total electronic energy is given by

$$E_e = \mathrm{Tr}[\underline{R}^{\alpha}\underline{H}] + \mathrm{Tr}[\underline{R}^{\beta}\underline{H}] + \tfrac{1}{2}\mathrm{Tr}[\underline{R}^{\alpha}\underline{G}^{\alpha}] + \tfrac{1}{2}\mathrm{Tr}[\underline{R}^{\beta}\underline{G}^{\beta}]$$

Occasionally one finds an author who associates the energy of a system with the sum of orbital energies of the occupied orbitals. The total energy is not equal to the sum of one electron energies[3], the assumption being, if one takes this approach, that the electron interaction terms cancel the nuclear repulsion contributions. Such an assumption, if energy differences are being considered, may be dangerous.

References : Chapter 3

1. M. Born, J.R. Oppenheimer, Ann. Physik., 84, 457 (1927).

2. J.A. Pople, R.K. Nesbet, J. Chem. Phys., 22, 69 (1954).

3. C.C.J. Roothaan, Rev. Mod. Phys., 23, 69 (1951).

4. P.O. Lowdin, J. Chem. Phys., 18, 365 (1950).

4.0 MOLECULAR ORBITAL METHODS APPLIED TO TRANSITION METAL SYSTEMS

4.1.0 Introduction

Very powerful computers and the development of effective techniques for calculating molecular integrals have at last made feasible rigorous non-empirical calculation of large coordination compounds. More importantly, it has also become possible to check the reliability of approximate computation procedures (reliability of various basis sets) and the validity of approximation approaches to the interpretation of the calculation results. When this has been achieved, valid approximation schemes may then be used routinely on chemically significant systems.

We adopt the Davies and Webb classifications[1] of MO techniques into the categories (i) semi-empirical, (ii) semi-quantitative and (iii) ab-initio.

A semi-empirical approach is one where approximations are not listed explicitly and some of the terms of the SCF operator in the LCAO-SCF F matrix are related directly to experimentally determined quantities.

If computational simplifications are introduced into the solution of the LCAO-SCF equations in a systematic manner using well defined approximations of reasonable accuracy, a semi-quantitative approach is evolved.

The ab-initio approach consists of solving the LCAO-SCF equations exactly, in terms of a given Hartree-Fock formalism in terms of a chosen MO expansion basis, but this basis may or may not be sufficiently extensive to guarantee realistic wave functions.

In each of these classifications we aim to discuss the different available approaches, but no attempt is made at exhaustive coverage (except for the hexafluoride systems) of individual MO studies of transition element systems in view of the many reviews and reports recently available[2-4].

Texts, review articles, and continued applications in the current literature attest to the continued interest in approximate calculations. Hückel theory[5], SCCC[6], ZDO[7], CNDO[8], INDO[9], X_α[10] and their various modifications[11] find their respective proponents expounding their merits. Too frequently the precautionary comments of the original authors concerning the applicability of the methods are ignored by subsequent users.

Several of the methods incorporate parameters to reduce the computational problems. Later applications alter the values until the final results agree with the users' preconceptions as to the "correct" values.

Seldom is an adequate study made of the implications that such variations have on the bonding description. Of equal significance is that such an approach makes no allowance for the unexpected yet truly correct answer.

Fenske's[12] assessment of an approximate calculational method is made by posing the following questions:

(1) Are the calculations used to study a single compound or a series of compounds?

(2) Are parameters used in the evaluation of the elements in the secular determinant?

If the answer is yes, then

(a) How many are employed?

(b) Are they held constant throughout the series of compounds? If not, what criteria are used to vary them?

(c) If they are varied, is there any statement made as to the sensitivity of the eigenvalues and eigenvectors to the variations in parameters?

(3) If a modification of a previously employed procedure is incorporated, what reasons are given for the change, and what alterations, if any, occur in the results?

(4) Does the method remain internally consistent throughout its applications to different systems?

(5) How closely does the approximate calculation adhere to the considerations and/or conclusions of more rigorous theory?

(6) What experimental results are correlated by the calculations? How independent are these correlations of possible parameter variations?

4.2.0 Ab-initio Methods

The accuracy of non-empirical (ab-initio) calculations by the MO LCAO SCF method depends on the completeness of the basis set of AO's which may be 'minimal' (i.e. include only AO's occupied in the ground state of the atoms of a molecule) or 'extended' (i.e. include additionally external AO's) and also on the functional type of the AO. Usually, AO's may be one (single ζ), two (double ζ) and, more rarely, many component combinations of Slater type functions (STF) with the radial part r^{n-1} exp $(-\zeta r)$. (n is the principal quantum number of AO's).

The orbital exponents (ζ) are found from calculations of isolated atoms, but, generally speaking, they must be optimized in molecular

calculations. A properly selected basis must be well balanced, ie. the minimal basis must include AO's of a sufficient accuracy [many - (analytical SCF) or at least double ζ AO's] and must be extended by adding external AO's from all the atoms of the molecule. Calculations of some small molecules have demonstrated that an unbalanced basis set causes a distortion of the wave function and electron distribution in a molecule[3].

The primary computational difficulty associated with the Fock matrix element lies in the evaluation of the electron interaction integrals $(\mu\nu|\rho\sigma)$ since each of the wavefunctions can be associated with a different atomic centre. Slater-type functions are quite successful in dealing with diatomic molecules, but substantial computational problems arise in the determination of multicentre integrals particularly in an ab-initio scheme. As larger and faster computers became available Huzinaga[13] suggested that the earlier recommendations by Boys[14] to use gaussian type orbitals (GTO's) be considered. Although GTO's have computational advantages, one needs a much larger basis set of such functions. Since the number of 2-electron-integrals one must calculate is proportional to the fourth power of the number of atomic functions, the number of integrals runs literally into the millions.

To facilitate a reduction in the integrals, symmetry considerations are utilized wherever possible to identify those integrals of identical value in the molecular system. Another device, used to reduce the size of the secular determinant, is to fit atomic Slater-type orbitals with a set of gaussian functions. This technique is denoted "near-ab-initio" because some simplifications are involved in multi-centre integral evaluation.

Several GTF ab-initio computations in the inorganic/transition metal area have been reported recently[15-18]. Unfortunately most GTF calculations are not of direct use as reference calculations for comparison with approximate STF based MO calculations such as those of this study. It is normally not possible to differentiate between the effects of, on one hand, matrix element and integral approximation , and with difference of bases used, on the other.

4.3.0 Semi-Quantitative Methods

The various neglect of differential overlap schemes by Pople et al[7-9], well suited for studying large organic molecules have been found lacking when applied to coordination compounds[3] where a diversity of bonding situations is encountered.

The various methodologies are as follows:

(i) CNDO - complete neglect of differential overlap

(ii) INDO - intermediate neglect of differential overlap

(iii) NDDO - neglect of diatomic differential overlap.

The last method is the most rigorous scheme, INDO provides intermediate accuracy whilst CNDO gives the roughest approximation. For a critique of these methods and the MCZDO method of Brown et al[19] the reader is referred to reviews by Burton[20] and Klimenko et al[3].

A further development of the NDO schemes has been reported by Halgren and Lipscomb[21] which allows partial retention of diatomic differential overlap (PRDDO). This scheme reduces the number of molecular integrals to approximately n^3 but to date, no applications of this method to transition metal complexes have appeared.

Pople et al stated that methods which employed the (CNDO) approximation should only employ "atom averaged" integral values if invariance to local orthogonal basis transformation be maintained. The rationale for this approximation is that integrals containing one electron charge distributions arising from the product of two different atomic orbitals tend to be smaller than integrals which contain only coincident product distributions. They also formulated an approximation scheme which both overcame the serious loss of detailed information in the "atom averaging" of the CNDO scheme, and also satisfied invariance requirements. In this scheme, the "Neglect of Diatomic Differential Overlap" (NDDO) approximation involves the explicit inclusion of all integrals involving monocentric product charge distributions (even those products of different orbitals on the same centre), but exclusion of integrals arising from the diffuse bicentric product of orbitals on different centres.

In both the schemes involving one or other of these approximations, along with the subsequent schemes involving the intermediate "Many Centre Neglect of Differential Overlap" (MCNDO-INDO) the NDO approximations are only used in evaluation of the two electron part of the LCAO SCF $\underline{F}$ matrix.

The zero differential overlap (ZDO) approximation is also used in the Pople et al parameterization of the MO methods using these approximations. The complete Roothaan LCAO SCF equations

$$\left.\begin{aligned} \underline{X}_F\, \underline{X}_C &= \underline{S}\, \underline{X}_C\, \underline{E} \\ |\underline{X}_F - \underline{S}\, \underline{E}| &= 0 \end{aligned}\right\}$$

become under the ZDO and NDO approximations

$$\underline{F}^{CNDO}\, \underline{C} = \underline{C}\, \underline{E}$$

or

$$\underline{F}^{NDDO}\, \underline{C} = \underline{C}\, \underline{E}$$

with the overlap matrix being approximated by a unit matrix ($\underline{S} = \underline{1}$). Lowdin[22] has described a symmetric orthogonalization of the atomic orbital basis which eliminates the overlap matrix $\underline{S}$ in a more rigorous manner. By defining a new orthogonalized basis $^{\lambda}C$ by

$$\chi_{\underline{C}} = \underline{S}^{-\frac{1}{2}} \lambda_{\underline{C}}$$

and defining $^{\lambda}F$,

$$\lambda_{F\ 1} = S^{-\frac{1}{2}} \chi_{\underline{F}}\ \underline{S}^{-\frac{1}{2}}$$

then in the new basis

$$\left.\begin{aligned} \lambda_{\underline{F}}\ \lambda_{\underline{C}} &= \lambda_{\underline{C}}\ \underline{E} \\ |\lambda_{\underline{F}} - \underline{E}| &= 0 \end{aligned}\right\}$$

In these terms the basis appropriate to the eigen vectors of the Pople et al parameterizations is in some doubt.

Many calculations in the transition metal area have been made using these methods and these will be discussed in Chapter 5.

Another approximate MO method has been developed recently - the so called scattered wave SCF - X_{α} method[23,24]. It is based on simplification of the Hartree-Fock equations by statistical approximation of the exchange potential with the expression $\alpha A\rho(1)^{-\frac{1}{3}}$ where $\rho(1)$ is the density of electrons with a given spin at point (1), and the parameter α may be selected using several ways. Moreover the SW method assumes that the space of the molecule is divided into zones of the following three types:

(1) spherical atomic zones

(2) an interatomic zone

(3) an outer zone lying outside the assumed spherical 'surface' of a molecule.

With a view to simplifying calculations, the molecular potential in the zones of the first and third types is averaged over the directions, and that in a zone of the second type over the volume. This permits, unlike conventional representation of the MO's in the form of LCAO's, the use of rapidly converging MO expansion in the eigenfunctions of zones, types 1 and 3, with spherically symmetrical potentials, and in special functions ('scattered waves') which account for the exponential asymptotic behaviour of MO's as we move off the atoms.

The requirement of continuity of MO's (and their derivatives) on adjacent spherical boundaries gives rise to secular equations whose solutions are used for determining the 'scattered wave' amplitudes and new eigenfunctions of first and second type zones etc until self-consistency. Since the calculation procedure does not require computation of many-centre electron interaction integrals computation times are quite moderate. By applying the SW technique to the consideration of complex ions, the crystal field stabilizing potential can very easily be taken into account through uniform distribution of the compensating charge of an opposite sign on the complex 'surface' (boundary of zone 3). A special calculation technique for determining orbital energies for the hypothetical states of a molecule approximately allows for the reorganisation of MO's when the molecule is ionized or excited.

An offshoot of the SW method is the Discrete Variational Method (HFS-DVM)[25-27] and investigations have been undertaken of the electronic structures of the tetrahedral -oxo- complexes[28].

4.4.0 Semi-Empirical Methods

In the various semi-empirical NDO approximation versions, separate integrals or whole matrix elements are treated as calculation parameters and are found from experimental (most frequently, spectroscopic) data for isolated atoms or ions. But, according to Coulson, "the number of sets of parameters is almost equal to the number of researchers working in this field", whereas the results depend significantly on the selected magnitudes of these parameters.

Recent contributions in the transition metal area have been made by Boudreaux's group[29,30]. The first method utilizes valence orbital ionization energies for incorporation into the diagonal elements of the Hamiltonian, and the Mulliken approximation for the off diagonal elements. Moderate success is achieved in calculating ground state wave functions for a series of transition metal hexafluoro complexes.

Their most recent development is the application of a modified Wolfsberg-Helmholz method to the study of transition metal halides. This scheme utilizes the Mulliken multicentre integral approximation and the Ruedenberg approximation for two centre kinetic energy integrals whilst the overlap integrals were calculated by numerical integration using the metal +1 functions of Richardson et al[31] and the fluoride (assumed 2ζ Fluorine) function of Clementi[32].

They also include a crude approximation to the site potential, its inclusion being essential to the valid operation of the Mulliken approximation in their calculations.

Perkins et al[33] have used a modified CNDO method to obtain an approximate ground state wave function and then carried out a multielectron configuration interaction calculation (which they call MECI).

It was found necessary to include additional electronic-interaction integrals in the excited state calculation. An analysis of the independent non zero two-electron integrals involving the d orbitals, in terms of the traditional ligand field parameters showed the CNDO method only included five of the 15 possible interactions and more importantly these are not identical.

The procedure they ultimately used in their MECI calculations to evaluate these two electron integrals was:

(i) to use the ligand field expression or

(ii) to employ the CNDO approximation if a ligand field expansion was not available.

Two values of the Wolfsberg-Helmholz proportionality constant k were used. This constant "defines" the magnitude of the off diagonal terms in the core Hamiltonian matrix and is normally the only parameter of the modified CNDO method.

The results of these calculations are presented in Chapter 5.

References : Chapter 4

1. D.R. Davies, G.A. Webb, Coord. Chem Rev., 6, 95 (1971).

2. D.A. Brown, W.J. Chambers, N.J. Fitzpatrick, Inorg. Chem. Acta, 6, 7 (1972).

3. M.E. Dyatkina, N.M. Klimenko, E.L. Rosenberg, Pure and Applied Chem., 38, 391 (1974).

4. Specialist Periodical Reports - Electronic Structure and Magnetism of Inorganic Compounds, Vols. 1-4, Chem. Soc., London.

5. R. Hoffmann, J. Chem. Phys., 39, 1397 (1963).

6. N.A. Basch, H.B. Gray, J. Am. Chem. Soc., 90, 5713 (1968).

7. J.A. Pople, Trans. Faraday Soc., 49, 1375 (1953).

8. J.A. Pople, D.P. Santry, G.A. Segal, J. Chem. Phys., 43, 5129 (1965).

9. J.A. Pople, D.L. Beveridge, P.A. Dobosh, J. Chem. Phys., 47, 2026 (1967).

10. K.H. Johnson, Advances in Quantum Chem., Vol. 7, P.O. Lowdin, Editor, Academic, New York, 1973, p. 143.

11. J.N. Murrell, A.J. Harget, Semi-empirical SCF MO Theory of Molecules, Wiley-Interscience, London-New York, 1972.

12. R.F. Fenske, Pure Appl. Chem., 27, 61 (1971).

13. S. Huzinaga, J. Chem. Phys., 42, 1293 (1965).

14. S.F. Boys, Proc. Roy. Soc. (London), A 200, 542 (1950).

15. E. Johansen, Chem. Phys. Lett., 17, 569 (1972).

16. K.J. Duff, Physical Review B 9, 66, (1974).

17. A.P. Mortola, H. Basch, J.W. Moskowitz, Int. J. Quantum Chem. 7, 725 (1973).

18. M.H. Wood, Theor. Chem. Acta, 36, 309 (1975).

19. R.D. Brown, K.R. Roby, Theor. Chem. Acta, 16, 175 (1970).

20. P.G. Burton, Coord. Chem. Revs., 12, 37 (1974).

21. T.A. Halgren, W.N. Lipscomb, J. Chem. Phys., 58, 1569 (1973).

22. P.O. Lowdin, J. Chem. Phys., 18, 365 (1950).

23. J.C. Slater, K.H. Johnson, Phys. Rev., B 5, 844 (1972).

24. K.H. Johnson, F.C. Smith, Phys. Rev., B 5, 831 (1972).

25. T. Parameswaran, D.E. Ellis, J. Chem. Phys., 58, 2088 (1973).

26. E.J. Baerends, D.E. Ellis, P. Ros, Chem. Phys., 2, 41, (1973).

27. A. Rauk, T. Ziegler, D.E. Ellis, Theor. Chem. Acta, 34, 49 (1974).

28. T. Ziegler, A. Rauk, E.J. Baerends, Chem. Phys., 16, 209 (1976).

29. A. Dutta-Ahmed, E.A. Boudreaux, Inorg. Chem., 12, 1590 (1973).

30. L.E. Harris, E.A. Boudreaux, Inorg. Chem. Acta, 9, 245 (1974).

31. J.W. Richardson, R.R. Powell, W.C. Nieuwpoort, J. Chem. Phys., 38, 796 (1963).

32. E. Clementi, J. Chem. Phys., 40, 1944 (1964); IBM Report RJ-256.

33. D.R. Armstrong, R. Fortune, P.G. Perkins, J. Chem. Soc., Dalton 9, 753 (1976).

5.0 LITERATURE RESULTS

5.1.0 Comparison of Literature Results for CrF_6^{3-}, FeF_6^{3-} and NiF_6^{4-} ions

Fenske et al[1] derived an approximate SCF method after noting shortcomings of the modified Wolfsberg and Helmolz[2] method in that calculated molecular orbital were frequently too covalent in character. Their method is now summarized.

(1) Matrix elements of the Secular Determinant

(a) Metal diagonal elements

The diagonal terms involving the metal wave functions χ_i are given by

$$H_{ii} = \langle\chi_i|\hat{H}|\chi_i\rangle = \langle\chi_i|-\tfrac{1}{2}\Delta + V_m|\chi_i\rangle + \langle\chi_i|\sum_j V_j|\chi_i\rangle \qquad 5.1$$

whilst these are approximated by

$$H_{ii} = \langle\chi_i|\hat{H}|\chi_i\rangle = E_\chi(q_m) + CF(q_j) \qquad 5.2$$

where $E_\chi(q_m)$ is the orbital energy of the metal electron in the free ion of charge q_m and $CF(q_j)$ is the crystal field potential, due to the ligand point charges, q_j.

(b) Ligand diagonal elements

For the electron in the ith orbital on ligand atom 1, μ_{il}

$$\langle\mu_{i2}|\hat{H}|\mu_{il}\rangle = \langle\mu_{il}|-\tfrac{1}{2}\Delta + V_1|\mu_{il}\rangle + \langle\mu_{il}|V_m + \sum_{j=2} V_j|\mu_{il}\rangle \qquad 5.3$$

when ligand-ligand overlap is neglected reduces in an analogous manner to the metal diagonal terms

$$\langle\phi_i|\hat{H}|\phi_i\rangle = E_\phi(q_j) - q_m\left(\frac{1}{r_m}|\phi_i\phi_i\right) - \sum_{j=2} q_j\left(\frac{1}{r_j}|\phi_i\phi_i\right). \qquad 5.4$$

(c) Off-diagonal elements $\langle\phi_i|\hat{H}|\chi_i\rangle$

They consider the matrix element $\langle\mu_{i2}|\hat{H}|\chi_i\rangle$, which involves the wave function of an electron on only one ligand atom and relate this to the desired matrix element as follows

$$\langle\phi_i|H|\chi_i\rangle = C\ \langle\mu_{il}|\hat{H}|\chi_i\rangle$$

where the constant, C, is the same coefficient which relates the diatomic overlap to the group overlap. The matrix element is then written as equation (5.3), above.

The first term becomes $E_{\chi i}(q_m)\ S(\mu_{il}, \chi_i)$. The last term becomes a sum of three centre integrals

$$\sum_{j=2} \langle\mu_{il}|V_j|\chi_i\rangle = -\sum_{j=2} q_j \left(\frac{1}{r_j}|\mu_{ii}\ \chi_i\right)$$

since it involves the wave functions of ligand atom 1 and the central metal with the charge distributions on all of the other ligand atoms and the sum of nuclear and electron charge densities on these centres is considered to be a point charge equal to the charge on the ligand.

The middle term $\langle\mu_{il}|V_1|\chi_i\rangle$ is approximated as

$$\left[R_a(6-q_1) - Z_1\right]\left(\frac{1}{r_1}|\mu_{il}\chi_i\right)$$

where R_a is chosen depending on whether μ_{il} and χ_i are σ- or π-bonding orbitals.

(2) The two- and three- centre integrals were calculated by the method of Shavitt[3] with further modifications where deemed necessary.

(3) Use of Richardson's[4] (+2) wave functions to evaluate integrals over the basis functions.

(4) The self consistent charge distribution is chosen by interpolation within the SCF procedure.

(5) External potential not included.

(6) Mulliken method utilized to obtain charges and orbital populations.

Brown and Burton[5] utilized a SUHF many centre zero differential overlap method in the study of the spin distributions in the transition metal hexafluorides. This scheme included:

(a) direct inclusion of all one- and two-centre one-electron integrals and all one-centre two-electron integrals,

(b) inclusion of only NDDU level multicentre two-electron integrals (the$(aa/bb)^S$),

(c) approximation of three-centre nuclear attraction integrals by the Ruedenberg formula in the core matrix,

(d) inclusion of the lattice potential in the Hamiltonian by precise evaluation of the Mandelung potential at each site of the cluster by the Ewald summation method.

Boudreaux and Dutta-Ahmed[6] have developed a semi empirical parameter free MO method which they have applied to the model systems MF_6^{n-} ($M = Ti^{3+}$, Cr^{3+}, Fe^{3+}, Ni^{2+}). The fundamentals of their method are now outlined.

(a) Only one-electron integrals are considered. Two-electron integrals between valence electrons in the molecular framework are not treated explicitly. These, however, are compensated for in a "spin pairing energy" correction to the calculated one-electron MO's.

(b) All parts of the Hamiltonian which are identifiable with the atomic cores are set equal to the orbital ionization energy with restricted charge dependence.

(c) All multicentre integrals are simplified using the Mulliken approximation.

(d) Only overlap integrals are calculated exactly; all other integrals which are not accounted for by (b) are evaluated on the basis of the point charge approximation.

(e) Lowdin orthogonalization is employed in the final analysis to arrive at populations.

(f) Explicit consideration is given to an external potential for stabilizing the complex ion.

Boudreaux and Harris[7] have used a modified Wolfsberg-Helmholz method to study first row transition metal fluoride and chloride complexes. The method is similar to that used by Hillier[8] for calculations on transition metal carbonyl complexes in that the modifications were derived from Richardson's simplified SCF Hamiltonian[6].

Their method is summarized as follows:

(a) Point charge electrostatic approximation is used for estimating nuclear attraction integrals.

(b) Site potential of the complex is incorporated by assuming that the stabilizing potential at the site of the complex MF_6^{-Q}, is uniformly distributed within a sphere of Radius R, upon whose surface resides a quantity of positive charge Q.

(c) Ruedenberg approximation for two-centre kinetic energy integrals.

(d) Orbital populations and atom charges are obtained from a population analysis of the Lowdin orbitals.

(e) Overlap integrals were calculated by numerical (16 point gaussian) integration using the metal, +1 functions of Richardson et al[4] and the fluorine functions of Clementi[9].

Several Multiple Scattering X_α studies have been made by Larson and Connoly's group[10-14] and their computational details are now given.

The MSX_α method is a self-consistent one-electron method where one uses a unique local potential function $V_\uparrow(x,y,z)$ for all the electrons of up spin and $V_\downarrow(x,y,z)$ for all electrons of down spin. These muffin tin potentials are spheres surrounding each atomic nucleus of the molecular ion and a constant average potential is used in the intersphere region. To obtain a local potential V one uses the Slater approximation[15] to exchange $V_\uparrow(r) = -6\alpha[(3/4\ \pi)\ p_\uparrow(r)]^{1/3}$ and similarly for $V_\downarrow$. Here $p_\uparrow$ and $p_\downarrow$ are the spherically averaged electronic charge densities of up- and down-spin, respectively. The parameter α is usually taken from atomic calculations where it has been optimized in such a way that the wavefunction, by some criterion, is as close as possible to the Hartree-Fock wavefunction. The value $\alpha = 0.72$ is said to be close to optimum for all the atoms involved in their calculations and has been used universally.

Other parameters have to be determined before a calculation is started. These include the radius and charge of the Watson sphere[16] and the radii of the muffin-tin spheres. The charge on the Watson sphere is chosen to neutralize the whole cluster whilst its radius is chosen to be equal to that of the outer sphere. The core orbitals (fluorine 1s and metal 1s, 2s, 2p) were in each iteration approximated by the corresponding free neutral atom SCF orbitals.

5.2.0 Relative Electronic Energy Levels

The relative electronic energy levels of the calculations discussed are given in table 5.1. No two calculations agree in the ordering of the energy levels and there is similar disagreement in the calculated orbital energies. Boudreaux and Ahmed[6] and Larson and Connolly[12] have reported the highest occupied MO's in CrF_6^{3-} FeF_6^{3-} and NiF_6^{4-} to be slightly negative.

5.1 Relative Electronic Energy Levels (eV)

	Fenske et al[1]	
	CrF_6^{3-}	FeF_6^{3-}
$3t_{1u}$	28.35	29.31
$2a_{1g}$	17.57	20.11
$2e_g$	11.23	7.42*
$2t_{2g}$	9.18*	5.44
t_{1g}	-1.21	-1.19
t_{2u}	-1.21	-1.19
$2t_{1u}$	-1.44	-1.42
$1t_{2g}$	-2.17	-2.36
$1a_{1g}$	-2.39	-2.69
$1t_{1u}$	-2.52	-2.70
$1e_g$	-3.91	-4.32

	Boudreaux and Dutta-Ahmed[6]		
	CrF_6^{3-}	FeF_6^{3-}	NiF_6^{4-}
$4t_{1u}$	2.87	-4.57	8.24
$3a_{1g}$	-5.72	-11.81	-6.94
$3e_g$	-12.53	-14.27*	-13.46*
$2t_{2g}$	-14.11*	-15.53	-14.32
$2a_{1g}$	-17.34	-17.41	-14.67
$3t_{1u}$	-17.58	-17.94	-15.05
$2e_g$	-18.35	-18.69	-15.92
$1t_{2u}$	-18.69	-18.82	-15.73
$1t_{1g}$	-18.89	-18.90	-16.02
$1t_{2g}$	-18.92	-19.09	-16.46
$2t_{1u}$	-19.12	-19.15	-15.84
$1e_g$	-29.65	-29.21	-27.87
$1a_{1g}$	-32.61	-30.54	-31.76
$1t_{1u}$	-33.50	-30.71	-29.43

Larsson and Connolly [12]

	CrF_6^{3-}		FeF_6^{3-}		NiF_6^{4-}	
	↑	↓	↑	↓	↑	↓
$4a_{1g}$	-.89	-	-.93	-	-.71	-
$3e_g$	-3.93	-.75	-6.85	-3.58*	-4.24	-2.68*
$2t_{2g}$	-5.88*	-2.38	-9.10	-5.32	-5.66	-3.87
$1t_{1g}$	-8.43	-8.48	-8.62	-8.32	-6.96	-6.81
$4t_{1u}$	-8.45	-8.48	-8.70	-8.40	-8.17	-6.93
$1t_{2u}$	-8.86	-8.90	-9.07	-8.78	-7.33	-7.19
$3t_{1u}$	-9.57	-9.56	-9.90	-9.59	-8.11	-7.97
$3a_{1g}$	-9.75	-9.67	-10.26	-9.86	-8.64	-8.48
$1t_{2g}$	-10.05	-9.85	-11.75	-9.92	-8.37	-8.09
$2e_g$	-10.09	-9.44	-12.26	-9.75	-8.41	-7.82
$2t_{1u}$	-27.22	-27.22	-27.49	-27.08	-25.71	-25.44
$1e_g$	-27.22	-27.22	-27.49	-27.08	--25.55	-25.44
$2a_{1g}$	-27.49	-27.49	-27.77	-27.49	-25.86	-25.71
$1t_{1u}$	-50.61	-46.50	-64.29	-58.40	-67.71	-65.51
$1a_{1g}$	-78.10	-73.86	-96.43	-90.41	-104.77	-102.58

* Highest occupied MO.

	Ab-initio[17]		Ab-initio RHF[18]
	NiF_6^{4-}		
	α	β	
$3e_g$	14.3586*		$3e_g$* 18.0608
$2t_{2g}$	13.1041	13.5690	$2t_{2g}$ 7.2080
$3t_{1u}$	12.6366	12.9178	$1t_{1g}$ 6.0384
$1t_{2u}$	12.4785	12.5202	$3t_{1u}$ 5.7392
$1t_{1g}$	12.4554	12.4892	$1t_{2u}$ 5.5488
$2t_{1u}$	10.6322	10.7663	$2e_g$ 5.3584
$2a_{1g}$	9.6541	9.9158	$2t_{1u}$ 4.5152
$1t_{2g}$	9.0905	10.6880	$1t_{2g}$ 4.1072
$2e_g$	7.0064	12.6681	$2a_{1g}$ 3.7264
$1a_{1g}$	-13.9090	-13.7871	$1e_g$ -19.3936
$1t_{1u}$	-13.9487	-13.8165	$1t_{1u}$ -19.5024
$1e_g$	-13.9620	-13.8157	$1a_{1g}$ -19.8016

Clack et al(a) 19

CrF_6^{3-}		FeF_6^{3-}	
$4t_{1u}$	29.89	$4t_{1u}$	31.52
$3a_{1g}$	27.64	$3a_{1g}$	29.43
$3e_g$	25.46	$3e_g$	8.02*
$2t_{2g}$	7.62*	$2t_{2g}$	3.92
$3t_{1u}$	3.67	$3t_{1u}$	2.77

(a) Values tabulated for α-spin

However, the other authors did not include the stabilizing potential of the lattice in their calculations and from our own results, this could result in the eigenvalues being about 15 eV too positive.

5.3.0 Orbital Populations and Atomic Charges

The results of previous calculations are presented in Table 5.2. These population analyses show that although the major charge density is in the 3d orbitals, small but significant contributions are found in the higher valence orbitals. The fluorine 2s and 2p orbitals are nearly fully populated. In comparing the predicted atomic charges it should be borne in mind that Fenske et al[1] utilized +2 wavefunctions whilst the other authors utilized +1 functions and hence the positive charge on the metal is enhanced.

5.4.0 Spin Densities

The extent to which the electron spin is transferred from a metal atom onto the ligands has for a long time been accepted as direct experimental evidence for covalent bonding in MF_6^{n-} complexes. The basic equations for this are well established[22,23] and are derived from the hyperfine interaction of an electron on the metal atom with the nuclear moment of the ligand. The important relations are

$$f_s = 2s\, A_s/A_{2s}$$

$$f_\sigma - f_\pi = 2s(A_\sigma - A_\pi)/A_{2p}$$

where A_s and $A_\sigma - A_\pi$ are hyperfine interaction parameters obtained from experiment, A_{2s} and A_{2p} are analagous quantities for the fluoride ion, s is the total spin of the metal ion and the f parameters are fractional spin densities.

5.2 Orbital Populations and Atomic Charges

	Total Populations					Atomic Charges	
	M(4p)	M(4s)	M(3d)	F(2s)	F(2p)	M	F
CrF_6^{3-} Observed[20]		0.07	4.40[a]			1.53+	
Fenske et al[1]			4.088		5.820	1.92+	0.82-
Brown et al[5]	-0.004	0.172	4.716		5.648	1.124+	0.648-
Boudreaux et al[6]	0.011	0.001	4.463	1.987	5.767	1.525	0.754-
Boudreaux & Harris[7]	0.48	0.24	3.91	1.91	--	1.47+	0.75-
FeF_6^{3-} Observed[20]		0.37	6.30[a]			1.33+	
Fenske et al[1]			6.014		5.827	1.96+	0.83-
Brown et al[5]	0.000	0.366	5.534		5.850	2.100+	0.850-
Boudreaux et al[6]	0.209	0.102	6.300	1.986	5.745	1.388+	0.731-
Boudreaux & Harris[7]	0.46	0.29	6.03	1.90	--	1.24+	0.70-
NiF_6^{4-}							
Brown et al[5]	0.023	0.373	8.034	--	5.921	+1.524	-0.921
Moskowitz et al[18]	0.062	0.071	8.023	1.985	5.986	+1.826	-0.971
Boudreaux et al[6]	0.005	0.042	8.916	1.999	5.841	+1.038	-0.840
Soules et al[17]	0.453	0.618	8.070	1.977	5.681		
Wachters & Nieuwpoort[21]		.0127	8.055	1.995	5.988		

(a) The observed 3d population is really the total π electron population.

The A_s parameter arises from the well-known Fermi contact interaction which is a function of $|\phi_s|^2$, the square of a radial wave function of an α orbital at the fluorine nucleus, which given the s-electron density at the nucleus; A_σ and A_π , on the other hand, are functions of the operator $\frac{1}{r^3}$ for the fluorine 2p orbitals.

Additional expressions relating spin densities to molecular orbital coefficients have been derived by Shulman and Sugano[24]

$$f_s = C_{eg/3}$$

$$f_\sigma - f_\pi = C_{eg/3} - C_{t2g/4}$$

where C_{eg} and C_{t2g} are the coefficients for the highest occupied e_g and t_{2g} orbitals.

From the data presented in Table 5.3 most treatments have managed to produce reasonable estimates of $f_\sigma - f_\pi$, at least for CrF_6^{3-}.

5.5.0 Other Studies

The ions of interest to the present study are FeF_6^{3-}, CrF_6^{3-} and NiF_6^{4-}. However, many calculations have been performed on other first row hexafluoro anions and these will now be summarized.

A semi-empirical based, revised INDO method has been applied to the calculation of charge transfer spectra of first row transition metal complexes by Van der Lugt[25], TiF_6^{3-} has been studied by Tondello[26] who has used the CNDO approach. Clack[27,28] has calculated PE curves and equilibrium geometries of NiF_6^{4-} using his INDO approach, and has related these curves for some $3d^6$ complexes to Tanabe-Sugarno diagrams. The most recent study[29] investigates the High spin-low spin crossover in $3d^5$ systems, their results being comparable to that predicted from pressure dependent magnetic moments.

5.3 Comparison of Reported Experimental and Theoretical Spin Densities

$f_\sigma - f_\pi$ (%)

	CrF_6^{3-} (d^3)	FeF_6^{3-} (d^5)	NiF_6^{4-} (d^8)
Observed	-4.9 ± 0.8[a]	$+3.4 \pm 1.0$[c]	+3.30[a]
	-6.0 ± 1.0[b]	+7.63[b,d]	+3.8[c]
Ab-initio[e]	-5.22		+3.22
Ab-initio[f]: UHF	--	--	+6.32
: RHF	--	--	+4.80
Modified EHM[g]	--	--	+8.3
CNDO[h]	--	--	+1.4
MCZDO[i]	-4.742	+5.140	+0.46
CNDO[j]	-4.1	+7.31	+3.3
Semi-Empirical[k]	-4.989	+2.977	+6.563
Modified EHM[l]	-3.07	+2.80	--
MSXd[m]	-5.8	+5.8	+6.3
Semi-Empirical[n]	-5.2	+4.2	--
Ab-initio[o]	--	--	2.86

(a) R.G. Shulman, K. Knox, Phys. Rev. Letts., 4, 603, (1960).

(b) L. Helmholz, A.V. Guzzo, R.N. Sanders, J. Chem. Phys., 35, 1349, (1961).

(c) J. Owen, J.H.M. Thornley, Rep. Progr. Physics 29, 675, (1966).

(d) L. Helmholz, J. Chem. Physics, 31, 172, (1959).

(e) T.F. Soules Ph.D., Thesis 1969, Purdue University.

(f) J.W. Moskowitz, C. Hollister, C.J. Hornback, H. Brasch, J. Chem. Phys., 53, 2570, (1970).

(g) J. Malek, K. Polak, Phys. Stat. Solidi (B), 52, 407, (1972).

(h) G.C. Allen, D.W. Clack, J. Chem. Soc., A, 2668, (1970).

(i) R.D. Brown, P.G. Burton, Theoret. Chem. Acta, 18, 309, (1970).

(j) D.W. Clack, N.S. Hush, J.R. Yandle, J. Chem. Phys., 57, 3503,(1972).

(k) A.D. Ahmed, E.A. Boudreaux, Inorg. Chem., 12, 1590, (1973).

(l) L.E. Harris, E.A. Boudreaux, Inorg. Chem. Acta, 9, 245, (1974).

(m) S. Larsson, J.W.D. Connoly, J. Chem. Physics, 60, 1514, (1974).

(n) R.F. Fenske, K.G. Caulton, D.D. Radtke, C.C. Sweeney, Inorg. Chem., 5, 960, (1966).

(o) A.J.H. Wachters, W.C. Nieuwpoort, Phys. Rev. B 5, 4291, (1972).

The electronic structures of iron and titanium hexafluoro complexes have been studied[30] using a non-empirical variant of Fenske's method to take two-electron two-centre integrals into account. Calculations for the TiF_6^{3-} complex concerned the overlap integrals, as well as the one-electron two-centre and three-centre integrals. Two-electron two-centre integrals were calculated for all complexes taking 756 nodal points. Except for TiF_6^{3-} neither the relative position of the level nor the metal charge was affected by taking the 2s AO of F into account. The influence of such orbitals in TiF_6^{3-} was due to the high values of the 3d and 2s overlap integrals. The $3e_g$ and $2t_{2g}$ MO were not purely metallic, being a superposition of the 2p and 2s AO of F. The fraction of 4s and 4p orbitals was low in all complexes. The influence of the 3d orbitals changed sharply from doubly to trebly charged ions.

The 3d series transition metal tetroxyanions have been the subject of many theoretical and experimental investigations. The first UV-visible absorption spectra of the permanganate ion (MnO_4^-) was published in 1938 by Teltow[31] and more recent experimental work[32-40] has resulted in the almost definite assignments of all the bands occurring with excitation energies up to ~7eV.

The first molecular orbital study undertaken to investigate the nature of the ground and excited states of the ion was by Wolfsberg and Helmholz[2], and they assigned the first two low lying intense bands of the absorption spectra to $t_1 \longrightarrow t_2$ and $t_2 \longrightarrow t_2$ electronic transitions. Many other semi-empirical studies have since been made [41-51] resulting in many different assignments of the absorption spectra. A review of the early work has been given by Ballhausen and Gray[52].

The first reported ab-initio SCF calculation of the ground state of MnO_4^- was that due to Hillier and Saunders[53] who used a minimal basis set of Slater type orbitals, each STO being expanded in terms of three GTF's. They also calculated the excited states using a configuration interaction procedure. These workers subsequently improved their agreement with the experimental absorption spectra by using a double zeta basis of 3d STO's and by describing the oxygen 2p STO's in terms of four instead of three GTF's[54]. The spectrum of the CrO_4^{2-} ion was also calculated and compared with experiment[55]. Dacre and Elder[56] also obtained a minimal basis set description of the ground state of MnO_4^- using a larger basis of primitive GTF's of near HF quality. They noted that the form of the MO's of e symmetry was quite sensitive to the basis set used and suggested that this fact could account for the difficulties encountered in providing a satisfactory interpretation of the observed absorption spectra.

Hillier and co-workers[57,58] have used ab-initio MO calculations with STO/3G bases to assist the assignment of both the X-ray emission spectra and the valence region XPE spectra of salts containing various oxyanions MO_4^{n-}.

The MnO_4^- ion has been the object of further ab-initio studies. In the first of these, Basch et al[59] employed a minimal basis of contracted GTF's except for double zeta manganese 3d and oxygen 2p representations. These workers also calculated the excited states by virtual orbital theory. In the second extensive study Johansen[60] has used a similar basis to that of Basch et al and he has compared his results with those obtained by the MS-X_α method. In the third study by Wood[61] the bases used were double zeta in metal 4s, 4p and oxygen 2s, 2p and triple zeta for metal 3d representation.

These C.-I. calculations are the most extensive performed for the excited states of MnO_4^- however the results obtained are only in fair agreement with results from the experimental spectra.

Johansen[62] has performed an ab-initio HF calculation and CI on permanganate ion to calculate the deformation density, which is the difference between the electron density distribution and the corresponding density obtained from a superposition of the constituent spherically averaged atoms. Peaks, similar to those found in diffraction experiments, are found at short distances from the transition metal atoms which are interpreted in terms of the specific electronic occupations of the d orbitals.

The electronic triplet transition energies of MnO_4^-, CrO_4^- and $PdCl_6^{2-}$ and the electronic structures and Pd-X bond strengths of PdX_4^{2-} (X = Cl,Br) and PdX_6^{2-} (X = F,Cl,Br) were obtained[63] by the CNDO method.

MS - X_α scattered wave calculations of the MnO_4^- ion have been reported[64,65].

In these calculations, the lattice is simulated by a sphere of positive charge around the ion and orbital energies of the same order as the best LCAO-SCF calculation are obtained. The agreement between calculated and experimental spectra is good.

Connoly et al[66] have applied the MS X_α method to the study of vanadate and chromate ions using the same approximations as the previous work on the permanganate ions. This allows complete comparison of the results for these three isoelectronic complexes. The predicted ordering of the electronic energy levels is in agreement with that predicted by ligand field theory.

The magnitude of the orbital energies are reasonable as they allow a fairly accurate description of the optical properties and the X-ray spectra of these complexes.

Another variant of the HFS technique is the Discrete Variational Method (HFS-DVM) developed by Ellis et al[67]. Two studies utilising this method for studying the electronic structures of transition metal oxyanions have been reported[68,69].

The results from these ground and excited state calculations have shown that all of the complexes have d-orbital populations close to that of the corresponding M^{2+} ions, where two (n+1)s electrons have been removed from M. Thus no transfer of charge was found for the excited states. The calculated singlet transition energies are in good agreement with experimental values and calculated A/D values from the theory of MCD support the uniform assignment of the d° complexes:

$t_1 \longrightarrow 2e(\nu_1)$, $4t_2 \longrightarrow 2e(\nu_2)$, $t_1 \longrightarrow 5t_2(\nu_3)$ and $4t_2 \longrightarrow 5t_2(\nu_4)$.

Transition Metal Halides

Original theoretical interest was centred on NiF_6^{4-} ion which was taken as a hypothetical isolated cluster in perovskite fluoride crystals of the form $KNiF_3$. Basch et al[70] have reported several studies of this and other similar systems. Soules et al[17] as well as investigating CrF_6^{3-} have studied NiF_6^{4-}. The many centre integrals in their method have been approximated with the Mulliken method although their calculations, when CI is included, provide a good calculated electronic spectrum of $KNiF_3$. Wachters and Nieuwpoort[21] have performed ab-initio calculations on several states of the NiF_6^{4-} ion using an extended GTF basis set.

Several non ab-initio studies of the NiF_6^{4-} ion have been made notably Offenhartz[71] and Malek and Polak[72]. Offenhartz employed the 'average of configuration' Roothaan method whilst the second study utilized a parameter free SCCC and obtained values of the covalency parameter and the crystal field splitting constant.

The MnF_6^{4-} 'cluster' has also been extensively studied notably by Freeman and Ellis[73], Matsuoka[74] and Lohr[75]. Freeman and Ellis have performed a fully variational calculation and the charge and spin densities result in a nuclear form factor which is contracted relative to the free ion value. The second study was performed using a RHF method. All many centre integrals were evaluated rigorously however, the poor agreement obtained between calculated and experimental parameters was attributed to the core electrons being treated as point charges. Lohr has used the INDO method in the investigation of the radial expansion of 3d orbitals in $KMnF_3$, $RbMnF_3$ and MnF_2.

Since two adjacent hexafluoride 'clusters' in these perovskite compounds share a common fluorine corner they have recently been studied with regard to the electronic pair interactions of the metal centres[76].

In some ways, theoretical inorganic chemistry is developing as its experimental counterpart has; simply change the ligand and perform more calculations. It would seem justified to develop and test better models for the simpler complexes such as the hexafluorides and the oxyanions before proceeding to more chemically significant problems. Despite this, calculations are now appearing for the chloro and cyano analogues as evidenced by Hillier et al[77] who have studied $CoCl_4^{2-}$ and Clack and Monshi[78] who investigated $Fe(CN)_6^{4-}$ and $Fe(CN)_6^{3-}$.

References : Chapter 5

1. R.F. Fenske, K.G. Caulton, D.D. Radtke, C.C. Sweeney, Inorg. Chem., 5, 951, (1966).

2. M. Wolfsberg, L. Helmholz, J. Chem. Phys., 20, 837, (1952).

3. I. Shavitt, Methods in Computational Phys., Vol. 2, Academic Press New York, 1963, p. 1.

4. J.W. Richardson, W.C. Nieuwpoort, R.R. Powell, W.F. Edgell, J. Chem. Phys., 36, 1057, (1962).

5. R.D. Brown, P.G. Burton, Theor. Chem. Acta, 18, 309, (1970).

6. A. Dutta-Ahmed, E.A. Boudreaux, Inorg. Chem., 12, 1590, (1973).

7. L.E. Harris, E.A. Boudreaux, Inorg. Chem. Acta, 9, 245, (1974).

8. M.F. Guest, M.B. Hall, I.H. Hillier, Mol. Phys., 25, 629, (1973).

9. E. Clementi, J. Chem. Phys., 40, 1944, (1964); IBM Report RJ-256.

10. S. Larsson, E.K. Vinikka, M.L. De Siqueira, J.W.D. Connolly, Int. J. Quantum Chem. Symp. No. 8, 145, (1974).

11. S. Larsson, Physics Letters, 45A, 185, (1973).

12. S. Larsson, J.W.D. Connolly, J. Chem. Phys., 60, 1514, (1974).

13. S. Larsson, J.W.D. Connolly, Chem. Phys. Letts., 20, 323, (1973).

14. M.L. De Siqueira, S. Larsson, J.W.D. Connolly, J. Phys. Chem. Solids, 36, 1419, (1975).

15. J.C. Slater, Phys. Rev., 76, 1592, (1949).

16. R.E. Watson, Phys. Ref., 111, 1108, (1958).

17. T.F. Soules, J.W. Richardson, D.M. Vaught, Phys. Rev. B, 3, 2186, (1971).

18. J.W. Moskowitz, C. Hollister, C.J. Hornback, H. Basch, J. Chem. Phys., 53, 2570, (1970).

19. G.C. Allen, D.W. Clack, M.S. Farrimond, J. Chem. Soc. A, 2728, (1971).

20. G. Leonhardt, A. Meisel, J. Chem. Phys., 52, 6189, (1970).

21. A.J.H. Wachters, W.C. Nieuwpoort, Phys. Rev., B 5, 4291, (1972).

22. W. Marshall, R. Stuart, Phys. Rev., 123, 2048, (1961).

23. A. Abragam, Principles of Nuclear Magnetism, Clarendon Press, Oxford, 1962, p.172.

24. R.G. Shulman, S. Sugarno, Phys. Rev., 130, 506, (1963).

25. W. Th. A.M. Van der Lugt, Int. J. Quant. Chem., 6, 859, (1972).

26. E. Tondello, Gazz. Chem. Italiana, 104, 953, (1974).

27. D.W. Clack, Mol. Phys., 27, 1513, (1974).

28. D.W. Clack, W. Smith, J. Chem. Soc. Dalton 18, 2015, (1974).

29. D.W. Clack, W. Smith, Theor. Chim. Acta, 36, 87, (1974).

30. V.A. Glebor, V.S. Nefedov, Koord. Khim, 1, 202, (1975).

31. J. Teltow, Z. Phys. Chem. B 40, 397, (1938); B 43, 198, (1939).

32. A. Carrington, M.C.R. Symons, J. Chem. Soc., 3373, (1956).

33. S.L. Holt, C.J. Ballhausen, Theor. Chim. Acta (Berl.), 7, 313, (1967).

34. P. Mullen, K. Schwochau, C.K. Jorgensen, Chem. Phys. Letts., 3, 49, (1969).

35. P. Day, L. DiSipio, L. Oleari, Chem. Phys. Letts., 5, 533, (1970).

36. L.W. Johnson, S.P. McGlynn, Chem. Phys. Letts., 10, 595, (1971).

37. L.W. Johnson, E. Hughes Jr., S.P. McGlynn, J. Chem. Phys., 55, 4476, (1971).

38. L.W. Johnson, S.P. McGlynn, J. Chem. Phys., 55, 2985, (1971).

39. J.C. Collingwood, P. Day, R.G. Denning, D.J. Robbins, L. DiSipio, L. Oleari, Chem. Phys. Letts., 13, 567, (1972).

40. C.J. Ballhausen, I. Trabjerg, Mol. Phys., 24, 689, (1972).

41. C.J. Ballhausen, A.D. Liehr, J. Mol. Spectry., 2, 342, (1958); 4, 190, (1960).

42. R.F. Fenske, C.C. Sweeney, Inorg. Chem., 3, 1105, (1964).

43. A. Viste, H.B. Gray, Inorg. Chem., 3, 1113, (1964).

44. L. Oleari, G. DeMichelis, L. DiSipio, Mol. Phys., 10, 97, (1966); 10, 111, (1966).

45. R.D. Brown, B.H. James, M.F. O'Dwyer, K.R. Roby, Chem. Phys. Letts. 1, 459, (1967).

46. J.P. Dahl, H. Johansen, Theor. Chim. Acta (Berl.), 11, 8, (1968).

47. J.P. Dahl, C.J. Ballhausen, Advan. Quantum Chem., 4, 170, (1968).

48. R.M. Canadine, R.M., I.H. Hillier, J. Chem. Phys., 50, 2984, (1969).

49. M. Astier, Mol. Phys., 19, 209, (1970).

50. R.D. Brown, B.H. James, T.J.V. McQuade, M.F. O'Dwyer, Theor. Chim. Acta. (Berl.), 17, 279, (1970).

51. R.D. Brown, B.H. James, M.F. O'Dwyer, Theor. Chim. Acta. (Berl), 17, 362, (1970).

52 C.J. Ballhausen, H.B. Gray, Coordination Chem., A.E. Martell (Ed.) New York: Van Nostrand 1971.

53. I.H. Hillier, V.R. Saunders, Proc. Roy. Soc. (Lond.) A 320, 161, (1970).

54. I.H. Hillier, V.R. Saunders, Chem. Phys. Letts., 9, 219, (1971).

55. P. Day, L. DiSipio, L. Oleari, Chem. Phys. Letts., 5, 533, (1970).

56. P.D. Daire, M. Elder, Chem. Phys. Letts., 11, 377, (1971).

57. J.A. Connor, I.H. Hillier, V.R. Saunders, M.H. Wood, M. Barber, Mol. Phys., 24, 497, (1972).

58. J.A. Connor, I.H. Hillier, V.R. Saunders, M. Barber, Mol. Phys., 23, 81, (1972).

59. A.P. Mortola, H. Basch, J.W. Moskowitz, Int. J. Quantum Chem., 7, 725, (1973).

60. H. Johansen, Chem. Phys. Letts., 17, 569, (1972).

61. M.H. Wood, Theor. Chim. Acta, 36, 309, (1975).

62. H. Johansen, Acta Crystall., A 32, 353, (1976).

63. S. Sakaki, H. Kato, Bull. Chem. Soc. Jap., 46, 2227, (1973).

64. K.H. Johnson, F.C. Smith, Chem. Phys. Letts., 10, 219, (1971).

65. K.H. Johnson, F.C. Smith, Phys. Rev. B5, 831, (1972).

66. V.A. Gubanov, J. Weber, J.W.D. Connolly, J. Chem. Phys., 63, 1455, (1975).

67. E.J. Baerends, D.E. Ellis, P. Ros, Chem. Phys., 2, 41, (1973).

68. A. Rauk, T. Ziegler, D.E. Ellis, Theor. Chim. Acta. 34, 49, (1973).

69. A. Rauk, T. Ziegler, E.J. Baerends, Chemical Physics, 16, 209, (1976).

70. J.W. Moskowitz, C. Hollister, C.J. Hornback, H. Basch, J. Chem. Phys., 53, 2570, (1970).

71. P.O.D.Offenhartz, Phys. Rev. B 6, 2876, (1972).

72. J. Malek, K. Polak, Phys. Stat. Solidi B 52, 407, (1972).

73. A.J. Freeman, D.E. Ellis, Phys. Rev. Lett., 24, 516, (1970).

74. O. Matsuoka, J. Phys. Soc. Jap., 28, 1296, (1970).

75. L.L. Lohr, J. Chem. Phys., 55, 27, (1971).

76. J. Ferguson, H.V. Gudel, E.R. Krausz, Mol. Phys., 30, 1139, (1975).

77. I.H. Hillier, J. Kendrick, F.E. Mabbs, C.D. Garner, J. Am. Chem. Soc., 98, 395, (1976).

78. D.W. Clack, M. Monshi, Mol. Phys., 31, 1607, (1976).

6.0 The ESEMO Method

6.1.0 Introduction

The computational demands of ab-initio calculations limits their use for routine studies of simple molecules and, more importantly, for large molecules of chemical significance, ab-initio electronic structure calculations are prohibitive in cost. On the other hand most less rigorous MO methods, whilst computationally less demanding than ab-initio methods, fail to be of any real predictive value for large low-symmetry molecules. The need for a general, non-empirical MO method of intermediate complexity is clear.

Detailed analysis[1] of the form of the LCAO-SCF F matrix elements has shown that it is possible to formulate new molecular orbital schemes of intermediate complexity between present semi-quantitative and ab-initio techniques. This chapter begins with an analysis of the F-matrix structure followed by a description of the matrix element formalism employed in this study. In the next section the methods used in the evaluation of these matrix elements are outlined, followed by further details of the actual methods used in this study.

6.2.0 Structure of the F-matrix

The individual contributions to an element $F_{\mu\nu}$ of the F-matrix in Roothaan's equations comprise:

(1) the kinetic energy of the one-electron distribution defined by the product $(\mu\nu)$ of orbitals μ and ν, $\langle\mu|T|\nu\rangle$,

(2) the attraction of various nuclei of the molecule for that one-electron distribution, $\langle\mu|\sum_{N} V^{N}|\nu\rangle$ and

(3) the interaction of other one-electron distributions ($\lambda\sigma$), occupied with $P_{\lambda\sigma}$ electrons, with the distribution ($\mu\nu$). The bond order elements $P_{\lambda\sigma}$ are calculated from the normalized contribution of the orbitals λ and σ to the various occupied molecular orbitals. This coulomb interaction is always accompanied by an exchange term which reflects the fact that electrons of like spin, respectively $P^{\alpha}_{\mu\nu}$ and $P^{\alpha}_{\lambda\sigma}$ in number for the up-spin case, in both the distributions ($\mu\nu$) and ($\lambda\sigma$) will tend to avoid each other, leading to an overall term $\sum_{\lambda\sigma} \lambda\sigma(\mu\nu|\lambda\sigma) - P^{\alpha}_{\lambda\sigma}(\mu\sigma|\lambda\nu)$ within each $F_{\mu\nu}$.

The magnitude of the individual terms may be roughly judged from consideration of the diffuseness of individual one-electron orbital distributions, and the distance between the charge distributions involved in each interaction, and accordingly it is helpful to arrange the contributions to the F elements according to the number of nuclear centres involved in each interaction. Then in an AO or hybrid orbital nuclear centred basis set $\{\chi\} = \mu,\nu,\lambda,\sigma$ we have, in the UHF formalism, for the α electron set,

$$\chi F^{\alpha}_{\mu_A\nu_A} = \left[\langle\mu_A|T+V^A|\nu_A\rangle + \sum_{\lambda,\sigma}^{A}\left(P_{\lambda\sigma}(\mu_A\nu_A|\lambda_A\sigma_A) - P^{\alpha}_{\lambda\sigma}(\mu_A\sigma_A|\lambda_A\nu_A)\right)\right] + \left[\sum^{B\neq A}\langle\mu_A|V^B|\nu_A\rangle + \sum_{\lambda,\sigma}^{B\neq A} P_{\lambda\sigma}(\mu_A\nu_A|\lambda_B\sigma_B)\right] + \chi D^{\alpha}_{\mu_A\nu_A} \qquad 6.1$$

and

$$\begin{aligned}\chi F^{\alpha}_{\mu_A\nu_B} = \Big[&\langle\mu_A|T+V^A+V^B|\nu_B\rangle - \sum_{\lambda\sigma}^{BA} P^{\alpha}(\mu_A\sigma_A|\lambda_B\nu_B) \\ &+ \sum_{\lambda,\sigma}^{A}\left(P_{\lambda\sigma}(\mu_A\nu_B|\lambda_A\sigma_A) - P^{\alpha}_{\lambda\sigma}(\mu_A\sigma_A|\lambda_A\nu_B)\right) \\ &+ \sum_{\lambda,\sigma}^{B}\left(P_{\lambda\sigma}(\mu_A\nu_B|\lambda_B\sigma_B) - P^{\alpha}_{\lambda\sigma}(\mu_A\sigma_B|\lambda_B\nu_B)\right)\Big] \\ &+ \left[\sum^{C\neq A,B}\langle\mu_A|V^C|\nu_B\rangle - \sum_{\lambda,\sigma}^{C\neq A,B} P_{\lambda\sigma}(\mu_A\nu_B|\lambda_C\sigma_C)\right] + \chi D^{\alpha}_{\mu_A\nu_B}\end{aligned} \qquad 6.2$$

Here the matrix D contains the interactions originating from the interaction of two SBD distributions, or where one SBD integral is premultiplied by a two-centre Bond order matrix element.

Of the terms of F, the one centre $\chi_F{}^\alpha$ elements where $\mu_A = \nu_A$ (the diagonal $\chi_F{}^\alpha$ elements) can be seen to arise from a sum of terms equal to kinetic energy and nuclear attraction of the distribution $(\mu_A\mu_A)$ to nucleus A, reduced by the repulsive interaction of $(\mu_A\mu_A)$ with other electrons on A. This first group of terms in the diagonal F element is often parameterized from ionization potential data (WH-EHMO, SCCC-MO and the CNDO, INDO and NDDO formalisms of Pople et al). The second group of terms in the diagonal elements corresponds to the overall coulomb interaction (nuclear attraction reduced by electronic coulomb replusion) of $(\mu_A\mu_A)$ with other atoms B of the molecule. This type of term is often simplified by taking the interaction to be well represented by the interaction of $(\mu_A\mu_A)$ with the point charge of B. In other cases, notably the CNDO methods, these contributions are simplified by neglecting integrals containing non coincident product distributions $(\lambda_B\sigma_B)$, $\lambda \neq \sigma$.

Since the determination of the coefficients of each AO μ,ν,λ,σ ... in each molecular orbital of the system proceeds by a diagonalization of the F^α matrices, the degree of mixing of the AO's to form MO's very much depends on the magnitude of the off-diagonal connecting F^α elements and the off-diagonal one-centre F^α elements contribute to this mixing.

However, it is the two-centre off-diagonal $\chi_F{}^\alpha$ elements $\chi_{F^\alpha_{\mu_A\nu_B}}$, which play the greatest part in the mixing of the AO's to form MO's. Inspection of the composition of these elements[2] shows that the magnitude of these elements depends upon a complex interplay of positive and negative terms corresponding to repulsive and attractive terms respectively.

In some highly simplified MO methods, these elements are evaluated simply through some proportionality to the geometric or arithmetic means of the diagonal elements, $F^{\alpha}_{\mu_A\mu_A}$ and $F^{\alpha}_{\nu_B\nu_B}$, and in other methods, notably all the NDO methods, CNDO, INDO and NDDO, these two-centre F^{α} elements are parametrized directly from ab-initio calculations on some 'appropriate' diatomic, AB. This latter situation is demanded by the fact that the NDO two-electron integral approximations themselves would eliminate all but minor two-electron contribution to these elements; it of course neglects any contribution from the last two three-centre terms of equation 6.2.

Since the balance between attractive and repulsive terms in these elements will vary particularly widely through inorganic systems where even the qualitative bonding existing between any given pair of atoms can vary greatly from compound to compound, it would appear important to allow for the consequent changes in the degree and nature of covalency from compound to compound by accurately evaluating the balance of contributions to the $\chi_{F^{\alpha}_{\mu_A\nu_A}}$ elements in each case rather than imposing the constraint of a predetermined balance within each parameterized $F_{\mu_A\nu_B}$.

6.3.0 Matrix Element Formalism

The overall scheme described in References 3-5 is denoted as ESEMO. Detailed analysis of the complete Hartree-Fock-Roothaan LCAO-SCF-MO scheme suggests that all four centre, and most three centre, two-electron integrals can be eliminated from the full set of repulsion integrals, and need not be evaluated, if only those terms entering the LCAO SCF F matrix elements involving at most a single bicentric orbital product distribution are retained.

Further studies[6] on HF, H_2O, NH_3, FCN, O_3, OF_2 and the n-alkane series up to pentane utilizing methods which increase in complexity (and rigour) from the basic ESEMO method$^{(E)}$ of equations 6.1 and 6.2 above through to an ab-initio method have been made. These results indicate improvement in the quality of the wavefunction when <u>all</u> single bicentric orbital products are included in the F matrix (see below) denoted <u>ES</u> and further improvement when all diatomic integrals were included as well, denoted <u>ESD</u>, (ESD in fact includes only two centre exchange integrals above ES).

It therefore appeared reasonable that in this present study on the transition metal hexafluoride complexes we begin with methods E and ES with the plan of ultimately developing ESD. We also evaluated a third formalism denoted $ES/_2$ which was a hybrid form of E and ES. The three methods we investigated E, ES and $ES/_2$ will now be discussed.

Using $\hat{T}$ for the kinetic energy operator, and superscripts on the nuclear attraction operators, V, and subscripts on each orbital to denote the atomic centre to which the operator or the orbital belongs, and with the two-electron integral

$$(\mu\nu|\lambda\sigma) = \int \chi_\mu(1)\ \chi_\nu(1)\ ({}^1/r_{12})\ \chi_\lambda(2)\ \chi_\sigma(2)\ d\tau\ ,$$

the explicit form of the one and two centre matrix elements of ${}^{\chi}F$ (given by equations 6.1 and 6.2) are respectively

$$
\begin{aligned}
{}^{\chi}F_{\mu_A\nu_A} = & \underline{\langle \mu_A | \hat{T} + \hat{V}^A + \textstyle\sum{}' \hat{V}^B | \nu_A \rangle} \\
& \underline{+ \sum_\lambda^A \sum_\sigma^A P_{\lambda_A\sigma_A} [(\mu_A\nu_A|\lambda_A\sigma_A) - \tfrac{1}{2}(\mu_A\sigma_A|\lambda_A\nu_A)]} \\
& \underline{+ \sum_\lambda^{B\neq A} \sum_\sigma^{B\neq A} P_{\lambda_B\sigma_B}} [(\mu_A\nu_A|\lambda_B\sigma_B) - \tfrac{1}{2}(\mu_A\sigma_B|\lambda_B\nu_A)] \\
& + \sum_\lambda^{A} \sum_\sigma^{B\neq A} P_{\lambda_A\sigma_B} [(\mu_A\nu_A|\lambda_A\sigma_B) - \tfrac{1}{2}(\mu_A\sigma_B|\lambda_A\nu_A)] \\
& \text{-- -- -- -- -- -- -- -- -- -- --}
\end{aligned}
$$

$$+\sum_{\lambda}^{B\neq A}\sum_{\sigma}^{A} P_{\lambda_B\sigma_A}\left[(\mu_A\nu_A|\lambda_B\sigma_A)-\tfrac{1}{2}(\mu_A\sigma_A|\lambda_B\nu_A)\right]$$

$$+\sum_{\lambda}^{B\neq A}\sum_{\sigma}^{C\neq A,B} P_{\lambda_B\sigma_C}\left[(\mu_A\nu_A|\lambda_B\sigma_C)-\tfrac{1}{2}(\mu_A\sigma_C|\lambda_B\nu_A)\right], \qquad 6.3$$

$$\chi_{F_{\mu_A\nu_B}} = \langle\mu_A|\hat{T}+\hat{V}^A+\hat{V}^B+\sum{}''\hat{V}^C|\nu_B\rangle$$

$$+\sum_{\lambda}^{A}\sum_{\sigma}^{A} P_{\lambda_A\sigma_A}\left[(\mu_A\nu_B|\lambda_A\sigma_A)-\tfrac{1}{2}(\mu_A\sigma_A|\lambda_A\nu_B)\right]$$

$$+\sum_{\lambda}^{B}\sum_{\sigma}^{B} P_{\lambda_B\sigma_B}\left[(\mu_A\nu_B|\lambda_B\sigma_B)-\tfrac{1}{2}(\mu_A\sigma_B|\lambda_B\nu_B)\right]$$

$$+\sum_{\lambda}^{A}\sum_{\sigma}^{B} P_{\lambda_A\sigma_B}\left[(\mu_A\nu_B|\lambda_A\sigma_B)-\tfrac{1}{2}(\mu_A\sigma_B|\lambda_A\nu_B)\right]$$

$$+\sum_{\lambda}^{B}\sum_{\sigma}^{A} P_{\lambda_B\sigma_A}\left[(\mu_A\nu_B|\lambda_B\sigma_A)-\tfrac{1}{2}(\mu_A\sigma_A|\lambda_B\nu_B)\right]$$

$$+\sum_{\lambda}^{C\neq A,B}\sum_{\sigma}^{C\neq A,B} P_{\lambda_C\sigma_C}\left[(\mu_A\nu_B|\lambda_C\sigma_C)-\tfrac{1}{2}(\mu_A\sigma_C|\lambda_C\nu_B)\right]$$

$$+\sum_{\lambda}^{A}\sum_{\sigma}^{C\neq A,B} P_{\lambda_A\sigma_C}\left[(\mu_A\nu_B|\lambda_A\sigma_C)-\tfrac{1}{2}(\mu_A\sigma_C|\lambda_A\nu_B)\right]$$

$$+\sum_{\lambda}^{B}\sum_{\sigma}^{C\neq A,B} P_{\lambda_B\sigma_C}\left[(\mu_A\nu_B|\lambda_B\sigma_C)-\tfrac{1}{2}(\mu_A\sigma_C|\lambda_B\nu_B)\right]$$

$$+\sum_{\lambda}^{C\neq A,B}\sum_{\sigma}^{A} P_{\lambda_C\sigma_A}\left[(\mu_A\nu_B|\lambda_C\sigma_A)-\tfrac{1}{2}(\mu_A\sigma_A|\lambda_C\nu_B)\right]$$

$$+\sum_{\lambda}^{C\neq A,B}\sum_{\sigma}^{B} P_{\lambda_C\sigma_B}\left[(\mu_A\nu_B|\lambda_C\sigma_B)-\tfrac{1}{2}(\mu_A\sigma_B|\lambda_C\nu_B)\right]$$

$$+\sum_{\lambda}^{C\neq A,B}\sum_{\sigma}^{D\neq A,B,C} P_{\lambda_C\sigma_D}\left[(\mu_A\nu_B|\lambda_C\sigma_D)-\tfrac{1}{2}(\mu_A\sigma_D|\lambda_C\nu_B)\right]. \qquad 6.4$$

Three distinct versions of the matrix element formalism are being studied and they are denoted as follows:

(i) E which includes $(\mu_A\nu_B|\lambda_A\sigma_A)$, $(\mu_A\nu_B|\lambda_B\sigma_B)$, $(\mu_A\nu_B|\lambda_C\sigma_C)$ in $F_{\mu_A\nu_B}$ ONLY.

(ii) $ES/_2$ which includes $(\mu_A\nu_B|\lambda_A\sigma_A)$, $(\mu_A\nu_B|\lambda_B\sigma_B)$ in BOTH $F_{\mu_A\nu_B}$ and $F_{\mu_A\nu_A}$.

whilst $(\mu_A\nu_B|\lambda_C\sigma_C)$ are included in $F_{\mu_A\nu_B}$ ONLY.

(iii) ES which includes $(\mu_A\nu_B|\lambda_A\sigma_A)$, $(\mu_A\nu_B|\lambda_B\sigma_B)$, $(\mu_A\nu_B|\lambda_C\sigma_C)$ in BOTH $F_{\mu_A\nu_B}$ and $F_{\mu_A\nu_A}$.

Method E thus includes only those terms in 6.3 and 6.4 underlined in solid line. Method ES includes all those of method E plus the terms underlined in dashed lines in 6.3 and 6.4 whilst in method $ES/2$ the terms underlined with dotted lines are left out of 6.3.

The real distinction between E and ES lies in the fact that the single bicentric distribution integrals (ab/aa), ab/bb) and (ab/cc) are only included when premultiplied by a <u>one centre</u> bond order matrix element in method E, while method ES includes every occurrence of such integrals regardless of the nature of the premultiplying bond order element.

6.4.0 <u>Evaluation of Integrals</u>

The one centre integrals contributing to the one centre <u>F</u> matrix elements are characterised by including integrals with the largest individual magnitudes of all integrals of the SCF equations.

In other words, the strongest interactions experienced by valence electrons of one centre are those interactions firstly with the nucleus and inner shells of the core, and with other valence electrons, of the same centre. In particular it is necessary to employ accurate orbital representations for both the valence orbitals themselves, and the inner shell orbitals, so that these individually large monocentric interactions are estimated accurately. The evaluation of monocentric integrals only occupies a minor fraction of the time required for a complete SCF calculation. All one centre integrals in this study have been evaluated exactly in terms of the multizeta basis.

The various multicentre integrals involved in the approximate F-matrix present varying degrees of difficulty in their evaluation. For large molecular calculations a compromise must be reached, since evaluation techniques for the integrals must be as rapid as possible on one hand, while on the other, the sensitivity of the approximate F-matrix to these integrals requires a certain minimal accuracy in the evaluation of the integrals. One of the major aims of this work is to delineate such an optimal compromise.

Evaluation of two centre integrals is greatly simplified by the use of standard diatomic axes to evaluate integrals between various atom pairs in a molecule, with subsequent transformation of those integrals to molecular parallel axes. This is especially important as in the diatomic axes system, full use can be made of the symmetry of orbitals on each centre with respect to the diatomic axis (i.e. σ,π,δ local symmetry for normal atomic bases (s,p,d)) and this symmetry guarantees that a large number of the integrals in the diatomic axes system are identically zero.

The use of standard diatomic axes, with subsequent transformation to molecular axes, allows ready evaluation of all integrals between equivalent pairs of atoms in the molecule to be achieved with only one set of diatomic integrals for each set of equivalent pairs required. Since the actual transformation is of course much faster than integral evaluation, this procedure produces quite considerable time savings, particularly in high symmetry molecules. For example, for an accurately octahedral hexafluoroanion MF_6^{n-}, only three sets of integrals over diatomic axes are required, M-F, $F_{opposite}$-$F_{opposite}$ and $F_{adjacent}$ - $F_{adjacent}$ to obtain all the two centre molecular integrals required.

The two centre integrals required for the approximate matrix element formalism of this chapter are the one electron integrals $\langle\mu_A|\hat{T}|\nu_B\rangle$, $\langle\mu_A|V^B|\nu_B\rangle$ and $\langle\mu_A|V^B|\mu_A\rangle$, the two electron integrals $(\mu_A\nu_A|\lambda_B\sigma_B)$, and the non-NNDO integrals of the form $(\mu_A\nu_B|\lambda_B\sigma_B)$. Exact evaluation of all two-centre one-electron integrals is retained. For the two-centre two-electron integrals several techniques, apart from exact evaluation in the STF basis, are available to approximate these integrals without the prohibitive cost of exact evaluation:

(i) numerical approximation through the use of single STF's (with Burns exponents which emphasise behaviour of multi-zeta functions out from the nucleus) are capable of reproducing integral values to within a few percent[7].

(ii) the use of the Ruedenberg integral approximation where any bicentric distribution is projected onto a one-centre set of distributions.

(iii) exact evaluation after fitting gaussian functions to the STF basis.

The methods used in this study were methods (ii) and (iii). Thus the matrix element methods using the Ruedenberg approximation will be referred to as E, $^{ES}/_{2}$, ES. The corresponding versions using the technique of fitted gaussian functions to the STF's to evaluate the time consuming $(\mu_A \nu_B | \lambda_A \sigma_A)$ type integrals (otherwise evaluated using the Ruedenberg approximation) are denoted as EG, ESG and $^{ES}/_{2G}$.

In the latter three methods, multicentric two-electron integrals were evaluated either as a two or three gaussian fit to each STF of the multi-zeta basis.

In all these methods the Ruedenberg approximation, method (ii) has been uniformly applied to both one- and two-electron integrals over three centres which are retained in the E, ES and $^{ES}/_{2}$ approaches (i.e. the (ab/cc) and $\langle a|V^C|b\rangle$ integrals are treated eqivalently and are obtained by expansion in terms of (aa/cc) and (bb/cc), and $\langle a|V^C|a\rangle$ and $\langle b|V^C|b\rangle$ integrals respectively).

6.5.0 Core - Valence Separation

In order to simplify molecular calculations, the usefulness has long been recognized of effecting a division of the full set of orbitals of a molecule, which are taken to be largely unaffected by bonding (the atomic-like inner shells), and the set of (outer-most) valence orbitals of each atom, which contribute in the LCAO sense, most substantially to the highest occupied molecular orbitals of the molecule. The nature of the electrons in the valence orbitals is such that their joint character changes markedly on bond formation, unlike those of the inner shells, and these valence electrons are primarily responsible for bonding effects.

Making use of this core/valence separation in molecular calculations means that only the electrons of the valence orbitals need be considered explicitly in any LCAO-SCF procedure, as the inner shell orbitals of each core are regarded as fixed, and serve only to contribute a fixed potential, acting on the valence electrons. This potential is a central potential at each atomic site, and is assumed not to change on bond formation. Since the interaction terms between valence electrons, and the nucleus and inner shell electrons dominate the calculation of relative stability and electronegativity of the various valence orbitals in individual MO's considerable care must be taken in evaluating these terms.

In this work a "point-charge-core-electron" approximation is invoked to estimate the electrostatic effect of core electrons on other centres on both the one and two centre charge distributions of the first centre[8]. However, parallel calculations have been performed which explicitly account for the overlap of core orbitals with neighbouring valence atomic orbitals using a projection technique[9].

6.6.0 Basis Sets Used

Bearing in mind that the purpose of this study was to evaluate the matrix element methods outlined in 6.3 we chose what could be termed a minimal basis set to represent the metal ions studied. The basis used was Richardson's[10] +1 basis which is double zeta in the 3d representations and single zeta for the other orbitals. We chose to represent the Fluorines with Clementi's[11] atomic double zeta basis. Two core-valence separations were made in the study of CrF_6^{3-} and FeF_6^{3-}.

The first included only metal 3d, 4s and fluorine 2s, 2p orbitals in the valence set whilst the metal 1s through 3p, and Fluorine 1s were regarded as non-polarizable core orbitals.

The second included the metal 3s and 3p orbitals as well. These separations reduce the valence orbitals to 30 and 34 respectively as compared to 45 for the full calculations on these complexes.

Richardson has employed a Schmidt orthogonalization for orbitals of the same symmetry and has obtained the representations by comparison with accurate HFAO radial distributions. These are available for a range of 3d representations appropriate to the degree of ionization of the metal atom, though all other orbital representations, including the 4s, are considered to remain unchanged for the various configurations. Full details of the actual basis sets used in this study are given in Appendix 1.

6.7.0 Wavefunction Interpretation

The normal Mulliken population analysis is carried out for each single determinant wave function and the Mulliken spin densities have also been computed. In addition to this analysis, however, a special feature of the program is the capability for employing the Roby "projected-charge" analysis[12]. The Roby analysis determines the total electron density associated with a particular atom of the molecule by operating on the total calculated electron distribution with a sum of projectors onto each orbital of that atom. This analysis is completely complementary to the Mulliken analysis in that the total number of electrons shared by a particular atom in the molecule can be computed rather than just the net charge on the atom, and Roby's method has the decided advantage of yielding well defined values to quantities such as atom populations and bond orders.

For each wave function the dipole moment is routinely calculated by evaluation of $\langle r \rangle$ directly, and then the delocalized canonical MO's

are localized using the Foster and Boys[13] criterion of maximizing the separation of centroids of each electron distribution. These localized orbitals are extremely useful in interpreting the contributions to the dipole moment, in pinpointing changes in the wavefunction calculated under different circumstances and in providing a valence-bond-like picture of the molecular electron distribution.

Finally, in the case of UHF calculation, single annihilation[14] of the major spin contaminant to the UHF wavefunction is routinely performed and the calculated $\langle S^2 \rangle$ before and after annihilation is monitored.

References : Chapter 6

1. R.D. Brown, P.G. Burton, Chem. Phys. Letts., 20, 45, (1973).
2. P.G. Burton, Coord. Chem. Revs., 12, 37, (1974).
3. P.G. Burton, R.D. Brown, Chemical Physics, 4, 220, (1974).
4. P.G. Burton, Chemical Physics, 4, 226, (1974).
5. P.G. Burton, Chemical Physics, 6, 419, (1974).
6. P.G. Burton, N.R. Carlsen, to be published.
7. P.G. Burton, Ph.D. Thesis, Monash, 1973.
8. N.M. Klimenko, M.E. Dyatkind, J. Struct. Chem., 10, 112, (1969).
9. S. Huzinaga, A.A. Cantu, J. Chem. Phys., 55, 5543, (1971).
10. J.W. Richardson, W.C. Nieuwpoort, R.R. Powell, W.F. Edgell, J. Chem. Phys., 36, 1057, (1962).
11. E. Clementi, J. Chem. Phys., 40, 1944, (1964); IBM Report RJ-256.
12. K.R. Roby, Mol. Phys., 24, 81, (1974).
13. J.M. Foster, S.F. Boys, Rev. Mod. Phys., 32, 300, (1960).
14. T. Amos, L.C. Snyder, J. Chem. Phys., 41, 1773, (1964) (Corrected).

7.0 RESULTS AND DISCUSSION

7.1.0 Introduction

The results will be discussed firstly in terms of the gross charge distribution and secondly in terms of the spin distribution. The localization of molecular orbitals, which has been carried out routinely in this study, provides a single number (the centroid of the σ-bonding MO) which is a measure of the extent of delocalization along the M-F bonds. The spin distribution, on the other hand, results from a complex interplay of spin delocalization and spin polarization phenomena. The comparison of our results with experiment will reflect not only on electrostatic and covalency effects in each cluster, but on the ability of our model scheme to adequately account for exchange effects which are centrally important to all magnetic phenomena.

7.2.0 Charge Distributions

Localization of orbitals provides a simple pictorial way of interpreting the cluster wavefunction. The centroid of each localized bonding orbital is the "centre of gravity" of the charge distribution along the bond axis. It is this σ-bond that should provide an indicator of the bonding in these compounds since variations within our model should be reflected by the M-F bond centroid position changes.

The localized orbitals of the systems studied were all generally similar in form, as might be expected, although differences in detail were observed in the nature of these orbitals particularly between different systems. Centred on each fluorine atom were four sp^3 type hybrids, three of which had identical centroids greater than the M-F bond length from the metal, while the fourth, the σ-bonding orbital, centroid was located between the metal and fluorine atoms.

The remaining orbitals are localized on the central metal and these orbitals are characteristic of the metal. The rotational orientations of these lone pairs is arbitrary within the structure of the octahedron but the total α-distribution, β-distribution and their difference should correlate with the map provided by magnetic neutron diffraction.

The complete results of this work are given in Table 1 of Appendix 2 but for ease of discussion Tables 1-5 of this chapter provide the basis for the present analysis.

7.2.1 CrF_6^{3-}

We shall discuss the results in terms of gradual degradation of our model, and note the effect relative to that of ESG : HCC : Small Core : Crystal. The results given by this method indicate that $\langle r \rangle_\beta$ by 0.06Å and also that $\langle r \rangle_\alpha$ is 0.533Å from F^- whilst $\langle r \rangle_\beta$ is 0.463Å from F^-.

If we remove more occurrences of (ab/aa) integrals in the F matrix formalism (which we do when we go from ESG to ES/2G to EG) there is an increase in both $\langle r \rangle_\alpha$ and $\langle r \rangle_\beta$ by 0.05Å each time.

By degrading the core representation (PCC for HCC) we decrease $\langle r \rangle_\alpha$ and $\langle r \rangle_\beta$ by about 0.04Å but $\langle r \rangle_\alpha$ is still less than $\langle r \rangle_\beta$ by 0.052Å.

In going from ESG to ES the integral representation is degraded and there is an increase in both $\langle r \rangle_\alpha$ and $\langle r \rangle_\beta$ although $\langle r \rangle_\beta$ versus $\langle r \rangle_\beta$ is variable.

When valence size is decreased by going from small core to large core $\langle r \rangle_\beta$ is decreased by 0.025Å (0.024 PCC) and $\langle r \rangle_\alpha$ is decreased by 0.010 (0.002 PCC) which indicates that there is not enough metal-core repulsion.

Table 1 : ESG : HCC Approximation

	Large Core	Small Core	Small Core with Crystal
CrF_6^{3-} (M-F 1.933Å)			
Bonding orbital centroids*			
α	1.399	1.402	1.409
β	1.445	1.474	1.470
$f_\sigma - f_\pi$ (Mulliken) %	-4.028	-4.988	-5.017
" (Roby) %	-2.690	-3.428	-3.452
" (Projected) %	-2.246	-2.460	-2.495
FeF_6^{3-} (M-F 1.910Å)			
Bonding orbital centroids*			
α	1.612	1.603	1.603
β	1.388	1.412	1.408
$f_\sigma - f_\pi$ (Mulliken) %	+10.590	+8.663	+8.723
" (Roby) %	+7.464	+5.874	+5.830
" (Projected) %	+10.474	-	+8.609
NiF_6^{4-} (M-F 2.006Å)			
Bonding orbital centroids*			
α		1.687	1.692
β		1.460	1.516
$f_\sigma - f_\pi$ (Mulliken) %		+11.256	+8.621
" (Roby) %		+8.285	+6.010
" (Projected) %		+11.000	+8.441

* distance from metal in Å

Table 2 : ES/2G : HCC Approximation

	Large Core	Small Core	Small Core Crystal
CrF_6^{3-}			
Bonding orbital centroids*			
α	1.456	-	1.461
β	1.499	-	1.519
$f_\sigma - f_\pi$ (Mulliken) %	-3.299	-4.410	-4.410
" (Roby) %	-2.254	-3.050	-3.065
" (Projected) %	-1.422	-1.720	-1.741
FeF_6^{3-}			
Bonding orbital centroids*			
α	1.598	1.594	1.594
β	1.390	1.404	1.402
$f_\sigma - f_\pi$ (Mulliken) %	+10.809	+9.239	+9.298
" (Roby) %	+7.645	+6.353	+6.410
" (Projected) %	+10.892	+9.304	+9.360

* distance from metal in Å.

Table 3 : EG : HCC Approximation

CrF_6^{3-}	Large Core	Small Core	Small Core Crystal
Bonding orbital centroids			
α	-	-	1.516
β	-	-	1.572
$f_\sigma - f_\pi$ (Mulliken) %	-4.240	-5.550	-5.559
" (Roby) %	-2.696	-3.467	-3.552
" (Projected) %	-2.203	-2.587	-2.673
FeF_6^{3-}			
Bonding orbital centroids			
α	1.622	1.597	1.597
β	1.375	1.383	1.381
$f_\sigma - f_\pi$ (Mulliken) %	+10.031	+9.648	+9.648
" (Roby) %	+7.523	+6.607	+6.708
" (Projected) %	+10.512	+9.519	+9.518

Table 4 : ESG : PCC Approximation

	Large Core	Small Core	Small Core Crystal
CrF_6^{3-}			
Bonding orbital centroids			
α	1.368	1.369	1.366
β	1.421	1.446	1.418
$f_\sigma - f_\pi$ (Mulliken) %	-4.152	-5.515	-1.550
" (Roby) %	-2.894	-4.015	-4.009
" (Projected) %	-2.143	-2.405	-2.427
FeF_6^{3-}			
Bonding orbital centroids			
α	1.605	1.599	1.599
β	1.369	1.385	1.381
$f_\sigma - f_\pi$ (Mulliken) %	+11.784	+10.438	+10.300
" (Roby) %	+8.363	+7.331	+7.227
" (Projected) %	+11.658	+10.487	+10.159

Table 5 : ES : HCC Approximation

	Large Core	Small Core	Small Core Crystal*
CrF_6^{3-}			
Bonding orbital centroids			
α	1.520	-	1.414
β	1.532	-	1.604
$f_\sigma - f_\pi$ (Mulliken) %	-1.650	-10.11	-13.18
" (Roby) %	-0.784	-13.39	-13.46
FeF_6^{3-}			
Bonding orbital centroids			
α	-	1.622	-
β	-	1.517	-
$f_\sigma - f_\pi$ (Mulliken) %	-	-4.516	-
" (Roby) %	-	-4.379	-

* This calculation converged to a different state.

When the crystal potential is removed $\langle r \rangle_\alpha$ decreases by 0.007Å whilst $\langle r \rangle_\beta$ increases by 0.004Å.

7.2.2 FeF_6^{3-}

In this case ESG : HCC : small core : crystal indicates that $\langle r \rangle_\alpha$ is greater than $\langle r \rangle_\beta$ by 0.195Å which places $\langle r \rangle_\alpha$ 0.307Å from F^- and $\langle r \rangle_\alpha$ 0.502Å from F^-.

There is a small decrease in both $\langle r \rangle_\alpha$ and $\langle r \rangle_\beta$ (by 0.01 and 0.03Å respectively) when more (ab/aa) integrals are removed by going from ESG through ES/2G to EG.

A further decrease in both $\langle r \rangle_\alpha$ and $\langle r \rangle_\beta$ (0.005 and 0.03 respectively) is noted when the core representation HCC is degraded to PCC but $\langle r \rangle_\alpha$ is still greater than $\langle r \rangle_\beta$ by about 0.2Å.

As we degrade the integral representation ESG to ES there is an overall increase in $\langle r \rangle_\alpha$ and $\langle r \rangle_\beta$ but the trend is variable.

When the valence size is decreased, small core to large core, $\langle r \rangle_\alpha$ increased by 0.009 (0.005 PCC) whilst $\langle r \rangle_\beta$ decreased by 0.024 (0.026 PCC)

No change is noted in $\langle r \rangle_\alpha$ when the crystal potential is removed however $\langle r \rangle_\beta$ increased by 0.004Å.

7.2.3 NiF_6^{4-}

$\langle r \rangle_\alpha$ is greater than $\langle r \rangle_\beta$ by 0.176Å for ESG : HCC : small core : crystal which puts $\langle r \rangle_\alpha$ 0.314Å from F^- and $\langle r \rangle_\beta$ 0.492Å from F^-. When the crystal potential is removed $\langle r \rangle_\alpha$ decreased by 0.005Å whilst $\langle r \rangle_\beta$ decreased by 0.056Å.

7.2.4 The Series CrF_6^{3-}, FeF_6^{3-} and NiF_6^{4-}

It appears that $\langle r \rangle_\alpha$ is significantly greater than $\langle r \rangle_\beta$ for d^5 and d^8 systems (about 0.21Å for FeF_6^{3-} and 0.17Å for NiF_6^{4-}) whereas $\langle r \rangle_\alpha$ is only slightly less than $\langle r \rangle_\beta$ for d^3 (about 0.06Å for CrF_6^{3-}). So removing a sigma antibonding electron (i.e. e_g^*) causes $\langle r \rangle_\alpha$ to move towards the metal since there is less repulsion in the σ system. Adding π* electrons (i.e. t_{2g}^*) going from d^5 to d^8 causes $\langle r \rangle_\beta$ also to move towards the fluorine presumably for the same reason of π* being localized on the metal (like σ*) causing increasing repulsion for the σ bonding pair.

If we remove valence electrons from the SCF and place them in core (non-polarizable 3s + 3p electrons) all changes in centroid lengths are less than 0.025Å and are mainly decreased. The point charge core causes movement of $\langle r \rangle_\alpha$ towards the metal in CrF_6^{3-} and away from the metal in FeF_6^{3-} whilst $\langle r \rangle_\beta$ in both systems moves closer to the metal by about 0.025Å when compared to the small core values. Thus the point charge representation of 3s and 3p electrons allows the bonding electrons to move too close to the metal nucleus. However, the HCC correction doesn't alter this by much, so the correction by HCC doesn't work perfectly to overcome the increase in size of the core (i.e. Metal core orbitals don't overlap strongly with Fluorine contracted valence orbitals).

The overall comparison of matrix element method and integral precision leads to difficult to interpret variations in $\langle r \rangle_\alpha$ and $\langle r \rangle_\beta$ with regard to sign. Removal of (ab/aa) integrals from F matrix elements (ESG → ES/2G → EG and ES → ES/2 → E) leads to centroid variations which differ in a non uniform way between CrF_6^{3-}, FeF_6^{3-} and NiF_6^{4-}.

However, the magnitudes of the variations are smaller for (ESG → ES/2G) than for (ESG → EG) significantly. Thus the (ab/aa) integrals in the diagonal one-centre F-matrix elements is the most important addition to the original ESEMO (E), while extra (ab/cc) integrals in two-centre F-matrix elements have secondary importance; presumably many more cancellations occur for (ab/cc) contributions (other than Pcc (ab/cc) of course) in $F_{\mu_A\nu_B}$ than for the P_{AB} (aa/ab) contribution in $F_{\mu_A\nu_A}$ as one would expect from inspection.

Degrading the numerical precision of (ab/aa) integrals in general leads to an increase in centroid length in either small core or large core CrF_6^{3-} and FeF_6^{3-} calculations. Thus the Ruedenberg approximation doesn't work the same for integrals mainly involving metal orbitals as it does for fluorine orbitals but no generalization is possible as the variations are system dependent. However the large variation in $\langle r \rangle_\alpha$ and $\langle r \rangle_\beta$ when the Ruedenberg approximation is used point to the necessity of avoiding this approximation for (ab/aa)'s. This is as one would expect theoretically, since $\langle a|V^a|b\rangle$'s are already evaluated exactly in either scheme and hence exact (ab/aa)'s should be required to get good "balance".

The analysis so far indicates a dependence on the method of integral evaluation for the ESEMO integrals. Table 6 gives numerical values for several types of selected integrals evaluated by the Ruedenberg approximation, two fitted GTF's per STF and three fitted GTF's per STF. Inspection of the table reveals considerable variation between integral values as evaluated by the Ruedenberg formula and 2 GTF's/STF. The improvement in precision in going from two fitted gaussians to three fitted gaussians is not great, particularly when weighed against the computational effort involved.

Table 6 : Numerical Values of Integrals Evaluated by Different Techniques : FeF_6^{3-}

$(\mu_A \nu_A | \lambda_B \sigma_B)$

	Burns	Multi-Zeta	Multi-Zeta (2G)	Multi-Zeta (3G)
ss|ss	7.69516446	7.98521765	7.9906403	7.9826578
ss|ππ	8.06482820	8.35736924	8.3645864	8.3549043
ss|sπ	-1.27595044	-1.21608352	-1.2305456	-1.2159546
σπ|σπ'	0.0970040	0.02745703	0.0275187	0.0274546
πδ|sσ	0.18435187	0.16429741	0.1667077	0.1642295
δδ|σσ	7.29181121	7.28665984	7.2745760	7.2838902
ss|ss	5.33059698	5.33053286	5.3299457	5.3299804
ss|ππ	5.27258974	5.26909037	5.2681023	5.2688614

FeF_6^{3-}

$(\mu_A \nu_B | \lambda_B \sigma_B)$

		Ruedenberg	2G/STF	3G/STF
ss	ss	-.4463442	-.3329516	-.3306966
sσ	σσ	.0342412	.0457608	.0449873
sσ	σπ	.0020398	-.0325711	-.0347256
sσ	πs	.0159748	.0404992	.0406709
sσ	πσ	.0224458	.0940046	.0950193

FeF_6^{3-}

$(\mu_A \nu_B | \lambda_A \sigma_A)$

		Ruedenberg	2G/STF	3G/STF
ss	ss	2.2010477	.8395354	.8263487
ss	ππ	.1089950	.1582440	.1566829
ss	σσ	.1311993	.2585738	.2548236
ss	ππ	.0911034	.2019588	.1989922
ss	ππ	1.9441962	1.9343879	1.9060173
ss	σδ	1.2180665	1.7882483	1.7629084
ss	πδ	-.630124	-.0244789	.0042695
ss	δδ	.0126953	.0387195	.0388450
ss	σs	.1420393	.2842744	.2808798
σs	ss	.0090440	.0017115	.0020400
σs	πδ	-.0164883	.1357536	.1575390
σs	δδ	.001687	.0014281	.0010167
σs	σδ	.1823782	.1317858	.1530299
σs	σs	.0917831	.1418288	.1647827
ss	ss	-.0589648	.0417989	.0592791
sσ	ss	1.8604698	1.6864660	1.615327

For instance, to evaluate all integrals for a S.C. HCC calculation using the Ruedenberg approximation takes 89 minutes, using 2 GTF's/STF takes 201 minutes and 3 GTF's/STF takes 352 minutes.

It is assumed that the core orbitals are initially non overlapping and that each inner shell orbital of the cores behaves as an inner SCF molecular orbital. When use is made of the Huzinaga-Cantu Core (HCC) effective hamiltonian, valence orbitals which overlap core orbitals are destabilized. The effect is similar to an anti bonding destabilization of the valence orbitals as though each formed predominantly the antibonding component of a bonding/antibonding couple with each overlapping core function. The destabilization of each orbital depends on its degree of overlap with core functions and is thus in accord with simple chemical bonding concepts. These destabilizations are given in Table 7. The effective "electronegativity" of metal outer valence orbitals is significantly affected (2 - 3 eV) by this connection. This indicates that relegation of Fluorine 1s and Metal 1s, 2s and 2p orbitals to the non-polarizable core is reasonable only in conjunction with the HCC connection. Further, there are grounds for persisting with the Metal 3s and 3p orbitals in the core when HCC hamiltonian is used. Overall the HCC approximation produces better SCF results than the PCC approximation although in the FeF_6^{3-} bonding orbital centroids the differences are minimal. It appears that if we discard the 3s and 3p orbitals from the valence shell and place them in the core we should utilize the Huzinaga-Cantu Core approximation to obtain best results because the variation of results between LC and SC under the HCC approximation is less than that under the PCC approximation. This also is an important result because it indicates that the HCC approximation is better able to accommodate the extensiveness of the 3s and 3p than the PCC model.

Table 7 : Corrections to H-Matrix

	CrF_6^{3-}		FeF_6^{3-}		NiF_6^{4-}
Orbitals' Corrections	L.C.	S.C.	L.C.	S.C.	S.C.
M $3d_{z^2}$	2.507660	2.507660	1.297626	1.297626	0.349074
M $3d_{x^2-y^2}$	2.507660	2.507660	1.297626	1.297626	0.349074
M 4s	2.915508	2.915508	2.874122	2.874122	2.03901
M 3s	0.000058		0.000016		0.00003
M $3p_x$	0.000132		0.000027		0.00002
M $3p_y$	0.000132		0.000027		0.00002
	0.000132		0.000027		0.00002
M $3p_z$	0.004669	0.076041	0.004856	0.063606	0.002302
F $2p_x$	0.057853	0.493526	0.059875	0.461717	0.030799
F $2p_y$	0.000275	0.008492	0.000299	0.007123	0.000126
F $2p_z$	0.000275	0.008492	0.000299	0.007123	0.000126

Thus, although the energy of interaction of core orbitals and neighbouring orbitals can be estimated by PCC there is a significant overlap effect which we need to account for. In other words if we skimp on the SCF and put more orbitals in the core we really do need the HCC treatment to correct for neighbouring core orbital to valence orbital overlaps.

Complete details of the best wavefunctions for each of the systems CrF_6^{3-}, FeF_6^{3-} and NiF_6^{4-} are given in Table 4 of Appendix 2. From the atomic orbital occupancy of these systems as derived by the Mulliken analyses of our cluster wavefunctions, the occupation of the central ions 4s orbital is significant. One can infer from this substantial involvement of the 4s orbital in the bonding of the octahedral fluoride complexes. For this reason the basis set representation for the 4s orbital is presumably quite important in the accurate analysis of transition metal complexes. It is the author's opinion that improved results could be obtained after some optimization of Richardson's single zeta representation for the 4s orbital in the molecular environment. However, the primary object was to test the behaviour of the model as a preliminary step in obtaining optimum results.

It was found that the fluorine ligand $2p\pi$ orbitals were consistently almost completely occupied (>97%) consistent with the accepted non-π-bonding characteristics of the fluorine ligand, covalent bonding occurring predominantly through the $2p\sigma$ orbitals.

It can be seen from Tables 1-4 of Appendix 2 that the inclusion of the extra cluster lattice potentials appropriate to each system in its crystalline lattice (assuming all metal and fluoride ions throughout the crystal have the SCF charges of the corresponding ions in the cluster) has little effect on the cluster wavefunctions derived on the

assumption that the cluster is completely "isolated", i.e. cases where this cluster approximation is crystallographically reasonable (CrF_6^{3-} in K_2NaCrF_6 and FeF_6^{3-} in K_2NaFeF_6). Again these results show the stronger influence of the cluster in the NiF_6^{4-} in $KNiF_3$ case. In the former complexes, a large number of highly symmetrically disposed ions surround the clusters and so there is little electrostatic differentiation between central ion and ligand. The actual values of the extra-cluster potentials at the central ion and at the ligand are given in Table 8.

It appears that for the cubic systems considered the central ion is in fact stabilized slightly with respect to the fluoride ions by the purely electrostatic potential of the surrounding lattice. This is contrary to the impression one would gain from considering purely nearest neighbour ions around each cluster. This has an attendant small influence on the charge distribution. Overall however the lattice has a powerful stabilizing influence on the electronic structure of the anions (see Fig. 1).

The crystal potential has a negligible effect on $\langle r \rangle_\alpha$ and $\langle r \rangle_\beta$ in CrF_6^{3-} and FeF_6^{3-} as one might expect since these complexes exist as isolated clusters in their crystal lattices. On the other hand, order of magnitude greater changes (0.056Å in $\langle r \rangle_\beta$) occur for NiF_6^{4-} when the crystal potential is removed. The crystal potential moves $\langle r \rangle_\beta$ out strongly toward the fluorine ($\langle r \rangle_\alpha$ less strongly) in response to the proximity of other Ni^{2+} atoms on the other side of F^- outside the cluster. So the cluster approximation is much worse for shared clusters.

The electrostatic differentiation between "Ni^{++}" and "F^-" in $KNiF_3$ which we estimate from a self-consistent Madelung potential calculation to be ~2.4 eV favouring F^- is an order of magnitude greater

Table 8 : SCF Electrostatic Potentials at Cluster ion Sites due to extra-cluster Lattice (SUF Contribution to $^{\chi}H_{\mu\mu}$)

$\langle\mu|V^{\ell}|\mu\rangle$ (eV)

System	Lattice	μ on M	μ on F
CrF_6^{3-}	K_2NaCrF_6	-15.995	-15.694
FeF_6^{3-}	K_2NaFeF_6	-16.544	-16.250
NiF_6^{4-}	$KNiF_3$	-25.028	-27.408

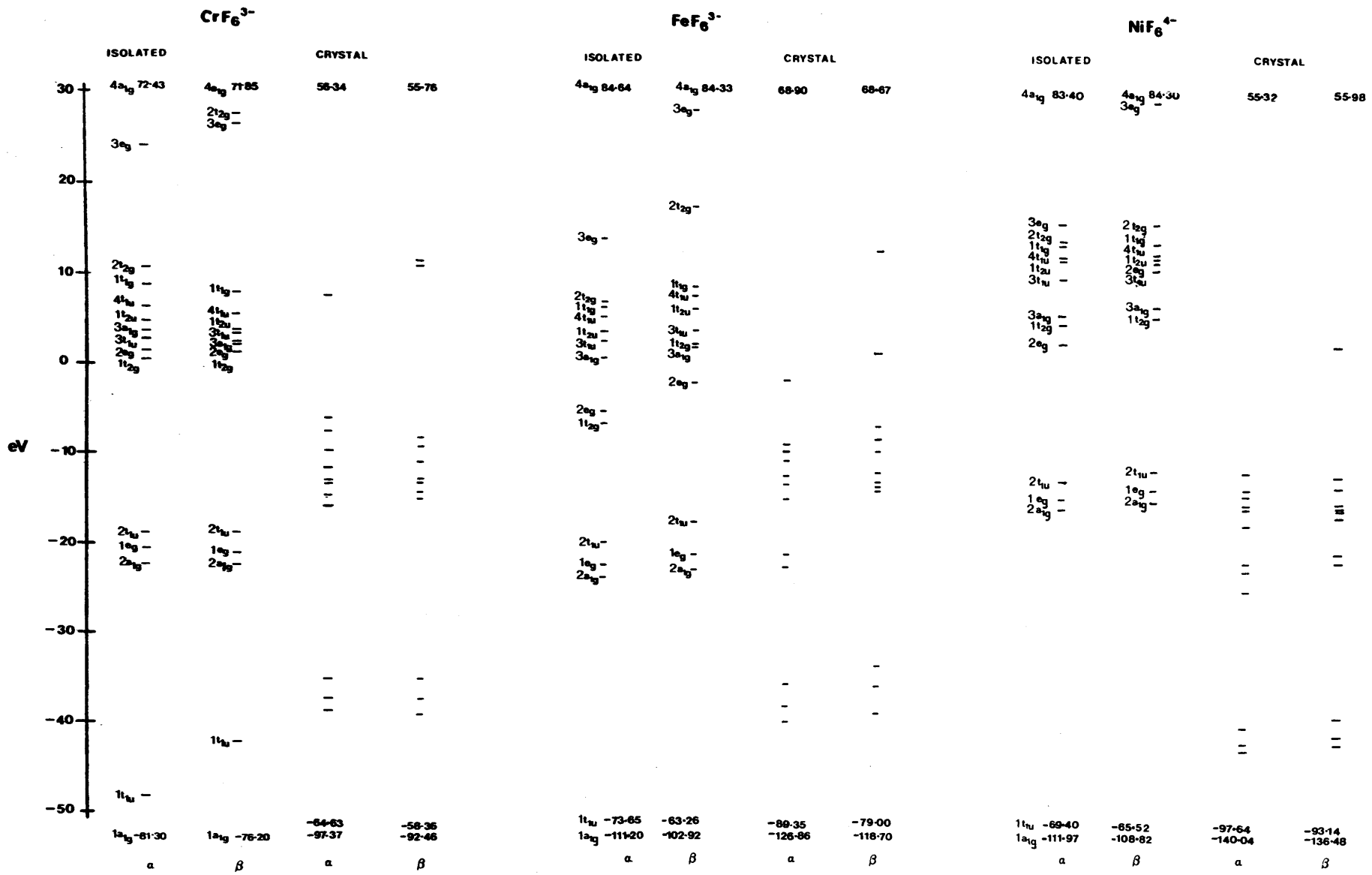

Fig. 1. Electronic Energy Levels and Orbital Symmetries for the Best Calculations on CrF_6^{3-}, FeF_6^{3-}, NiF_6^{4-}

NOTE: The crystal potential does not change the ordering of energy levels within any one complex.

than for the isolated cluster systems K_2NaCrF_6 and K_2NaFeF_6. This is the most sophisticated determination of the influence of the lattice potential yet attempted and the results lead one to completely reject the common assumption of early cluster computations (on $KNiF_3$) that the crystal environment caused a "flat" potential across the cluster and so could be ignored.

7.2.5 Localized Orbital Plots

Electron density plots have been made for the best calculations on the series CrF_6^{3-}, FeF_6^{3-} and NiF_6^{4-} (ESG : HCC : Small Core : Crystal) and these are presented in Figs. 2 - 4 overleaf.

The CrF_6^{3-} α-bond is pear-shaped and extends over most of the Cr - F internuclear region whilst the corresponding FeF_6^{3-} and NiF_6^{4-} orbitals are more oblate and are localized towards the fluorine. This is in accord with the increasing ionic character from CrF_6^{3-} - FeF_6^{3-} - NiF_6^{4-} and also the fact that the latter two complexes have antibonding σ electrons, unlike d^3 systems. The β-bonding orbitals are all similar in shape and size.

CRFG SMALL CORE SINGLE ZETA PLOTS ESG + CRYSTAL POT FIG 2a
CHROMIUM-FLUORINE ALPHA BONDING MO +XTAL POT

MAP THROUGH Y= .0000000 DIMENSIONS X= 4.0000000 BY Z= 4.0000000
DENSITY MAXIMUM .10000000+01 FACTOR BETWEEN INTERVALS .50000000+00
THE DENSITIES ARE SCALED TO .10000000+01

A	1	.35367432-05
		.19073486-05
C	2	.38146973-05
		.76293945-05
D	3	.15258789-04
		.30517578-04
G	4	.61035156-04
		.12207031-03
I	5	.24414063-03
		.48828125-03
K	6	.97656250-03
		.19531250-02
L	7	.39062500-02
		.78125000-02
O	8	.15625000-01
		.31250000-01
Q	9	.62500000-01
		.12500000+00
S	0	.25000000+00
		.50000000+00
U	-	.10000000+01

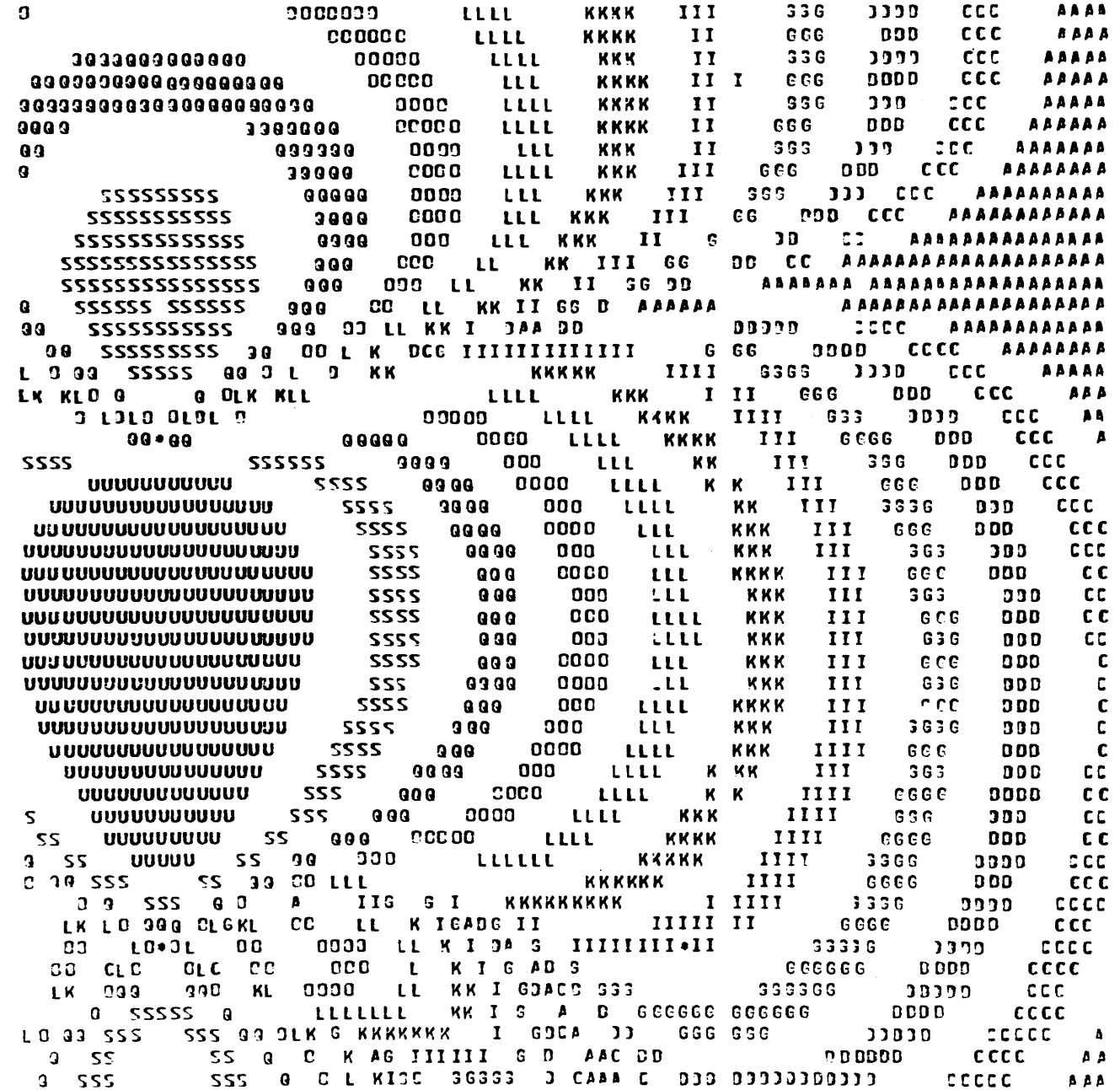

CRF6 SMALL CORE SINGLE ZETA PLOTS ESG • CRYSTAL POT FIG 2b
CHROMIUM-FLUORINE BETA BONDING MO •XTAL POT

MAP THROUGH Y= .0000000 DIMENSIONS X= 4.0000000 BY Z= 4.0000000
DENSITY MAXIMUM .10000000•01 FACTOR BETWEEN INTERVALS .50000000•00
THE DENSITIES ARE SCALED TO .10000000•01

A	1	.95367432-06
		.19073486-05
C	2	.38146973-05
		.76293945-05
D	3	.15258789-04
		.30517578-04
G	4	.61035156-04
		.12207031-03
I	5	.24414063-03
		.48828125-03
K	6	.97656250-03
		.19531250-02
L	7	.39062500-02
		.78125000-02
O	8	.15625000-01
		.31250000-01
Q	9	.62500000-01
		.12500000•00
S	0	.25000000•00
		.50000000•00
U	-	.10000000•01

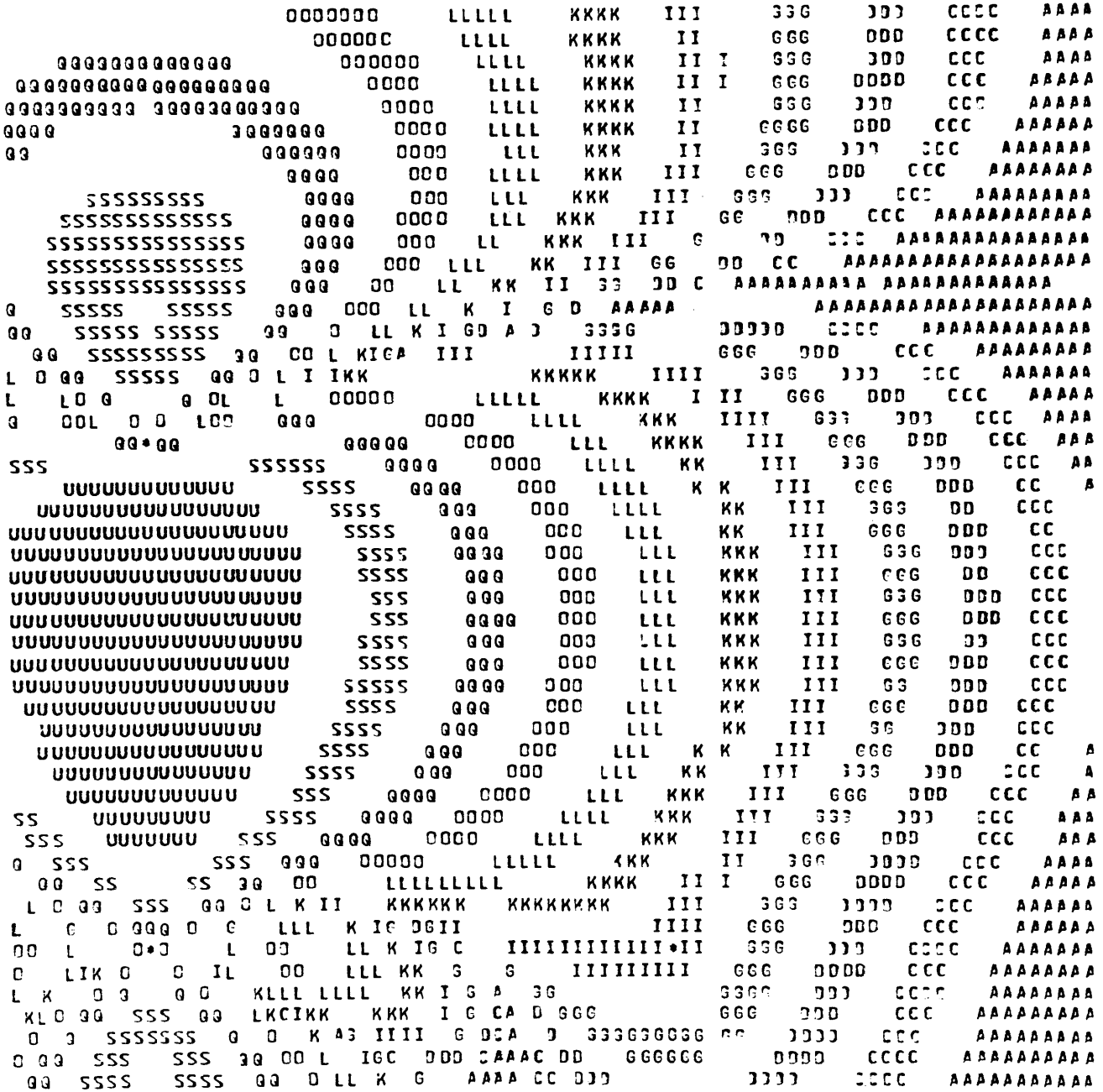

FEF6 10 FN BASIS SINGLE ZETA PLOTS
FE-FL ALPHA BONDING MO IN X-Z PLANE

FIG 3a

MAP THROUGH Y= .0000000 DIMENSIONS X= 4.0300000 BY Z= 4.0000000
DENSITY MAXIMUM .10000000+01 FACTOR BETWEEN INTERVALS .50000000+00
THE DENSITIES ARE SCALED TO .10000000+01

A	1	.95367431-06
		.19073486-05
C	2	.38146973-05
		.76293945-05
D	3	.15258789-04
		.30517578-04
G	4	.61035156-04
		.12207031-03
I	5	.24414063-03
		.48828125-03
K	6	.97656250-03
		.19531250-02
L	7	.39062500-02
		.78125000-02
O	8	.15625000-01
		.31250000-01
Q	9	.62500000-01
		.12500000+00
S	0	.25000000+00
		.50000000+00
U	-	.10000000+01

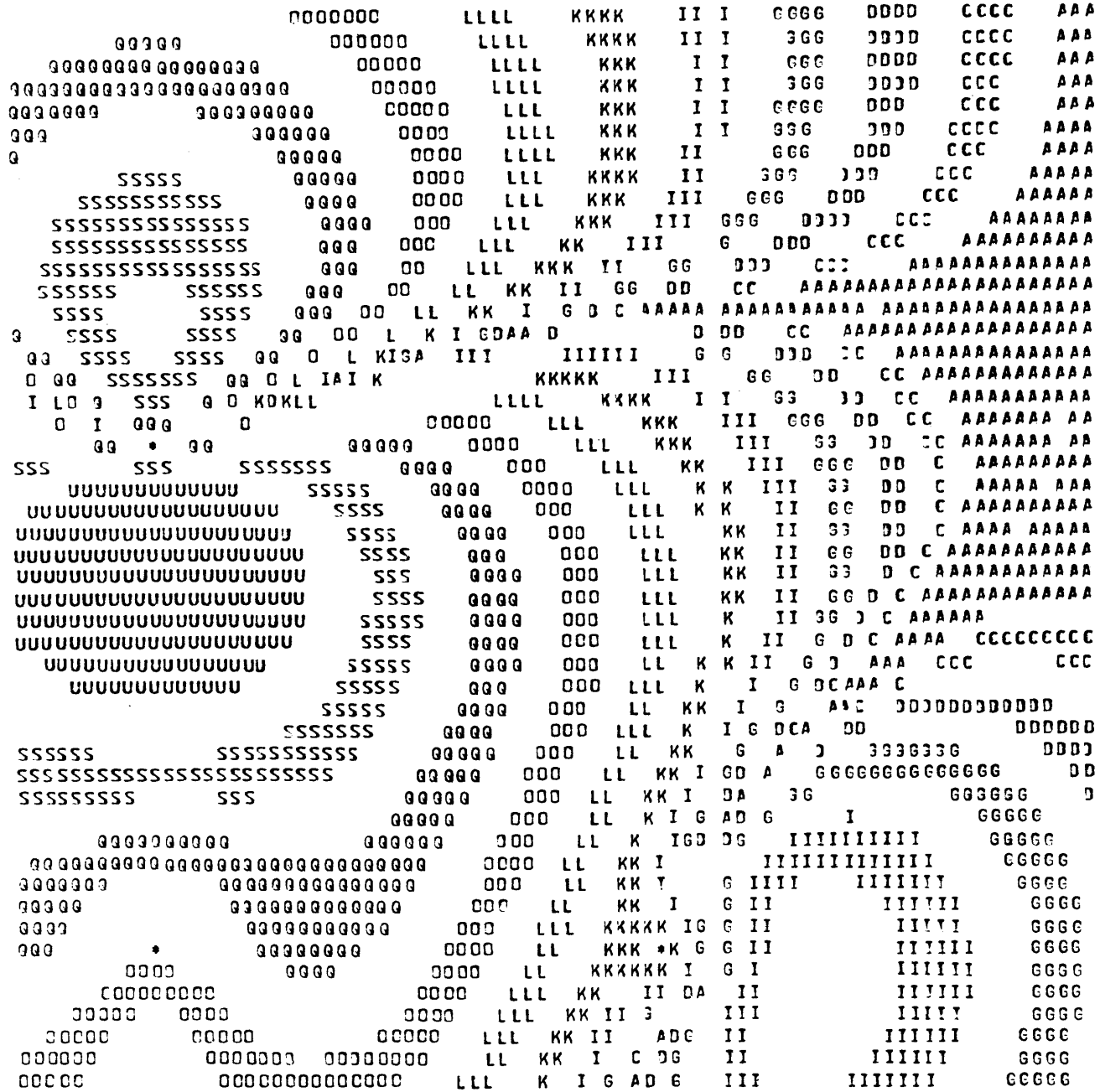

FEF6 10 FN BASIS SINGLE ZETA PLOTS FIG 3b
FE-FL BETA BONDING MO IN X-Z PLANE

MAP THROUGH Y= .0000000 DIMENSIONS X= 4.0000000 BY Z= 4.0000000
DENSITY MAXIMUM .10000000+01 FACTOR BETWEEN INTERVALS .50000000+00
THE DENSITIES ARE SCALED TO .10000000+01

A	1	.95367432-06
		.19073486-05
C	2	.38146973-05
		.76293945-05
D	3	.15258789-04
		.30517578-04
G	4	.61035156-04
		.12207031-03
I	5	.24414063-03
		.48828125-03
K	6	.97656250-03
		.19531250-02
L	7	.39062500-02
		.78125000-02
O	8	.15625000-01
		.31250000-01
Q	9	.62500000-01
		.12500000+00
S	0	.25000000+00
		.50000000+00
U	-	.10000000+01

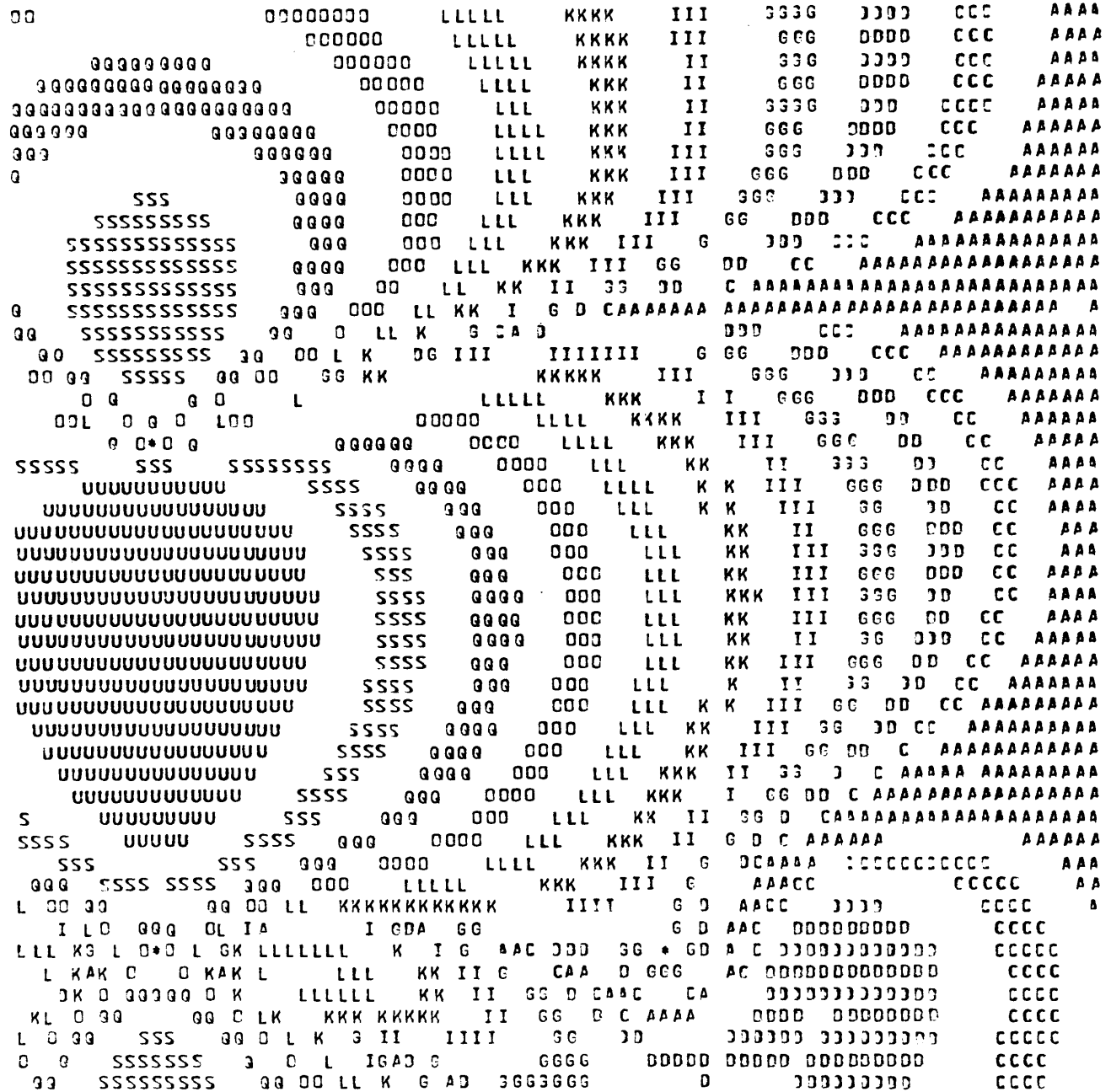

NIF6 10 FN BASIS SINGLE ZETA PLOTS
NI-FL ALPHA BONDING MO IN X-Z PLANE + CRYST POT

FIG 4a

MAP THROUGH Y= .0000000 DIMENSIONS X= 4.0000000 BY Z= 4.0000000
DENSITY MAXIMUM .1000000+01 FACTOR BETWEEN INTERVALS .50000000+00
THE DENSITIES ARE SCALED TO .10000000+01

A	1	.95367432-06
		.19073486-05
C	2	.38146973-05
		.76293945-05
D	3	.15258789-04
		.30517578-04
G	4	.61035156-04
		.12207031-03
I	5	.24414063-03
		.48828125-03
K	6	.97656250-03
		.19531250-02
L	7	.39062500-02
		.78125000-02
O	8	.15625000-01
		.31250000-01
Q	9	.62500000-01
		.12500000+00
S	0	.25000000+00
		.50000000+00
U	-	.10000000+01

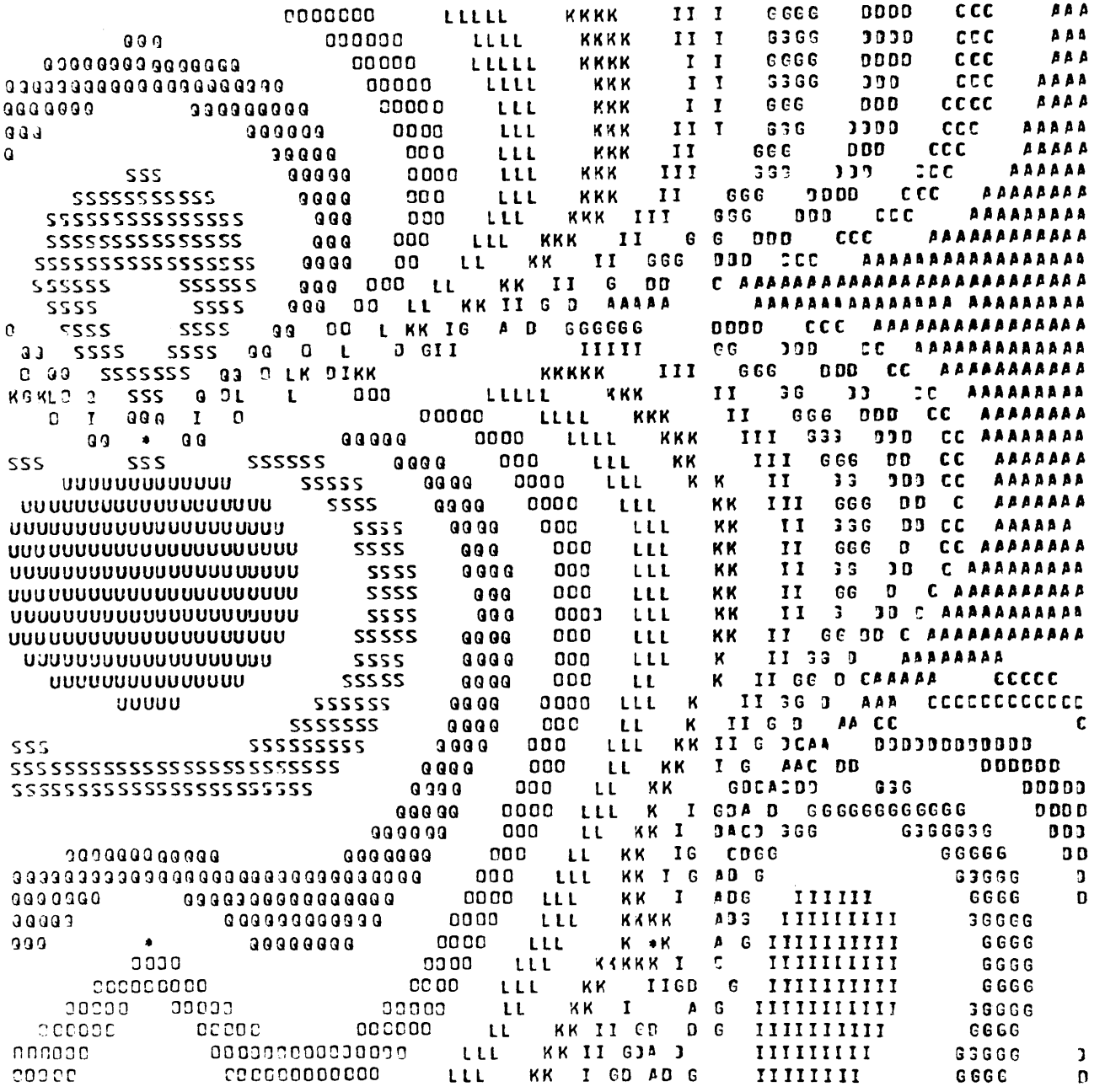

NIF6 10 FN BASIS SINGLE ZETA PLOTS
NI-FL BETA BONDING MO IN X-Z PLANE • CRYST POT

FIG 4b

MAP THROUGH Y= .0000000 DIMENSIONS X= 4.0000000 BY Z= 4.0000000
DENSITY MAXIMUM .10000000•01 FACTOR BETWEEN INTERVALS .50000000•00
THE DENSITIES ARE SCALED TO .10000000•01

A	1	.95367432-06
		.19073486-05
C	2	.38146973-05
		.76293945-05
D	3	.15258789-04
		.30517578-04
E	4	.61035156-04
		.12207031-03
I	5	.24414063-03
		.48828125-03
K	6	.97656250-03
		.19531250-02
L	7	.39062500-02
		.78125000-02
O	8	.15625000-01
		.31250000-01
Q	9	.62500000-01
		.12500000•00
S	0	.25000000•00
		.50000000•00
U	-	.10000000•01

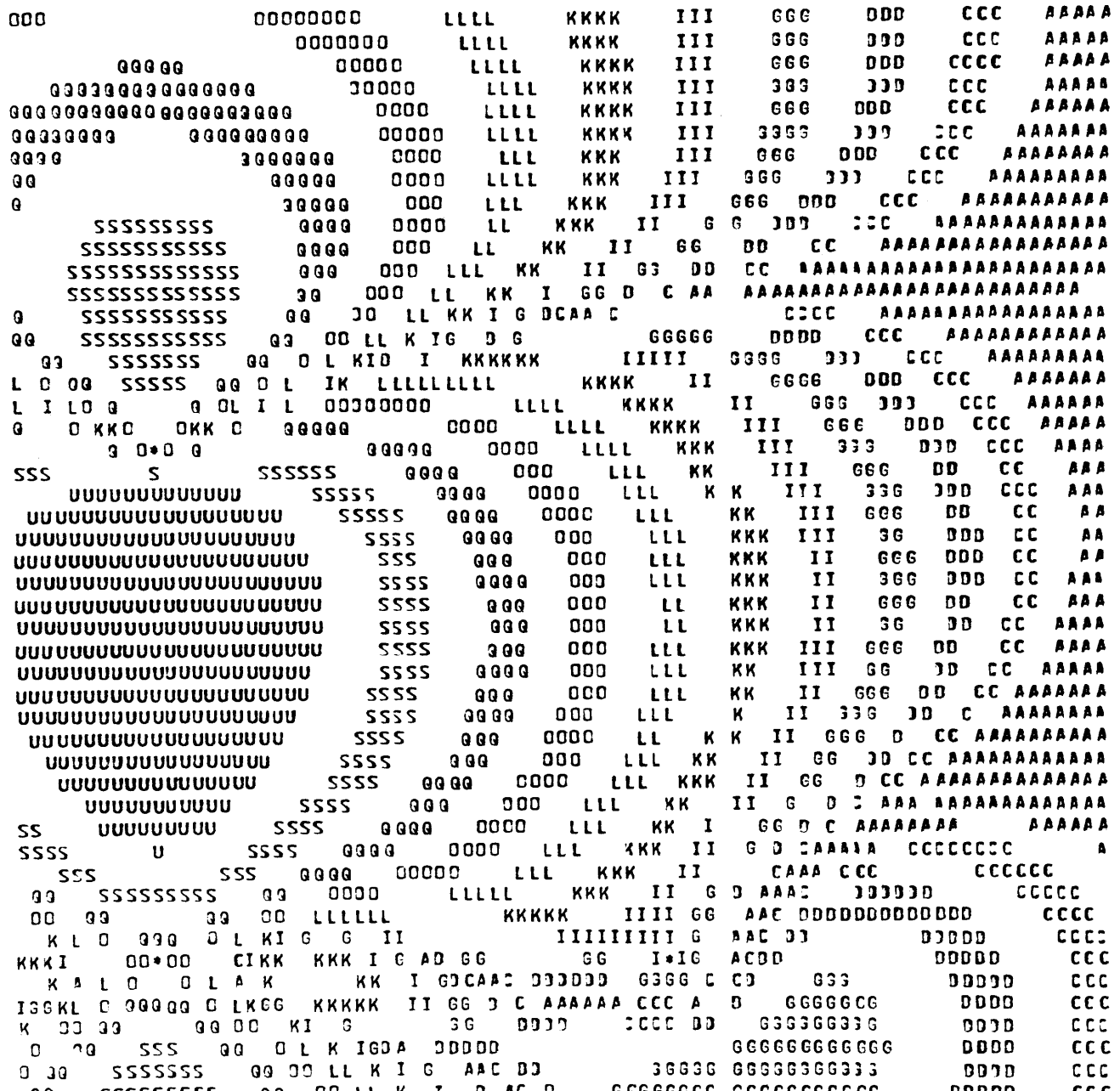

7.3.0 Spin Distributions

We shall discuss our analysis of the spin distributions in terms of gradual degradation of our model, in an analagous manner to our discussion of charge distributions in 7.2. Table 9 provides a summary of our results of $f_\sigma - f_\pi$ values for each system utilizing the conventional Mulliken Analysis, Roby Projected Charge Analysis and Projection Analysis after spin projection has removed contaminating multiplets.

7.3.1 CrF_6^{3-}

Relative to ESG, $ES/_2G$ ($f_\sigma - f_\pi$) values are all more positive by about 0.6% but the EG values are all slightly more negative again. Thus as we remove more (ab/aa) integrals we initially unbalance the wavefunction ($ES/_2G$) and then as we remove more (EG) we overcorrect.

Degrading the core representation (using PCC) produces values which are more negative but the most dramatic effect is observed when the integral representation is degraded since $f_\sigma - f_\pi$ values of the order of -13% are obtained. The effect is clear; when the ESEMO integrals are evaluated exactly, the covalency parameter homes in on the experimental value even though imbalances caused by approximate SBD integrals caused errors of opposite sign with the large and small valence bases.

Table 9 : $f_\sigma - f_\pi$ values (%)

		CrF_6^{3-}	FeF_6^{3-}	NiF_6^{4-}
Relative to ESG : HCC : Small Core : Crystal	(M)	-5.017	+8.723	+8.621
	(R)	-3.452	+5.830	+6.010
	(P)	-2.495	+8.609	+8.441
1) Remove more (ab|aa) integrals (ESG → $ES/_2G$ → EG)				
$ES/_2G$	(M)	-4.410	+9.298	
	(R)	-3.065	+6.410	
	(P)	-1.741	+9.360	
EG	(M)	-5.559	+9.648	
	(R)	-3.552	+6.708	
	(P)	-2.673	+9.518	
2) Degrade core representation (HCC → PCC)			*	
	(M)	-5.550	+10.44	
	(R)	-4.009	+7.33	
	(P)	-2.427	+10.49	
3) Degrade integral representation (ESG → ES)			*	
	(M)	-13.18	-4.516	
	(R)	-13.46	-4.379	
	(P)	-8.32	-2.281	
4) Decrease valence size (Small core → Large core)	(M)	-4.028	+10.590	
	(R)	-2.690	+7.464	
	(P)	-2.246	+10.474	
5) Remove crystal potential	(M)	-4.988	+8.663	+11.256
	(R)	-3.428	+5.874	+8.285
	(P)	-2.460	+8.703	+11.000

* These results are for no crystal potential.

M: conventional Mulliken Analysis

R: Roby Projected charge Analysis

P: Projection Analysis.

7.3.2 FeF_6^{3-}

As we removed more (ab/aa) integrals from the F-matrix, $f_\sigma - f_\pi$ became more positive. The effect was more pronounced in going from (ESG → EG) than from (ESG → $ES/_2G$).

The degradation of the core representation (PCC instead of HCC) resulted in values of $f_\sigma - f_\pi$ becoming more positive by about 1.5%, which is quite significant. Again, the most dramatic affect on $f_\sigma - f_\pi$ values is noted when the integral representation is degraded since reductions of about 13% were noted.

Decreasing the valence size caused values to become more positive by about 1.5% whilst the removal of the crystal potential made no significant difference.

For FeF_6^{3-} the differences in $f_\sigma - f_\pi$ before and after spin annihilation of higher multiplets from the wavefunction are nowhere near as large as for CrF_6^{3-}.

7.3.3 NiF_6^{4-}

Only one study of NiF_6^{4-} was made in the interests of economy. The method chosen was ESG : HCC : Small Core : since this had produced the best results for CrF_6^{3-} and FeF_6^{3-} and the only factor varied was the crystal potential. The effect of the crystal potential on the covalency parameter was quite dramatic in that a reduction of 2.5 percentage units in $(f_\sigma - f_\pi)$ a fractional change of greater than a fifth was recorded for all population analysis methods. Agreement with experiment (+3.3, +3.8%) is only moderate (+8.441%).

7.3.4 CrF_6^{3-}, FeF_6^{3-} and NiF_6^{4-}

From the analysis of the spin distributions of CrF_6^{3-} and FeF_6^{3-} it is obvious that the employment of accurate ESEMO integrals is necessary to produce a spin distribution which is close to experimental. In CrF_6^{3-} the considerable reduction in $(f_\sigma - f_\pi)$ after spin annihilation of the wavefunction may result from the presence of a reasonable amount of higher multiplets in the wavefunction as evidenced by $\hat{S}^2$ before annihilation. This may indicate that the single determinant representation (for CrF_6^{3-} at least) would be improved by configuration interaction.

Method ESG : HCC : Small Core : Crystal has produced the best results when compared to experimental values, except in the case of the "shared cluster" $NiF_6^{4-}/KNiF_3$ system. Reference to Table 5.3 shows that several investigators have had moderate success in reproducing experimental $(f_\sigma - f_\pi)$ values.

All investigations with the exception of a modified EHM study[1] and the CNDO and INDO studies[2] outlined in Appendix 3 were within experimental error for CrF_6^{3-} whilst all values for FeF_6^{3-} known were within these limits. The most widely studied system NiF_6^{4-} is apparently the most difficult to reproduce as evidenced by the variability and spread of values. It is perhaps fitting that ab-initio and CNDO studies (representing extremes of rigour) produce the best results for this ion. Our results (Table 3, Appendix 2) are within experimental error for CrF_6^{3-} and quite close to experiment for FeF_6^{3-} although our values for NiF_6^{4-} are definitely too high. We do not attribute this error to our electronic structure computation scheme within the cluster, but to the cluster approximation itself.

It is rewarding that our method which is both computationally simple (compared to ab-initio) and parameter free, has been able to produce these results. It is interesting to note the proponents of the MSX_α model requested "an ab-initio spin polarized Hartree-Fock (SPHF) calculation of good quality to resolve the uncertainty" in their model[3]. In contrast to other studies (including our present one) their results indicate for CrF_6^{3-} that f_σ is large and negative, whereas f_π is small. They then state " they are perhaps somewhat inconclusive in view of the approximations made in the model". It would appear from these comments that despite the numerical value of $f_\sigma - f_\pi$ there is still some uncertainty in the MSX_α description of the spin distribution in these systems.

The fact that our inclusion of the crystal potential in NiF_6^{4-} had such a great effect on $f_\sigma - f_\pi$ is in direct contrast to Soules et al[4] who after approximate preliminary calculations concurred with Ellis et al[5] that the external Madelung potential had no effect on the calculated wavefunction. We reject that proposition.

Our orbital populations (Table 3, Appendix 2) have been analyzed in three different ways, the Lowdin populations, Mulliken Populations and Roby populations. At this stage the only widely used technique is the Mulliken population analysis scheme. Our results are comparable to those of Table 5.2 and indicate significant involvement of the 4s orbital in bonding.

The most significant result of this work is the demonstration of the effect of accurately evaluated ESEMO integrals on the quality of the wavefunction. For the two systems most extensively investigated, CrF_6^{3-} and FeF_6^{3-}, the accurate integrals have a levelling effect in that the three different matrix element methods produce results which are similar.

Overall method E performs the best of the methods using the approximate integrals. Remembering that E excludes those occurrences of the ESEMO integrals in both the diagonal and off-diagonal elements of the F-matrix, except where premultiplied with a one-centre bond order element while $ES/_2$ and ES include an intermediate number and all of these integrals respectively. There is a significant numerical difference in integral values calculated using the Ruedenberg approximation and using the fitted gaussian technique. Since in E, only a small subgroup of F-matrix occurrences of these approximate integrals are included in the F-matrix, there is little effect due to the poor numerical values of these integrals under the Ruedenberg approximation. However, progressive inclusion of these leads to poorer SCF results due to magnification of the effects of these numerical errors in these important integrals. Support for this is also given by the parallel results for the SC calculations, where in the SCF, the effect is more pronounced because more of these defective integrals are involved in these calculations.

This point is important because despite the numerical difference between accurate and approximate integrals there may be some cancellation of errors. Our work clearly demonstrates that this does not happen for the (ab/aa) type integrals' overall contribution to the F-matrix.

In the SO_2 investigation[6] it was obvious that there were problems with integral approximations. However, the investigation of the matrix element formalisms devoid of any integral approximations[7] has produced good results with a considerable saving in effort over ab-initio methods.

In this present study we still retain the Ruedenberg Approximation for the three centre nuclear attraction integrals. We are still not in a position with STF basis sets to evaluate these three centre integrals exactly.with reasonable computational effort. Our analysis seems to indicate for these ionic systems at least, there is some measure of justification for retaining this very cheap approximation. In the light of our results, we can no longer justify using accurate one-electron integrals for the two-centre matrix elements and approximate two-electron integrals which is what was done in the SO_2 study and in the approximate calculations of this present study.

There doesn't appear to be any evidence from these results that says, for these systems at least, that we need to go further in removing integral approximations. This is important because of the enormous amount of extra work involved with the three-centre nuclear attraction integrals due to the sheer number of them.

We have demonstrated that the Ruedenberg Approximation for two-centre integrals is poor whilst the other studies have utilized the Mulliken Approximation[8] which is known to be inherently worse[9]. As a result our method is more rigorous than all the others excepting possibly the MSX_α. We can produce maps of charge and spin distributions and produce energy levels just as can the MSX_α method proponents but we can in addition interpret our wavefunction in terms of orbitals.

Our results indicate the final model is behaving in an orderly and interpretable manner. It appears that all the integrals that are left our effectively do cancel as there is no suggestion that their omission is causing deleterious effects to the reliable prediction of quantities which can be compared with experiments.

References : Chapter 7

1. L.E. Harris, E.A. Boudreaux, Inorg. Chim. Acta, 9, 245, (1974).

2. S. Sakaki, H. Kikkawa, H. Kato, S. Goshida, Bull. Chem. Soc. Jap., 49, 76, (1976).

3. S. Larsson, E.K. Viinikka, M.L. DeSiquira, J.W.D. Connoly, Int. J. Quantum Chem., Symp. No. 8, 145, (1974).

4. T.F. Soules, J.W. Richardson, D.M. Vaught, Phys. Rev., B3, 2186 (1971).

5. D.E. Ellis, A.J. Freeman, P. Ros, Phys. Rev., 176, 688, (1968).

6. P.G. Burton, Chemical Physics, 6, 419, (1974).

7. P.G. Burton, N.R. Carlsen, Chemical Physics, In Press.

8. R.S. Mulliken, J. Chim. Phys. Physicochim. Biol., 46, 675, (1949).

9. P.G. Burton, PhD. Thesis, Monash, 1973.

8.0 CONCLUSION

It appears from this work that the development of better methods of calculating the ESEMO integrals has led to considerable improvement in their accuracy, and as a result of this greatly improved agreement with experimental spin distributions of the complexes studied and greater internal consistency of different matrix element formalisms was noted.

An important result of this work is the demonstration of similar results obtained with the three different matrix element methods providing accurate integrals were used. However, the most sophisticated ESEMO method, ESG is the one for which greatest promise is held of obtaining highly reliable wavefunctions on previously intractable molecular systems exhibiting greater covalency than the ionic fluorides tested here.

The ESEMO method, at the minimum acceptable degree of computational effort (exact one and two centre integrals, Ruedenberg approximated $\langle a|V^C|b\rangle$ and (ab/cc) integrals and three and four centre non-SBD integrals omitted), has yielded realistic and fairly reliable quantitative information on the charge and spin distributions within the cluster approximation to these systems.

The major outcome of this work is that progressive removal of approximations within our model led ultimately to dramatically improved results which were internally consistent and in acceptable agreement with experiment. We can say that this study has therefore defined the acceptable course to modelling the electronic structure of such metal complexes by establishing the minimum acceptable computational effort required to describe them within a given basis set.

We showed that degrading the final model by introducing computationally stimulated approximations of a chemically interpretable nature (degrading the core representation of the metals (LC → SC); introducing integrals (EG or ESG → E or ES); degrading the evaluation of the core/valence interaction HCC → PCC) in all cases removed the agreement of the final model results with experimental parameters.

Obvious areas for further investigation are the 4s metal orbital representation, the inclusion of configuration interaction, particularly in CrF_6^{3-} studies, with the view to obtaining reasonable calculated electronic spectra, and further testing on more general, less symmetric molecules is also warranted. Improvements in basis sets or progression beyond the HF level are clearly desirable to attain precise agreement with experiment for transition metal complex properties. Within the limits of the HF model and the basis sets we have employed we believe we have established a computationally efficient vehicle upon which such improvements may be soundly based.

Appendix 1. Details of Basis Sets Used

Metal Orbitals[a]

	Exponents			Coefficients		
	Cr	Fe	Ni	Cr	Fe	Ni
1s	23.70	25.70	27.70	1	1	1
2s	8.90	9.75	10.60	-.3624	-.3679	-.3727
				1.0636	1.0655	1.0672
2p	9.70	10.60	11.50	1	1	1
3s	4.06	4.48	4.90	.1415	.1455	.1489
				-.4792	-.4875	-.4945
				1.0970	1.0999	1.1024
3p	3.74	4.17	4.60	-.3075	-.3201	-.3308
				1.0462	1.0500	1.0533
$3d_1$	4.95	5.35	5.75	.4876	.5366	.5683
$3d_2$	1.60	1.80	2.00	.7205	.6678	.6292
4s	1.30	1.40	1.50	-.02145	-.02078	-.02018
				.07366	.07052	.06792
				-.1851	-.1744	-.1657
				1.0142	1.0125	1.0113

Ligand Orbitals[b]

	Exponent	Coefficient	
1s	7.91788	.76949	.31340
1s	11.01100	.23727	-.02923
2s	1.94665	.00076	-.40163
2s	3.09603	.00109	-.68011
2p	1.84539	.72531	
2p	4.17099	.35754	

(a) J.W. Richardson, W.C. Nieuwpoort, R.R. Powell, W.F. Edgell, J. Chem. Phys. 36, 1057, (1962).

(b) E. Clementi, IBM Report, RJ-256.

Appendix 2. Results of Calculations for CrF_6^{3-}, FeF_6^{3-} and NiF_6^{4-}

TABLE 1(a) : ALPHA LOCALIZED BONDING MOLECULAR ORBITALS

Centroids A°

H.C. Core Approximation

CrF_6^{3-}

	E	$ES_{/2}$	ES
Large	-	1.55680	1.52024
Core	-	*1.54980*	*1.51861*
Small	1.61521	1.17145	-
Core	*1.59911*	*1.16788*	*1.41353*

	EG	$ES_{/2}G$	ESG
Large	1.50298	1.45551	1.39908
Core	*1.49904*	*1.45182*	*1.39537*
Small	1.52148	-	1.40221
Core	*1.51619*	*1.46094*	*1.40952*

P.C. Core Approximation

CrF_6^{3-}

	E	$ES_{/2}$	ES
Large	1.51793	1.54432	1.50701
Core	*1.50682*	*1.53910*	*1.51260*
Small	1.60251	-	-
Core	*1.58456*	-	-

	EG	$ES_{/2}G$	ESG
Large	1.46823	1.42489	1.36766
Core	*1.46434*	*1.42154*	*1.36459*
Small	1.46720	1.42357	1.36946
Core	*1.46241*	*1.41972*	*1.36581*

Centroids/Bond Length

H.C. Core Approximation

CrF_6^{3-}

	E	$ES_{/2}$	ES
Large	-	.80538	.78647
Core	-	*.80176*	-
Small	.83560	.60603	-
Core	*.82727*	*.60418*	*.73126*

	EG	$ES_{/2}G$	ESG
Large	.77854	.75298	.72379
Core	*.77550*	*.75107*	*.72187*
Small	.78711	-	.72541
Core	*.78437*	*.75579*	*.72919*

P.C. Core Approximation

CrF_6^{3-}

	E	$ES_{/2}$	ES
Large	.78527	.79893	.77962
Core	*.77952*	*.79622*	*.78251*
Small	.82903	-	-
Core	*.81974*	-	-

	EG	$ES_{/2}G$	ESG
Large	.75956	.73714	.70753
Core	*.75755*	*.73541*	*.70594*
Small	.75903	.73646	.70847
Core	*.75655*	*.73446*	*.70658*

Table 1(a) - continued

FeF_6^{3-}

	E	$ES_{/2}$	ES	E	$ES_{/2}$	ES	E	$ES_{/2}$	ES	E	$ES_{/2}$	ES
Large	-	1.58565	-	1.59871	1.58270	-	-	.83018	-	.87702	.82864	-
Core	-	-	-	-	-	-	-	-	-	-	-	-
Small	1.55434	1.58395	1.62216	1.54226	1.57862	1.61658	.81379	.82930	.84930	.80747	.82650	.84638
Core	-	-	-	-	-	-	-	-	-	-	-	-

	EG	$ES_{/2}G$	ESG	EG	$ES_{/2}G$	ESG	EG	$ES_{/2}G$	ESG	EG	$ES_{/2}G$	ESG
Large	1.62254	1.59838	1.61156	-	1.59754	1.60503	.84950	.83685	.84375	-	.83641	.84047
Core	-	-	-	-	-	-	-	-	-	-	-	-
Small	1.59734	1.59374	1.60271	1.59329	1.60128	1.59934	.83630	.83442	.83911	.83418	.83837	.83735
Core	*1.59656*	*1.59368*	*1.60250*	*1.59273*	*1.58948*	*1.59851*	*.83590*	*.83439*	*.83901*	*.83389*	*.83219*	*.83691*

NiF_6^{4-}

		ESG
Small		1.68657
Core		*1.69164*

NiF_6^{4-}

		ESG
Small		.84076
Core		*.84329*

TABLE 1(b) : BETA LOCALIZED BONDING MOLECULAR ORBITALS

Centroids A°

H.C. Core Approximation — CrF_6^{3-}

	E	$ES_{/2}$	ES
Large	-	1.554326	1.531580
Core	-	*1.564583*	-
Small	1.75380	1.18828	-
Core	*1.73054*	*1.17871*	*1.60404*

	EG	$ES_{/2}G$	ESG
Large	-	1.49873	1.44493
Core	*1.54160*	*1.49501*	*1.44145*
Small	-	-	1.47423
Core	*1.57243*	*1.51855*	*1.47005*

P.C. Core Approximation — CrF_6^{3-}

	E	$ES_{/2}$	ES
Large	-	1.56277	1.519469
Core	*1.536290*	*1.572704*	*1.529683*
Small	1.736136	-	-
Core	*1.733017*	-	-

	EG	$ES_{/2}G$	ESG
Large	1.51969	1.47381	1.42134
Core	*1.51592*	*1.47029*	*1.41808*
Small	1.54251	1.49201	1.44629
Core	*1.53792*	*1.48783*	*1.44228*

Centroids/Bond Length

H.C. Core Approximation — CrF_6^{3-}

	E	$ES_{/2}$	ES
Large	-	.80410	.79233
Core	-	*.80941*	-
Small	.89798	.61473	-
Core	*.89526*	*.60978*	*.82982*

	EG	$ES_{/2}G$	ESG
Large	-	.77534	.74751
Core	*.79751*	*.77341*	*.74571*
Small	-	-	.76267
Core	*.97988*	*.78559*	*.76050*

P.C. Core Approximation — CrF_6^{3-}

	E	$ES_{/2}$	ES
Large	-	.80847	.78607
Core	*.79477*	*.81361*	*.79135*
Small	.51640	-	-
Core	*.89654*	-	-

	EG	$ES_{/2}G$	ESG
Large	.78618	.76245	.73530
Core	*.78423*	*.76063*	*.73362*
Small	.79799	.77198	.74812
Core	*.79561*	*.76920*	*.74614*

Table 1(b) - continued

FeF_6^{3-}

	E	$ES_{/2}$	ES
Large	-	1.58132	-
Core	-	-	-
Small	1.67815	1.27815	1.51663
Core	-	-	-

	E	$ES_{/2}$	ES
Large	1.718331	1.576811	-
Core	-	-	-
Small	1.22741	1.59427	1.41701
Core	-	-	-

FeF_6^{3-}

	E	$ES_{/2}$	ES
Large	-	.82792	-
Core	-	-	-
Small	.87861	.66919	.79405
Core	-	-	-

FeF_6^{3-}

	E	$ES_{/2}$	ES
Large	.89965	.82556	-
Core	-	-	-
Small	.64262	.83470	.74189
Core	-	-	-

	EG	$ES_{/2}G$	ESG
Large	1.37462	1.38974	1.38820
Core	-	-	-
Small	1.38322	1.40451	1.41162
Core	*1.38059*	*1.40156*	*1.40795*

	EG	$ES_{/2}G$	ESG
Large	-	1.37314	1.36856
Core	-	-	-
Small	1.36102	1.38224	1.38490
Core	*1.35814*	*1.37914*	*1.38098*

	EG	$ES_{/2}G$	ESG
Large	.71970	.72761	.72681
Core	-	-	-
Small	.72420	.73535	.73907
Core	*.72282*	*.73379*	*.73715*

	EG	$ES_{/2}G$	ESG
Large	-	.71892	.71652
Core	-	-	-
Small	.71258	.72369	.72508
Core	*.71107*	*.72206*	*.72303*

NiF_6^{4-}

		ESG
Small		1.45959
Core		*1.51583*

NiF_6^{4-}

		ESG
Small		.72761
Core		*.75565*

TABLE 2 : CALCULATIONS WHICH EMPLOYED THE RUEDENBERG APPROXIMATION FOR EVALUATION OF ESEMO INTEGRALS

	HUZINAGA-CANTU CORE HAMILTONIAN						POINT CHARGE CORE APPROXIMATION					
	E		$ES_{/2}$		ES		E		$ES_{/2}$		ES	
(a) CrF_6^{3-} Cr{3d,4s}, F{2s,2p} - Large Core												
LUMO (α) (β)	2.215	10.862	1.107	16.925	33.500	19.085	.2638	11.001	27.352	17.614	31.112	19.783
	10.707	*-4.910*	*14.063*	*1.334*	*17.837*	*3.329*	*7.558*	*-4.888*	*11.773*	*1.956*	*15.361*	*3.912*
HOMO (α) (β)	1.089	2.98	.7098	.3607	6.588	5.071	.051	- .031	.587	- .073	6.641	4.772
	-13.373	*-13.569*	*-14.346*	*-15.086*	*-9.064*	*-10.583*	*-15.453*	*-15.751*	*-14.937*	*-15.588*	*-9.091*	*-11.010*
At. Charges Cr	+1.230	*+1.203*	+1.480	*+1.462*	+1.156	*+1.128*	+1.109	*+1.082*	+1.375	*+1.394*	+1.072	*+1.045*
F	- .7049	*- .7005*	- .746	*- .743*	- .692	*- .688*	- .684	*- .680*	*- .733*	*- .729*	- .6784	*- .6742*
Mulliken ($f_\sigma - f_\pi$) %	-1.98		- .608		- 1.65		-2.15		- .789		-1.66	
	-2.080		*- .632*		*- 1.74*		*-2.22*		*- .813*		*-1.75*	
Roby Projected ($f_\sigma - f_\pi$) %	-3.39		- .597		- .784		-3.28		- .626		- .835	
	-3.523		*- .503*		*- .839*		*-3.37*		*- .744*		*- .881*	
(b) CrF_6^{3-} Cr{3s,3p,3d,4s}, F{2s,2p} - Small Core												
LUMO (α) (β)	38.392	38.001	38.426	39.288	27.632	27.966	27.374	37.448	N.C.		N.C.	
	22.847	*22.446*	*20.585*	*21.445*	*11.094*	*11.683*	*20.887*	*21.874*				
HOMO (α) (β)	26.558	20.191	32.986	28.196	23.063	8.278	20.424	21.007				
	11.096	*4.848*	*15.165*	*10.423*	*17.024*	*-7.232*	*12.158*	*5.653*				
At. Charges Cr	+1.447	*+1.426*	-1.311	*-1.335*	+ .669	*+ .647*	+1.429	*+1.408*				
F	- .741	*- .737*	- .281	*- .277*	- .611	*- .607*	- .738	*- .735*				
Mulliken ($f_\sigma - f_\pi$) %	-6.106	*-5.98*	-13.33	*-13.37*	-10.11	*-13.18*	-5.70	*-5.82*				
Roby Projected ($f_\sigma - f_\pi$) %	-8.90	*-9.28*	-16.64	*-16.67*	-13.39	*-13.46*	-8.58	*-8.70*				

TABLE 2 : continued

	HUZINAGA-CANTU CORE HAMILTONIAN						POINT CHARGE CORE APPROXIMATION					
	E		$ES/_2$		ES		E		$ES_{/2}$		ES	
(c) FeF_6^{3-} Fe{3d,4s}, F{2s,2p} - Large Core												
LUMO (α,β)	N.D.		71.731	21.842	N.D.		80.997	21.898	65.730	22.059	38.911	21.141
HOMO (α,β)			21.117	13.947			11.123	11.837	12.319	14.013	9.016	7.678
At. Charges Fe			+ .603				+1.422		+ .571		+1.103	
F			- .6005				- .737		- .595		- .689	
Mulliken ($f_\sigma - f_\pi$) %			-14.263				-4.286		-14.61		-12.00	
Roby Projected ($f_\sigma - f_\pi$) %			-15.689				-7.834		-15.33		-12.53	
(d) FeF_6^{3-} {Fe{3s,3p,3d,4s}, F{2s,2p} - Small Core												
LUMO (α) (β)	103.413	37.800	73.951	33.007	43.847	28.736	99.246	36.797	69.803	32.591	38.723	27.674
HOMO (α) (β)	26.867	20.002	22.815	18.982	16.414	7.399	27.179	20.139	23.211	19.394	16.538	7.328
At. Charges Fe	+1.213		- .0977		+ .6459		+1.164		- .2164		+ .5621	
F	- .7023		- .4837		- .6076		- .6941		- .4639		- .5936	
Mulliken ($f_\sigma - f_\pi$) %	-4.38		-3.909		-4.516		-3.616		-2.449		-3.492	
Roby Projected ($f_\sigma - f_\pi$) %	-4.36		-3.698		-4.379		-3.455		-2.228		-3.341	

NOTES (1) Values in italics are for crystal calculations.

(2) N.C. not converged to correct state.

(3) N.D. not done.

TABLE 3 : CALCULATIONS WHERE ESEMO INTEGRALS WERE EVALUATED BY GAUSSIAN FITS

(a) CrF_6^{3-} Cr{3d,4s}, F{2s,2p} - Large Core

	HUZINAGA-CANTU CORE HAMILTONIAN						POINT-CHARGE CORE APPROXIMATION					
	EG		$ES/_2G$		ESG		EG		$ES/_2G$		ESG	
LUMO (α) (β)	21.058	11.218	23.404	25.108	26.957	28.554	20.388	12.364	22.900	24.596	26.303	28.130
	5.210	*-4.795*	*7.466*	*9.157*	*10.662*	*12.099*	*4.411*	*-3.911*	*6.808*	*8.488*	*9.872*	*11.673*
HOMO (α) (β)	-1.210	-1.291	6.654	.948	11.403	7.547	-1.601	-1.846	8.021	.664	12.406	7.334
	-17.124	*-17.218*	*-9.382*	*-15.081*	*-5.003*	*-8.803*	*-17.642*	*-17.901*	*-8.188*	*-15.511*	*-4.153*	*-9.151*
At. Charges Cr	+1.033	*+ .9946*	+ .7902	*+ .76187*	+ .32977	*+ .3035*	+ .8556	*+ .8208*	+ .6096	*+ .5842*	+ .178	*+ .155*
F	- .6722	*- .6657*	- .6317	*- .6269*	- .5549	*- .5505*	- .6426	*- .6368*	- .6016	*- .5973*	- .529	*- .525*
Mulliken ($f_\sigma - f_\pi$) %	-4.240		-3.299	*-3.309*	-4.028	*-4.050*	-4.362		-3.43		-4.152	
	-4.321						*-4.405*		*-3.431*		*-4.160*	
Roby Projected ($f_\sigma - f_\pi$) %	-2.696		-2.254	*-2.261*	-2.690	*-2.706*	-2.939		-2.46		-2.894	
	-2.734						*-2.969*		*-2.456*		*-2.895*	
$\langle \hat{S}^2 \rangle$	3.764165	*3.764036*	3.761661	*3.761494*	3.760353	*3.760224*	3.768493	*3.768221*	3.762353	*3.762997*	3.762896	*3.762659*

Orbital Spin Densities after Spin Annihilation of SUHF Wavefunctions (%)

$\langle \hat{S}^2 \rangle$	3.750059	*3.750058*	3.750039	*3.750038*	3.750031	*3.750030*	3.750100	*3.750097*	3.750051	*3.750049*	3.750048	*3.750046*
f_{4s}	.4244	*.4213*	.3383	*.33820*	.35977	*.358493*	.4696	*.4666*	.36624	*.36573*	.3833	*.38176*
$f_{3d\pi}$	93.5873	*93.2731*	96.6759	*96.5964*	93.3342	*93.1995*	95.0317	*94.8201*	97.0055	*96.9396*	93.993	*93.8818*
$f_{3d\sigma}$	2.5835	*2.5806*	2.4988	*2.4848*	2.3958	*2.3819*	3.1225	*3.1038*	2.7288	*2.70268*	2.728	*2.7012*
$f_{2p\sigma}$	- .7020	*- .7041*	- .6753	*- .6736*	- .6553	*- .6527*	- .8292	*- .82843*	- .7367	*.73236*	- .7346	*.7293*
$f_{2p\pi}$	1.5007	*1.58023*	+ .7466	*+ .7677*	+1.5915	*+1.6261*	+1.10864	*+1.1633*	+ .65277	*.67109*	+1.4083	*1.43798*
($f_\sigma - f_\pi$) %	-2.203	*-2.284*	-1.422	*-1.441*	-1.147	*-2.279*	-1.938	*-1.992*	-1.389	*-1.403*	-2.143	*-2.167*

TABLE 3 : continued

(b) CrF_6^{3-} Cr{3s,3p,3d,4s}, F{2s,2p} - Small Core

HUZINAGA-CANTU CORE HAMILTONIAN

	EG		$ES_{/2}G$		ESG	
LUMO (α) (β)	19.67	12.959	21.52	23.56	24.038	26.415
	3.949	*-2.295*	*5.682*	*7.701*	*7.880*	*10.233*
HOMO (α) (β)	.939	.871	5.839	2.04	10.238	7.940
	-14.896	*-15.001*	*-10.084*	*-13.939*	*-6.023*	*-8.292*
At. Charges Cr	+1.185	*1.137*	+ .8813	+ *.8470*	+ .456	+ *.4240*
F	- .697	- *.6904*	- .646	- *.6421*	- .576	- *.5706*
Mulliken (f_σ-f_π) %	-5.550		-4.41		-4.988	
	-5.559		*-4.41*		*-5.017*	
Roby Projected (f_σ-f_π) %	-3.467		-3.05		-3.428	
	-3.5520		*-3.064*		*-3.452*	
$\langle\hat{S}^2\rangle$	3.780200	*3.779888*	3.773748	*3.773293*	3.770350	*3.770184*

POINT-CHARGE CORE APPROXIMATION

	EG		$ES_{/2}G$		ESG	
LUMO (α) (β)	19.051	13.89	21.094	23.188	23.532	26.025
	3.132	*-2.214*	*5.042*	*7.114*	*7.181*	*9.635*
HOMO (α) (β)	.599	- .197	7.487	1.533	11.454	8.010
	-15.415	*-16.242*	*-8.674*	*-14.635*	*-5.025*	*-8.407*
At. Charges Cr	+ .915	+ *.8750*	+ .642	+ *.6129*	+ .249	+ *.222*
F	- .652	- *.6458*	- .607	- *.6021*	- .541	- *.537*
Mulliken (f_σ-f_π) %	-6.123		-4.764		-5.515	
	-6.149		*-4.741*		*-5.550*	
Roby Projected (f_σ-f_π) %	-4.225		-3.501		-4.015	
	-4.254		*-3.485*		*-4.009*	
$\langle\hat{S}^2\rangle$	3.794619	*3.793696*	3.778656	*3.777924*	3.779338	*3.778763*

Orbital Spin Densities after Spin Annihilation of SUHF Wavefunctions (%)

$\langle\hat{S}^2\rangle$	3.750267	*3.750262*	3.750162	*3.750155*	3.750119	*3.750117*
f_{4s}	.6467	*.64107*	.4372	*.436801*	.4736	*.47177*
$f_{3d\pi}$	92.2934	*92.0087*	95.9843	*95.9113*	93.0454	*92.9119*
$f_{3d\sigma}$	3.7481	*3.7608*	3.6334	*3.6101*	3.4293	*3.4219*
$f_{2p\sigma}$	- .8779	- *.88790*	- .8872	- *.88691*	- .8682	- *.86805*
$f_{2p\pi}$	1.7089	*1.785057*	.83252	*.85404*	1.5917	*1.62645*
(f_σ-f_π) %	-2.5868	*-2.6730*	-1.7197	*-1.7410*	-2.4599	*-2.4945*

$\langle\hat{S}^2\rangle$	3.750583	*3.750559*	3.750235	*3.75024*	3.750247	*3.750238*
f_{4s}	.7941	*.78506*	.5013	*.49916*	.5391	*.53534*
$f_{3d\pi}$	94.0731	*93.8995*	96.3944	*96.3410*	93.7177	*93.6179*
$f_{3d\sigma}$	5.0748	*5.0355*	4.1716	*4.1183*	4.3149	*4.2704*
$f_{2p\sigma}$	-1.1411	*-1.14294*	-1.011745	*-1.00527*	-1.0455	*-1.0390*
$f_{2p\pi}$	1.1610	*1.21102*	.69478	*.71338*	1.3590	*1.38815*
(f_σ-f_π) %	-2.3021	*-2.3540*	-1.7065	*-1.7187*	-2.4045	*-2.4272*

TABLE 3 : continued

(c) FeF_6^{3-} Fe{3d,4s}, F{2s,2p} - Large Core

	HUZINAGA-CANTU CORE HAMILTONIAN						POINT-CHARGE CORE APPROXIMATION					
	EG		$ES_{/2}G$		ESG		EG		$ES_{/2}G$		ESG	
LUMO (α) (β)	89.564	14.450	96.481	18.411	84.215	18.188	84.620	14.822	91.493	18.884	79.076	18.714
	73.655	*-1.520*	*80.793*	*2.568*	*68.505*	*.7865*	*68.696*	*-1.179*	*75.766*	*3.000*	*63.332*	*2.841*
HOMO (α) (β)	6.684	5.032	9.832	4.914	16.434	8.392	6.462	4.898	9.614	4.842	16.270	8.291
	-9.156	*-10.807*	*-5.863*	*-10.813*	*2.358*	*-7.299*	*-9.401*	*-10.963*	*-6.118*	*-10.923*	*.8823*	*-7.446*
At. Charges Fe	+1.135	*+1.113*	+1.253	*+1.236*	+1.211	*+1.189*	+1.102	*+1.080*	1.2070	*+1.190*	+1.166	*+1.45*
F	- .6892	*- .6855*	- .7089	*- .7060*	- .7019	*- .6982*	- .6836	*- .6801*	- .7011	*- .6983*	- .694	*- .6908*
Mulliken ($f_\sigma - f_\pi$) %	+10.0314	*+10.608*	+10.809	*+10.865*	+10.590	*+10.637*	+11.687	*+11.7026*	+11.755	*+11.830*	+11.784	*+11.847*
Roby Projected ($f_\sigma - f_\pi$) %	+7.5230	*+7.5160*	+7.645	*+7.703*	+7.464	*+7.414*	+8.396	*+8.443*	+8.447	*+8.514*	+8.363	*+8.529*
$\langle \hat{S}^2 \rangle$	8.750378	*N.D.*	8.750137	*N.D.*	8.750226	*N.D.*	8.750448	*N.D.*	8.750128	*N.D.*	8.750296	*N.D.*

Orbital Spin Densities after Spin Annihilation of SUHF Wavefunctions (%)

$\langle \hat{S}^2 \rangle$	8.750000	*N.D.*	8.750000	*N.D.*	8.750000	*N.D.*	8.750000	*N.D.*	8.750000	*N.D.*	8.750000	*N.D.*
f_{4s}	- .814	*N.D.*	.474	*N.D.*	.483	*N.D.*	- .8795	*N.D.*	+ .4439	*N.D.*	- .5496	*N.D.*
f_{3d}	91.863	*N.D.*	94.680	*N.D.*	92.302	*N.D.*	92.726	*N.D.*	95.141	*N.D.*	93.061	*N.D.*
$f_{3d\sigma}$	54.211	*N.D.*	55.761	*N.D.*	55.323	*N.D.*	51.6008	*N.D.*	53.104	*N.D.*	52.2199	*N.D.*
$f_{2p\sigma}$	12.543	*N.D.*	12.220	*N.D.*	12.401	*N.D.*	13.3619	*N.D.*	13.0607	*N.D.*	13.3901	*N.D.*
$f_{2p\pi}$	2.031	*N.D.*	1.328	*N.D.*	1.922	*N.D.*	1.8152	*N.D.*	1.2137	*N.D.*	1.7325	*N.D.*
($f_\sigma - f_\pi$) %	10.518	*N.D.*	10.892	*N.D.*	10.479	*N.D.*	11.547	*N.D.*	11.847	*N.D.*	11.658	*N.D.*

TABLE 3 : continued

(d) FeF_6^{3-} Fe{3s,3p,3d,4s}, F{2s,2p} - Small Core

	HUZINAGA-CANTU CORE HAMILTONIAN						POINT-CHARGE CORE APPROXIMATION					
	EG		$ES/_2G$		ESG		EG		$ES/_2G$		ESG	
LUMO (α) (β)	93.115	15.571	98.769	18.086	84.640	17.462	89.504	15.991	95.154	18.654	80.659	18.107
	77.221	*- .3966*	*83.093*	*2.251*	*68.980*	*+1.669*	*73.580*	*- .0260*	*79.422*	*2.757*	*64.933*	*2.247*
HOMO (α) (β)	5.381	6.135	8.162	5.567	14.031	8.679	5.248	6.287	7.991	5.644	13.984	8.845
	-10.454	*-9.701*	*-7.537*	*-10.154*	*-1.591*	*-6.990*	*-10.630*	*-9.5929*	*-7.764*	*-10.131*	*-1.738*	*-6.884*
At. Charges Fe	+1.138	*+1.115*	+1.249	*+1.230*	+1.237	*+1.212*	+1.080	*+1.0593*	+1.182	*+1.164*	+1.168	*+1.144*
F	- .6897	*- .6859*	- .708	*- .705*	- .706	*- .702*	- .680	*- .6765*	- .697	*- .6940*	- .6947	*- .6908*
Mulliken ($f_\sigma - f_\pi$) %	+9.648	*+9.648*	+9.239	*+9.298*	+8.663	*+8.663*	+10.846	*+10.872*	+10.438	*+10.5129*	+10.214	*+10.300*
Roby Projected ($f_\sigma - f_\pi$) %	+6.607	*+6.7078*	+6.3528	*+6.410*	+5.874	*+5.830*	+7.690	*+7.724*	+7.331	*+7.403*	+7.145	*+7.227*
$\langle \hat{S}^2 \rangle$	8.750427	*8.750429*	8.750098	*8.750090*	N.D.	*8.750226*	8.750517	*8.75053*	8.750062	*8.750056*	8.750314	*8.750328*

Orbital Spin Densities after Spin Annihilation of SUHF Wavefunctions (%)

$\langle \hat{S}^2 \rangle$	8.750000	*8.750000*	8.750000	*8.750000*	N.D.	*8.750000*	8.750000	*8.750000*	8.750000	*8.750000*	8.750000	*8.750000*
f_{4s}	- .8663	*- .8789*	- .4395	*+ .4229*	N.D.	*- .5134*	- .9631	*- .9757*	+ .3522	*+ .3343*	- .6101	*- .6261*
$f_{3d\pi}$	91.716	*91.306*	93.598	*93.598*	N.D.	*90.8647*	92.651	*92.303*	94.324	*94.1036*	92.359	*92.060*
$f_{3d\sigma}$	56.606	*56.244*	59.340	*58.914*	N.D.	*59.564*	53.594	*53.202*	56.162	*55.721*	56.180	*55.624*
$f_{2p\sigma}$	11.5874	*11.6877*	10.9033	*11.0242*	N.D.	*10.891*	+12.5310	*12.641*	+11.9050	*+12.032*	+11.9844	*12,1418*
$f_{2p\pi}$	2.0680	*2.1705*	1.5995	*1.6638*	N.D.	*2.282*	1.8337	*1.920*	+1.418	*+1.473*	+1.9080	*1.9827*
($f_\sigma - f_\pi$) %	9.5194	*9.5182*	9.3038	*9.3604*	N.D.	*8.609*	10.6973	*10.721*	10.487	*10.559*	10.0764	*10.1591*

TABLE 4 : BEST CALCULATIONS FOR CrF_6^{3-}, FeF_6^{3-} AND NiF_6^{4-} (2G) AND FeF_6^{3-} (3G)

	CrF_6^{3-} : ESG		FeF_6^{3-} : ESG		FeF_6^{3-} (3G/STF) : ESG		NiF_6^{4-} : ESG	
LUMO (α) (β)	24.038	26.415	84.640	17.462	*70.587*	*2.529*	83.386	29.013
	7.880	*10.233*	*68.980*	*1.669*			*55.326*	*2.209*
HOMO (α) (β)	10.238	7.940	14.031	8.679	*4.974*	*-7.760*	15.775	15.630
	-6.023	*-8.292*	*-1.591*	*-6.990*			*-11.925*	*-12.187*
Lowdin Pop. Analysis								
Atomic Charges M	+.456	*+.420*	+1.237	*+1.212*	*+1.134*		+ .5122	*+.7114*
F	-.576	*-.571*	-.706	*-.702*	*-.689*		- .7520	*-.7852*
Population 3dσ	.8654	*.8768*	1.408	*1.413*	*1.422*		2.0000	*2.0000*
3dπ	1.0748	*1.0762*	1.094	*1.097*	*1.122*		1.4054	*1.3251*
4s	.5939	*.5998*	.6733	*.6766*	*.6642*		.6802	*.6417*
2pσ	1.7387	*1.7356*	1.8456	*1.8439*	*1.8446*		1.8267	*1.8555*
2pπ	1.9813	*1.9809*	1.9765	*1.9756*	*1.9694*		2.0000	*2.0000*
Mulliken Pop. Analysis								
Atomic Charges M	+.6561	*+.6194*	+1.374	*+1.347*	*+1.2705*		.6059	*.8203*
F	-.6093	*-.6032*	-.72911	*-.7245*	*-.7117*		.7676	*-.8034*

Table 4 : continued

	CrF_6^{3-}	ESG	FeF_6^{3-}	ESG	(3G/STF) FeF_6^{3-}	ESG	NiF_6^{4-}	ESG
Population 3dσ	.47021	*.47634*	1.0000	*1.0000*	*1.0000*		1.0000	*1.0000*
3dπ	1.0000	*1.0000*	1.0000	*1.0000*	*1.0000*		1.0000	*1.0000*
4s	.24546	*.24925*	.27811	*.28079*	*.2730*		.2844	*.2625*
2pσ	.85213	*.85049*	.9772	*.97706*	*.98155*		.9702	*.9718*
2pπ	1.0000	1.0000	1.0000	*1.0000*	*1.0000*		1.0000	*1.0000*
Mulliken $(f_\sigma - f_\pi)$ %	-4.988	*-5.017*	+8.663	*+8.723*	*+8.8291*		11.2562	*+8.6208*
Roby Projected Pop. Analysis								
Atomic Charges M	-1.219	*-1.253*	-.0210	*-.00101*	*-.0955*		-.37849	*-.17472*
F	-.8024	*-.7984*	-.8625	*-.86257*	*-.8524*		-.8722	*-.89998*
Population 3dσ	.67127	*.67656*	1.0000	*1.0000*	*1.0000*		1.0000	*1.0000*
3dπ	1.0000	*1.0000*	1.0000	*1.0000*	*1.0000*		1.0000	*1.0000*
4s	.64018	*.64323*	.65185	*.68359*	*.6795*		.65816	*.64046*
2pσ	.90694	*.90557*	.99101	*.99093*	*.9934*		.98804	*..98897*
2pπ	1.0000	1.0000	1.0000	*1.0000*	*1.0000*		1.0000	*1.0000*
Roby Projected $(f_\sigma - f_\pi)$ %	-3.428	*-3.452*	+5.874	*+5.830*	*+6.0366*		8.285	*+6.012*
$\langle \hat{S}^2 \rangle$	3.770350	*3.770184*	N.D.	*8.750226*	*8.750280*		2.00537	*2.000333*

Table 4 : continued

Spin D's after Spin Annihilation. (%)	CrF_6^{3-}	ESG	FeF_6^{3-}	ESG	(3G/STF) FeF_6^{3-}	ESG	NiF_6^{4-}	ESG
$\langle \hat{S}^2 \rangle$	3.750119	*3.750117*	N.D.	*8.750000*	*8.750000*		2.00000	*2.00000*
f_{4s}	.4736	*.4717*	N.D.	*-.5134*	*-.5485*		-.62759	*-.49566*
$f_{3d\sigma}$	3.429	*3.422*	N.D.	*59.564*	*58.691*		59.8741	*68.1317*
$f_{3d\pi}$	93.045	*92.911*	N.D.	*90.864*	*88.332*		0.0	*0.0*
$f_{2p\sigma}$	-.8682	*-.8681*	N.D.	*10.891*	*11.6221*		11.0217	*8.44123*
$f_{2p\pi}$	1.5917	*1.6264*	N.D.	*2.282*	*2.9149*		0.0	*0.0*
$(f_\sigma - f_\pi)$ %	-2.4599	*-2.4945*	N.D.	*+8.609*	*+8.707*		11.0217	*8.44123*

Appendix 3. A Recent Publication

This publication[1] has recently appeared outlining a semi-empirical UHF-MO study of compounds that we have looked at in our own work. Their calculated values for $f_\sigma - f_\pi$ are better than the previous CNDO studies[2] and this paper will now be briefly summarized.

(1) All valence orbitals were included.

(2) Parameterization is via orbital ionization potentials.

(3) Double zeta orbitals of Richardson were used for the d orbitals whilst Clementi's[3] single STO's are used for s and p orbitals.

(4) Either a CNDO or INDO type approximation was used.

Their results overemphasize the 4s and 4p orbitals in that for NiF_6^{4-} the values are .251 and .465 electrons respectively. Nonetheless the spin distribution predicted by them shows good agreement with experiment particularly before spin annihilation of the wavefunction. In comparing their CNDO and INDO methods they recognise that the former method doesn't show polarization effects on the MO energies and eigenvectors and hence is unsatisfactory in practical situations as wl well as being theoretically deficient in the treatment of open shell systems compared to the INDO scheme which includes the possibility of exchange polarization by including exchange integrals.

1. S. Sakaki, H. Kikkawa, H. Kato, S. Yoshida, Bull. Chem. Soc. Jap., 49, 76 (1976).

2. D.W. Clack, N.S. Hush, J.R. Yandle, J. Chem. Phys., 57, 3505 (1972).

3. E. Clementi, D.L. Raimondi, J. Chem. Phys., 38, 2686 (1963).